Chapter IV

CHARACTERIZATION

The IPNs and their homopolymer networks have been characterized using various techniques to investigate the following physical properties

1. Molecular weight between two crosslinks by swelling method
2 Transport properties Diffusion coefficient, sorption coefficient and permeability coefficient
3 Morphology by Dynamic mechanical and Scanning electron microscopy
4 Mechanical properties Ultimate tensile strength, ultimate elongation, modulus and hardness
5 Thermal properties by Thermogravimetry and Differential scanning calorimetry

4.1 MOLECULAR WEIGHT BETWEEN TWO CROSSLINKS (M_C)

Physical properties of crosslinked polymers are largely influenced by Mc, the average chain length between two crosslinks and hence the crosslink density The most widely used method to determine Mc of network polymers is swelling method When a crosslinked polymer is placed in contact with a suitable solvent, imbibition of the solvent takes place with consequent swelling of the specimen As a result, the three dimensional network gets extended until equilibrium swelling is achieved at which, the rate of imbibition of solvent equals rate of expulsion This equilibrium swelling is the key parameter to determine Mc

Experimental

Equilibrium swelling experiments were performed at 25 ± 0 5°C, of IPNs of various NCO/OH ratios and weight composition of PUR and UPE Identical experiments were also performed for pure homopolymer networks (PUR60, PUR92, IPE and OPE) For the swelling studies, circular samples of diameter ~1 5 cm were cut and the thickness were measured using a micrometer screw The samples, after taking the initial weights were soaked in various solvents with solubility parameter values (δ), in the range of 7 4 to 14 5 $(cal/cm^3)^{1/2}$ until an equilibrium weight was achieved in each case The samples were blot dried and immediately weighed This was repeated for three specimen from each network in order to ensure the reproducibility of the results. The equilibrium swelling was determined from the initial weight and the equilibrium swollen weight Density measurements of the samples were carried out at 25 ± 0.5°C by floatation method

Results and discussion

The equilibrium degree of swelling (Q) which is the reciprocal of volume fraction of polymer in swollen state (V_p), was calculated from the swelling data of samples in various solvents using the following relations

$$Q = \frac{1}{V_p} \quad \text{and} \quad V_p = \frac{W_p/d_p}{W_p/d_p + W_s/d_s}$$

Where

W_p - The dry weight of polymer

W_s - Weight of solvent taken up at equilibrium

d_p - Density of polymer

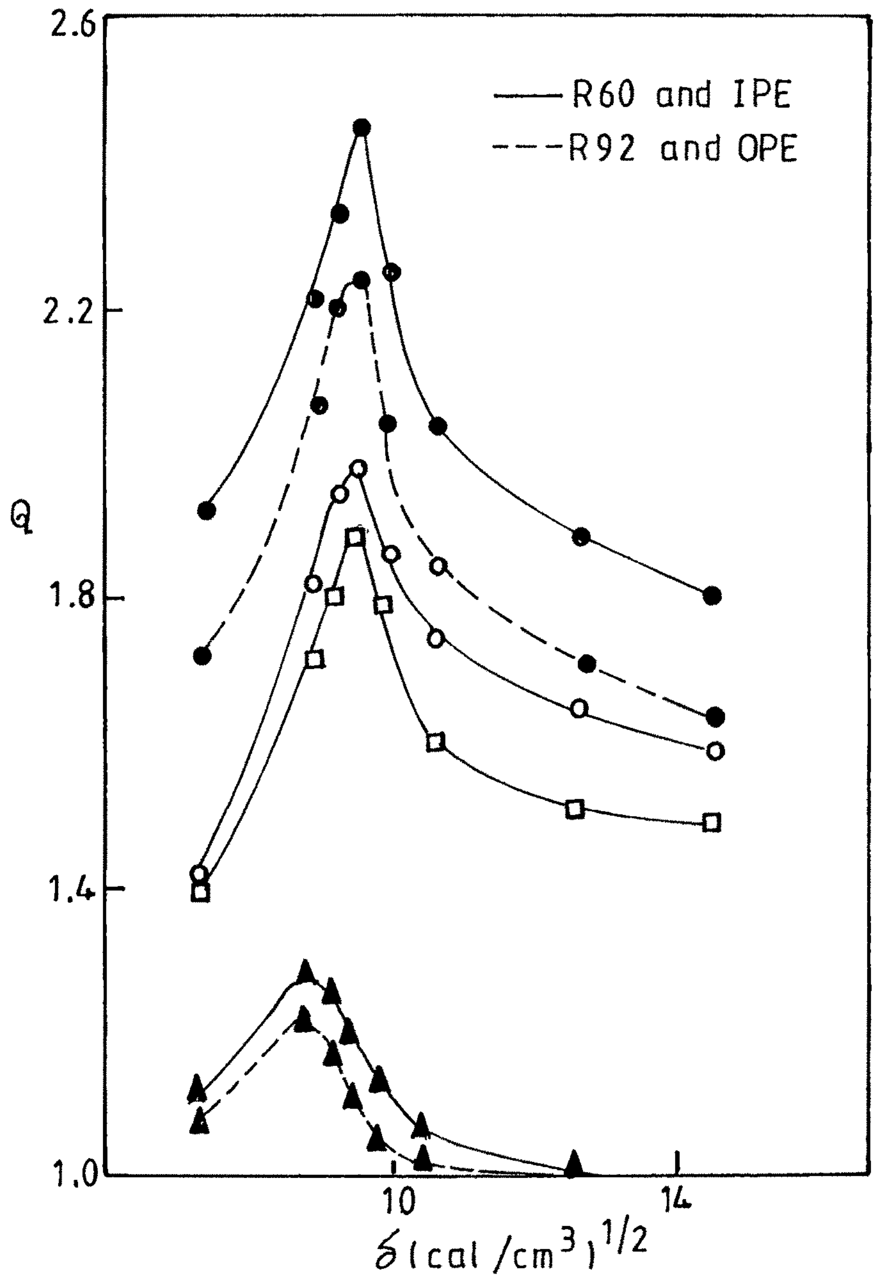

Fig 4.1 Plot of degree of swellıng (Q) vs solubılıty parameter of solvents (δ) for homopolymer networks PUR60(●, —), PUR92 (●,----), IPE (▲, —), OPE (▲,----) and IPNs PUR60(1 2)/IPE 60 40 (O, —) and PUR60(1 2)/OPE 60 40 (□, —)

d_s - Density of solvent

In order to determine the solubility parameter of IPNs, Q was plotted against δ of all solvents studied From the representative plot (Fig 4 1), it was found that chlorobenzene [$\delta = 9\ 5\ (\mathrm{Cal/cm^3})^{1/2}$] gave maximum value of Q for all the samples studied and hence was used for further sorption studies

The average molecular weight between two cross links (M_c), which is a direct measure of cross link density, was measured from the well known Flory-Rehner[1] equation as shown below

$$M_c = \frac{dV_1(V_p)^{1/3}}{\ln(1-V_p) + V_p + \chi_{12}V_p^2}$$

Where

V_1 - Molar volume of solvent

d - Density of network

χ_{12} - Polymer solvent interaction parameter, which was calculated using the equation[2]

$$\chi_{12} = B + \frac{V_1\ (\delta_p - \delta_s)^2}{RT}$$

where

δ_p - Solubility parameter of polymer

δ_s - Solubility parameter of solvent

R - Gas constant

T - Absolute temperature and

B - The lattice constant, which is generally taken as 0 34 for a good solvent

The degree of cross linking (ν) and the number of chains per unit volume (N) were also calculated for all the samples using the following relations[3,4]

$$\nu = \frac{1}{2M_c} \qquad\qquad N = \frac{d}{M_c}$$

The values of V_p, M_c and ν for all the systems studied in chlorobenzene are summarised in Table 4 1 From the table it can be confirmed that, the present system as a whole has got high cross link density In this section, the effect of composition of PUR and UPE, NCO/OH ratio of PUR and type of PUR and

Table 4.1: Values of Vp, Mc and ν for various IPNs based on IPE and OPE with PUR60 and PUR92

IPNs based on IPE

PUR	NCO/OH	Vp					Mc					$\nu \times 10^4$ (mole/g)				
		PUR:UPE (w/w%)					PUR:UPE (w/w%)					PUR:UPE (w/w%)				
		100:00	80:20	50:50	20:80	00:100	100:00	80:20	50:50	20:80	00:100	100:00	80:20	50:50	20:80	00:100
PUR60	1.2	0.394	0.458	0.522	0.683	0.820	1234	955	761	441	187	4.05	5.23	6.57	11.33	26.73
	1.5	0.401	0.529	0.506	0.661	,,	1010	785	758	405	,,	4.95	6.36	6.59	12.34	,,
	2.0	-	0.546	0.595	0.655	,,	-	774	667	407	,,	-	6.45	7.49	12.28	,,
PUR92	1.2	0.442	0.520	0.545	0.687	,,	1120	744	684	346	,,	4.46	6.72	7.31	14.15	,,
	1.5	0.484	0.543	0.552	0.688	,,	888	669	659	347	,,	5.63	7.47	7.58	14.40	,,
	2.0	-	0.552	0.564	0.701	,,	-	632	624	322	,,	-	7.91	8.01	15.82	,,

IPNs based on OPE

PUR	NCO/OH	Vp 100:00	Vp 80:20	Vp 50:50	Vp 20:80	Vp 00:100	Mc 100:00	Mc 80:20	Mc 50:50	Mc 20:80	Mc 00:100	ν 100:00	ν 80:20	ν 50:50	ν 20:80	ν 00:100
PUR60	1.2	0.394	0.479	0.526	0.688	0.848	1234	932	759	349	153	4.05	5.36	6058	14.32	32.67
	1.5	0.401	0.536	0.528	0.700	,,	1010	692	757	327	,,	4.95	7.22	6.60	15.29	,,
	2.0	-	0.549	0.594	0.701	,,	-	649	519	333	,,	-	7.70	9.93	15.01	,,
PUR92	1.2	0.442	0.539	0.578	0.701	,,	1120	696	579	327	,,	4.46	7.18	8.63	15.29	,,
	1.5	0.484	0.564	0.580	0.720	,,	888	600	577	297	,,	5.63	8.33	8.66	16.83	,,
	2.0	-	0.571	0.587	0.721	,,	-	580	557	298	,,	-	8.62	8.97	16.77	,,

UPE on M_c is dıscussed as ıt ıs interrelated to V_p and N accordıng to the above mentioned equatıons Effect of the above mentıoned parameters on swellıng ıs dıscussed ın sectıon 4 2, sınce ıt descrıbes the transport properties whıch are associated wıth swellıng phenomena

Effect of composition : For a gıven NCO/OH ratıo, V_p ıncreases while M_c decreases wıth ıncrease ın UPE content, ındıcating that swellıng of IPNs ın chlorobenzene is largely attrıbuted to PUR content rather than UPE content The value of M_c are maxımum and mınimum for homopolymer networks of PUR and UPE respectively Such low values of M_c ın UPE network seem to be the result of formatıon of shorter chains between two cross links compared to that of PUR The values of IPNs fall in between that of homopolymer networks dependıng on the contrıbutıon of PUR and UPE

Effect of crosslink density The effect of cross lınk densıty on V_p and M_c follow the same trend as observed for compositıonal varıatıon As NCO/OH ratıo of PUR ıncreases for a gıven composıtıon, the number of cross lınk poınts increases and ultimately the system becomes more rigıd ın nature wıth low values of M_c

Effect of polyol PUR network and its IPNs based on R92 polyol show low values of M_c compared to those based on R60 polyol, irrespectıve of the type of polyesters ınterpenetrated Thıs could be due to more number of hydroxyl groups present ın R92, whıch lead to more number of cross lınk points compared to the system based on R60.

Effect of polyester : UPE resıns based on orthophthalıc acid show relatively low values of M_c to that based on ısophthalic acıd The dense cross lınked structure resulted in case of the former is probably the reason for low values of M_c

4.2 TRANSPORT PROPERTIES

Polymers used for transport properties display their ability to resist the passage of penetrants like gases, vapours and organic liquids The transport of penetrant molecules through polymers is of great importance in many areas of technology like membranes, barrier plastics, foams and many other applications requiring protective packaging and shelf-life extension of food and beverages

Transport properties of various engineering polymers like PUR, cross linked polystyrene, natural rubber and various synthetic rubbers have been extensively studied by using organic solvents of various polarity and interacting groups and also by using aqueous salt solutions of acids by many researchers[3,5-8] However, transport properties of IPNs are rarely found in literature[9,10] even though they are widely used in many applications such as membranes, GPC, controlled release agents and enzyme immobilization[11-14] The transport phenomenon of penetrant in IPNs differ from other cross linked polymers as they consist of two components, one rubbery and the other glassy The behavior of rubbery polymers towards solvents would be different from glassy polymers as there is a difference in their free volume and molecular mobility[6]

Experimental

In the kinetic experiments, so called pat and weigh technique[15] was used for liquid sorption Circular samples (diameter ~1 5 cm) of definite thickness, after taking the dry weight were placed in chlorobenzene in a standard joint test tube for which temperature of 25 ± 0 5°C was maintained Specimen were taken out at regular intervals of time, solvent adhering to the surface is rubbed off, weighed immediately and replaced in the solvent This procedure was continued till equilibrium swelling was achieved. This was repeated for three specimens from each network in order to ensure the reproducibility of the values The time taken for wiping out the solvent from sample surface and weighing was kept minimum in order to minimise the error due to solvent evaporation.

Results and discussion

The sorption of penetrating species into polymer matrix is quantified in terms of mole percent uptake. The mole percent uptake (Q_t) at each time interval, from the results of swelling experiments, was calculated using the following relation[3]

$$Q_t = \frac{m_e/m_r}{m_i} \times 100$$

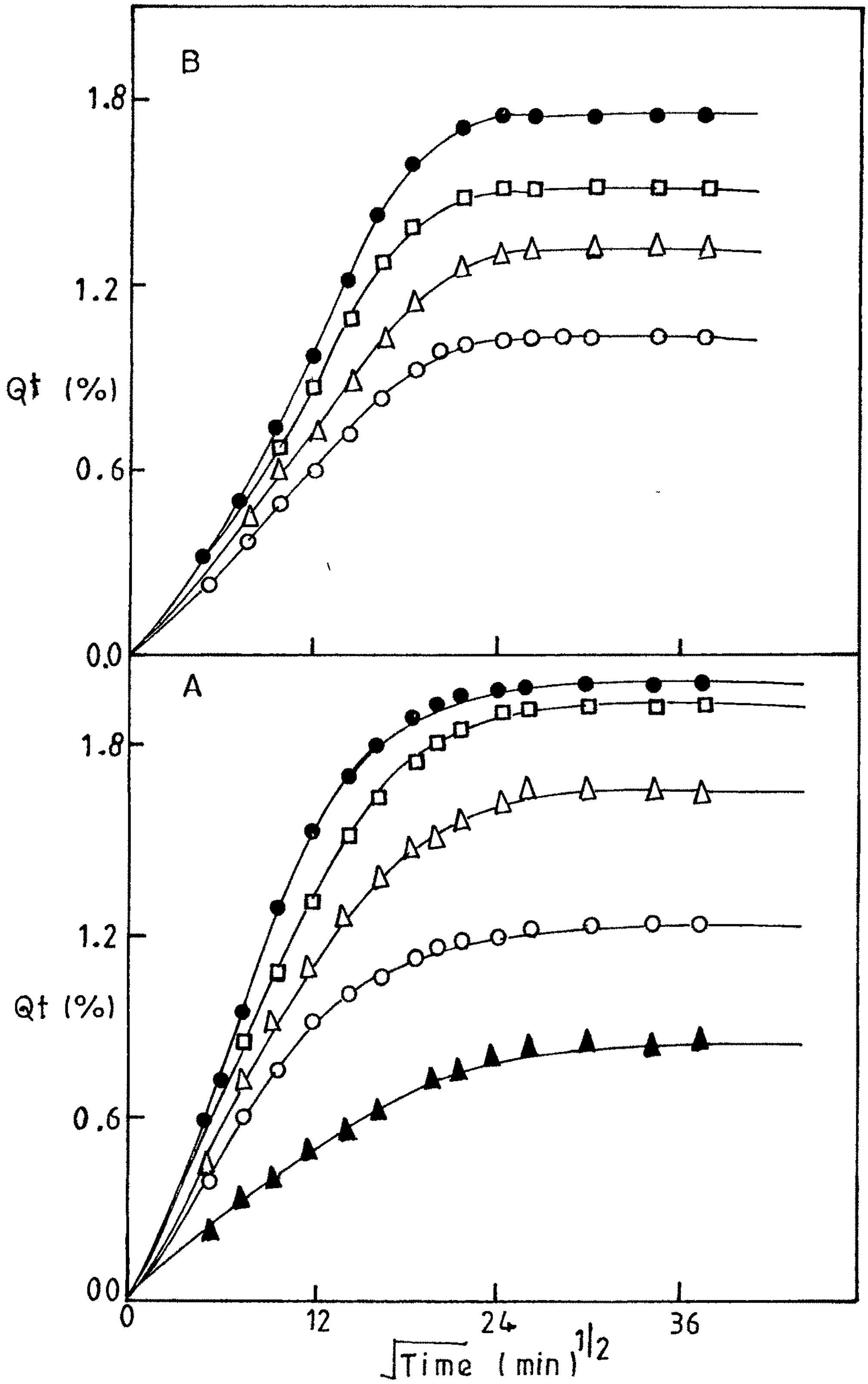

Fig 4.2 Sorption curves showing the mole percent uptake of homopolymer networks and IPNs based on PUR60/IPE (A) and PUR92/IPE (B) containing 100%(●), 80%(□),50%(Δ), 20%(O)and 00%(▲) PUR by weight

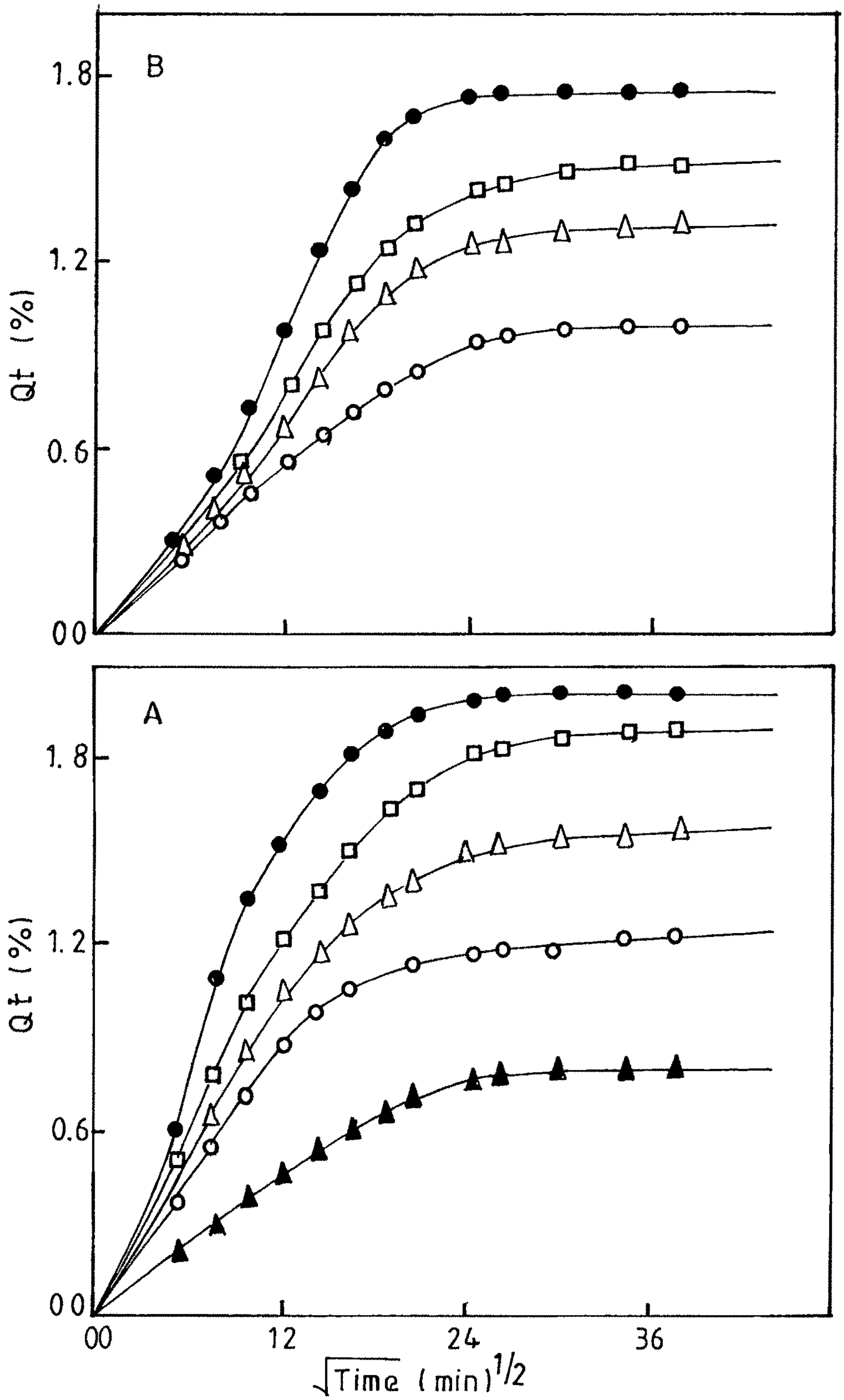

Fig 4.3 Sorption curves showing the mole percent uptake of homopolymer networks and IPNs based on PUR60/OPE(A) and PUR92/OPE(B) containing 100%(●), 80%(□), 50%(Δ), 20%(O) and 00%(▲) PUR by weight

where

m_e = Mass of solvent taken up at equilibrium

m_r = Relative molar mass of solvent

m_i = Dry mass of sample

At equilibrium swelling, Q_t was considered to be Q_∞, mole percent uptake at infinite time, the values of which are tabulated in Table 4 2 Figures 4 2 (A&B) and 4 3 (A&B) show the sorption curves of homopolymer networks and various IPNs at NCO/OH ratio of 1 2 obtained by plotting Q_t against $(\text{time})^{1/2}$ From the curves it is clear that, the homopolymer networks of PUR and UPE show the highest and the lowest values of Q_t respectively at a particular time The uptake capacity of IPNs were found to be intermediate between that of both constituents With increase in UPE content as well as NCO/OH ratio, sorption decreases and reaches a minimum value irrespective of the type of PUR and UPE used in all the IPNs The values of Q_∞ also follow the same trend

The whole phenomena can be explained on the basis of cross link density and composition of the network With increase in NCO/OH ratio, cross link density increases and the network becomes more dense and rigid Thus the ability of polymer chains to accommodate solvent molecules decreases. When NCO/OH ratio is 1.2, the chains would have maximum flexibility due to less cross link points and thus sorption capacity will be the highest With further increase in NCO/OH ratio to 1.5 and 2 0, flexibility of chains gradually decreases resulting in to less sorption and hence low values of Q_t and Q_∞ Coming back to Table 4 2, it is clear that IPNs made of R60 based PUR show more solvent uptake capacity compared to that made of R92 based PUR This may be due to more number of hydroxyl groups in the latter which lead to increase in crosslink density IPNs based on OPE show less swelling compared to that based on IPE The presence of orthophthalic acid in OPE moiety is probably responsible to provide less flexibility to chains compared to isophthalic acid based polyester This in turn result into low values of Q_t and Q_∞ The values of V_p and M_c, which are explained in section 4 1 also support the above reasoning

To understand the mechanism of sorption, the values of Q_t and Q_∞ were substituted into the general expression[16] which describes the transport kinetics

$$Q_t/Q_\infty = k\, t^n$$

Table 4.2 : Values of Q_∞, n and k for IPNs based on IPE and OPE with PUR60 and PUR92

IPNs based of IPE

PUR	NCO/	Q_∞ (mole %)					n					$k \times 10^2$				
		PUR:UPE (w/w %)					PUR:UPE (w/w %)					PUR:UPE (w/w %)				
	OH	100:00	80:20	50:50	20:80	00:100	100:00	80:20	50:50	20:80	00:100	100:00	80:20	50:50	20:80	00:100
	1.2	2.01	1.92	1.64	1.22	0.85	0.53	0.58	0.61	0.59	0.63	3.94	3.61	4.44	5.12	4.81
PUR60	1.5	1.96	1.74	1.39	1.09	,,	0.52	0.54	0.58	0.62	,,	5.84	4.11	2.84	3.52	,,
	2.0	-	1.51	1.31	0.99	,,	-	0.63	0.54	0.61	,,	-	3.84	5.16	4.13	,,
	1.2	1.74	1.51	1.31	1.02	,,	0.51	0.59	0.56	0.61	,,	4.11	3.21	3.22	5.41	,,
PUR92	1.5	1.67	1.45	1.20	0.94	,,	0.51	0.61	0.62	0.54	,,	6.10	2.42	5.04	4.12	,,
	2.0	-	1.34	1.09	0.90	,,	-	0.54	0.61	0.52	,,	-	3.16	6.11	5.06	,,

IPNs based on OPE

	1.2	.2.01	1.89	1.56	1.23	0.80	0.53	0.54	0.59	0.62	0.64	3.94	4.21	3.66	5.42	4.79
PUR60	1.5	1.96	1.70	1.40	1.04	,,	0.52	0.60	0.52	0.58	,,	5.84	3.99	4.11	4.84	,,
	2.0	-	1.49	1.29	0.95	,,	-	0.56	0.51	0.63	,,	-	4.63	4.44	3.82	,,
	1.2	1.74	1.50	1.32	0.99	,,	0.51	0.57	0.54	0.62	,,	4.11	2.98	5.48	4.01	,,
PUR92	1.5	1.67	1.37	1.17	0.82	,,	0.51	0.55	0.63	0.56	,,	6.10	3.62	4.23	5.33	,,
	2.0	-	1.28	1.05	0.84	,,	-	0.61	0.58	0.60	,,	-	5.12	4.71	5.01	,,

where k is a constant which depends on the structural characteristics of the polymer and its interaction with solvent The value of 'n' determines the mode of transport When n=1/2, diffusion obeys Fick's law Fickian diffusion occurs when segmental mobility of the polymer chain is faster than the rate of diffusion of penetrant molecules when n=1, the diffusion is said to be non-Fickian, which occurs when diffusion is much faster than polymer chain relaxation processes

In the present system, the values of 'k' and 'n' were obtained from the linear plot of log (Q_t/Q_∞) Vs log t (correlation coefficient >0 9) and are presented in Table 4.2 In all the cases, the magnitude of 'n' varies from 0 51 to a maximum of 0 64 This suggests that diffusion process deviates only slightly from normal Fickian behavior and may be treated as anomalous in nature

The transport of penetrant molecules through polymers is also quantified by another term, permeability (P) The permeability of small molecules in polymers usually occur through the following steps

1. Sorption of penetrating species into polymer matrix
2. Diffusion of penetrating species through polymer matrix
3. Desorption of penetrating species through polymer wall

The Sorption coefficient (S), which gives an idea about the equilibrium sorption of solvent was calculated using the relation[14]

$$S = m_\infty / m_p$$

where

m_∞ - Mass of solvents taken up at equilibrium

m_p - Initial mass of polymer

The Diffusion coefficient (D), which is a measure of the ability of the penetrant molecules to move among the polymer segment was calculated from the following equation[17]

$$D = \Pi \left[\frac{h\,\theta}{4\,Q_\infty} \right]^2$$

where

θ - Slope of the linear portion of the sorption curve

h - Thickness of the sample

Table 4.3 : Values of D, S and P for various IPNs based on IPE and OPE with PUR60 and PUR92

IPNs based on IPE

PUR	NCO/OH	$Dx10^6$ (cm^2/s) PUR:UPE (w/w %) 100:00	80:20	50:50	20:80	00:100	S (g/g) PUR:UPE (w/w %) 100:00	80:20	50:50	20:80	00:100	$Px10^6$ (cm^2/s) PUR:UPE (w/w %) 100:00	80:20	50:50	20:80	00:100
PUR60	1.2	3.51	3.62	4.38	5.83	8.47	2.30	2.11	1.61	1.12	0.82	8.07	7.64	7.05	6.53	6.94
	1.5	3.69	4.01	5.42	6.11	„	2.13	1.85	1.52	1.10	„	8.43	7.41	8.23	6.72	„
	2.0	-	4.82	5.85	7.19	„	-	1.54	1.31	0.99	„	-	7.43	7.66	7.12	„
PUR92	1.2	4.14	4.21	4.98	6.62	„	2.01	1.93	1.36	1.01	„	8.32	8.12	6.77	6.68	„
	1.5	4.51	4.63	5.84	6.42	„	1.90	1.72	1.20	0.93	„	8.56	7.96	7.00	5.97	„
	2.0	-	5.81	6.61	8.01	„	-	1.68	1.21	0.89	„	-	9.76	7.99	7.12	

IPNs based on OPE

PUR	NCO/OH	$Dx10^6$ 100:00	80:20	50:50	20:80	00:100	S 100:00	80:20	50:50	20:80	00:100	$Px10^6$ 100:00	80:20	50:50	20:80	00:100
PUR60	1.2	3.51	3.84	4.42	5088	8.63	2.30	2.10	1.58	1.09	0.78	8.07	8.06	6.98	6.40	6.73
	1.5	3.69	4.12	4.86	6.14	„	2.13	1.69	1.52	1.01	„	8.43	6.96	7.38	6.20	„
	2.0	-	5.03	6.01	7.22	„	-	1.56	1.26	0.94	„	-	7.84	7.57	6.78	„
PUR92	1.2	4.14	4.33	4.91	6.64	„	2.01	1.91	1.40	0.98	„	8.32	8.27	6.87	6.50	„
	1.5	4.51	4.81	5.93	7.04	„	1.90	1.70	1.19	0.94	„	8.56	8.17	7.05	6.61	„
	2.0	-	5.92	6.64	8.21	„	-	1.64	1.12	0.80	„	-	9.70	7.43	6.55	

The permeability coefficient, P which gives the combined effect of both D and S, was calculated using the equation

$$P = D \times S$$

The values of D, S and P for all the systems are summarised in Table 4 3. For a given NCO/OH ratio, diffusion coefficient increases and sorption coefficient decreases with increase in polyester content This signifies less affinity of solvent molecules with polyester moiety as can also be seen from their Q_∞ values. PUR networks show high sorption in presence of chlorobenzene This may be due to specific interaction of solvent molecules with PUR and more segmental mobility compared to UPE network The values of diffusion coefficients are slightly higher in pure PUR and IPNs based on R92 compared to that based on R60 polyol This is in contradiction to the general tendencies observed in swelling studies. (i e. systems based on R92 should show low values of D than that based on R60 as the former lead to more cross linked structure) The higher values of D in R92 based systems may be due to the formation of more number of urethane linkages, thereby rendering it more susceptible to attack by chlorobenzene molecules

It is also observed that sorption coefficient decreases with increase in NCO/OH ratio at a given composition At low NCO/OH ratio, the network structure is more flexible and mainly forms urethane linkages which may have specific interaction with chlorobenzene However, as the NCO/OH ratio increases, more of allophanate linkages would be formed, along with urethane linkages having less interaction with solvent molecules and hence reducing sorption. The permeability coefficient did not follow any particular trend with either change in composition or NCO/OH ratio in all the IPNs studied

The data of D, M_c and V_p were used to establish the following relationships proposed by de Gennes[18] for swollen polymer networks.

$$D \sim V_p^{\beta} \qquad \text{and} \qquad D \sim M_c^{-\gamma}$$

where $\beta = 3/4$ and 1 for a good and theta solvent respectively and $\gamma = 3/5$ These power laws are represented by straight lines as shown in Fig 4 4 (A&B), for IPNs based on R60 with IPE and OPE respectively having NCO/OH ratio 1 2 The exponent values of β for all the IPNs are nearly 1 which is agreeable with the foregoing theoretical prediction and other findings[19] within experimental errors This means that chlorobenzene is a poor solvent for the present IPN system at 25°C. The γ values were

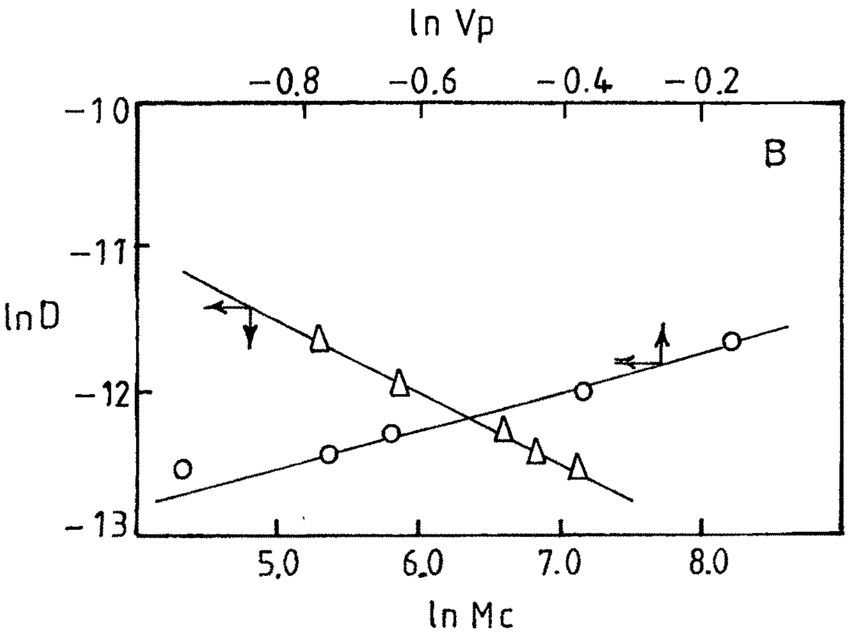

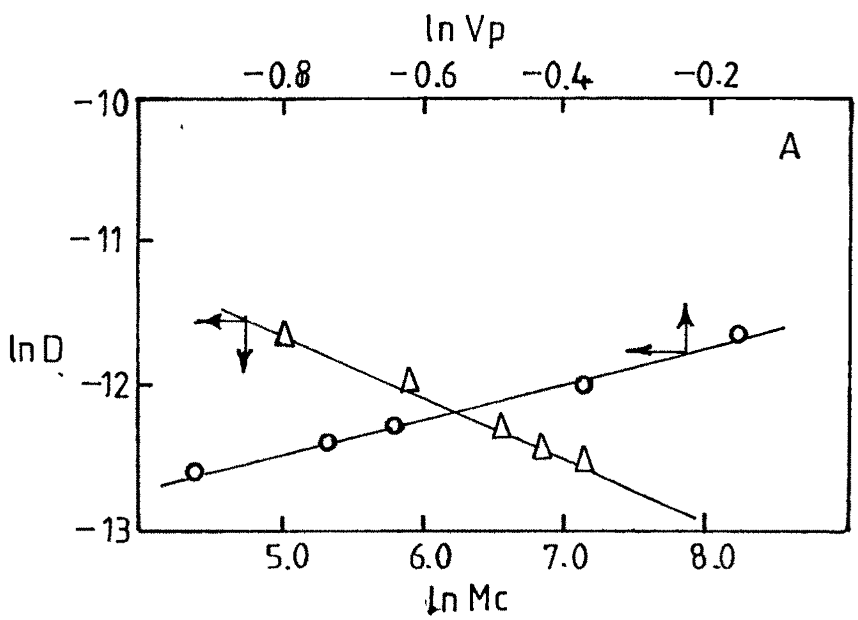

Fig 4.4 log-log plot of diffusion coefficient (D) against Mc (Δ) and Vp (O) for IPNs based on PUR60/IPE (A) and PUR60/OPE (B)

found to be in the range of 0 3 to 0 48 which are rather small compared to the theoretical prediction Incidentally Oikawa and Murakami[20] have investigated poly (dimethyl siloxane) gels in benzene by means of dynamic light scattering technique and obtained the values of γ as 0 29 K. Chee[21] also observed low values of γ for poly (ethyl methacrylate) crosslinked system

4.3 DYNAMIC MECHANICAL PROPERTIES

Dynamic mechanical properties are the mechanical properties where the materials undergo repeated small amplitude strains in a cyclic manner Molecules perturb in this way, store a portion of the imparted energy elastically and dissipate a portion in the form of heat[22] The quantity E', young's storage modulus is a measure of energy stored elastically where as E'', the loss modulus is a measure of energy lost as heat The ratio E'' to E' is called tan δ, the loss tangent, where δ is the angle between in-phase and out of phase components in cyclic motion

The dynamic storage modulus (E') provides an information regarding the inherent stiffness of the material under dynamic loading conditions The polymeric materials under use conditions are often in the dynamic stress and strain field such as parts of automobiles, aircraft and aerospace structures Thus knowledge of the dynamic modulus of such materials is indispensable for design of these materials The other two quantities loss modulus (E'') and/or mechanical damping (tan δ) are the measure of amount of energy dissipated as heat during deformation of the material The mechanical damping of the material is important as a property index, and for environmental and industrial applications Since noise is radiated by vibration, especially of metallic materials with small mechanical damping (0 001-0 004), the application of damping materials to the vibrating surface converts the energy into heat which is dissipated within the damping materials rather than being radiated as airborne noise Thus high damping is essential in decreasing the effect of undesirable vibrations and in reducing to safe limits as well as in playing a key role in all kinds of structural applications The mechanical damping (dissipation factor) is sensitive to many kinds of molecular motions, transitions, relaxation processes, structural heterogeneity and the morphology of multiphase systems Therefore interpretation of dynamic mechanical properties at the molecular level are of great importance in understanding the mechanical behavior of polymers

These dynamic tests have proven useful in evaluating the glass transition temperature (T_g), degree of crystallinity, molecular orientation, cross linking, phase-separation and structural or morphological changes resulting from processing and other features of molecular structures of polymer chains

For IPNs, which are an integral part of blends, information gathered from these properties give an idea about the compatibility of the components It also allow us to understand how one polymer can modify the dynamic mechanical properties of another component in IPN and ultimately aid in the design of IPNs with desirable physical properties Literature abounds with information regarding the behavior of IPN systems and their usefulness based on dynamic mechanical test method[23-27]

Experimental technique

Fılms casted of IPNs of dıfferent composıtıon and crosslınk densıty were cut ınto demensions of 60 x 5 x 0 5 mm The dynamıc mechanıcal data of the samples were obtained usıng a Perkın - Elmer 7 serıes thermal analysıs system The DMA temperature - tıme scan in 3 - point bendıng mode was performed at a frequency of 1 Hz, heatıng rate of 2°C/mın and over a temperature range of -120 to 250°C

Results and discussion

(I) IPNs based on PUR 60 and IPE

Dynamic mechanıcal analysıs ın terms of tan δ ,E^{I} and E^{II} by varyıng temperature for IPNs are dıscussed in the followıng sectıon

Glass transition behavior (Dissipation factor)

The following observatıons

1) The ınward shıfting of the glass transitıon temperatures, T_g of the components wıth, ultımately theır merger to yıeld a sıngle transıtıon

2) An increase ın the wıdth of the glass transıtıons whıch is usually measured as half-peak height or half-peak width (HPW)

are generally considered as evidence of mıxıng

Fıgure 4 5 shows the tan δ -temperature plots for PUR60(1 2)/IPE IPNs of dıfferent composıtıon and of the correspondıng homopolymer networks It is clear from the figure that for all IPNs there are two glass transıtion temperatures, ındıcatıng that complete mıxing has not occurred ın any of the IPNs The sıze of the tan δ peaks changed systematıcally wıth change ın concentratıon of the components ın IPNs, ı e decreased wıth increasıng polyester content All the IPNs showed relatıvely low tan δ_{max} values for ısophthalıc polyester (IPE) phase (hıgher T_g). Thıs shows that, the other component, polyurethane (PUR) which ıs rubbery at the T_g of the IPE component ıs present as a contınuous phase[28]

It is also observed from Fıg 4 5 is that, PUR glass transıtıon, at about 34°C, gaıns ın promınence and shıfts to slıghtly hıgher temperatures as PUR content decreases Also there seems to be an ınward shıftıng of the ındıvidual transitıons, ındıcatıng some segmental mixıng of the components

The tan δ - temperature curve of pure IPE exhıbıts two peaks, one located at around 98°C and a second small peak as shoulder at 195°C. Thıs could be due to exıstence of two dıfferent structures of IPE, polyester part and polystyrene(PS) part The peak observed at 98°C may be due to PS domaıns exıstıng ın the form of long crosslınkıng chaıns or homo polystyrene However, ın case of IPNs as observed ın

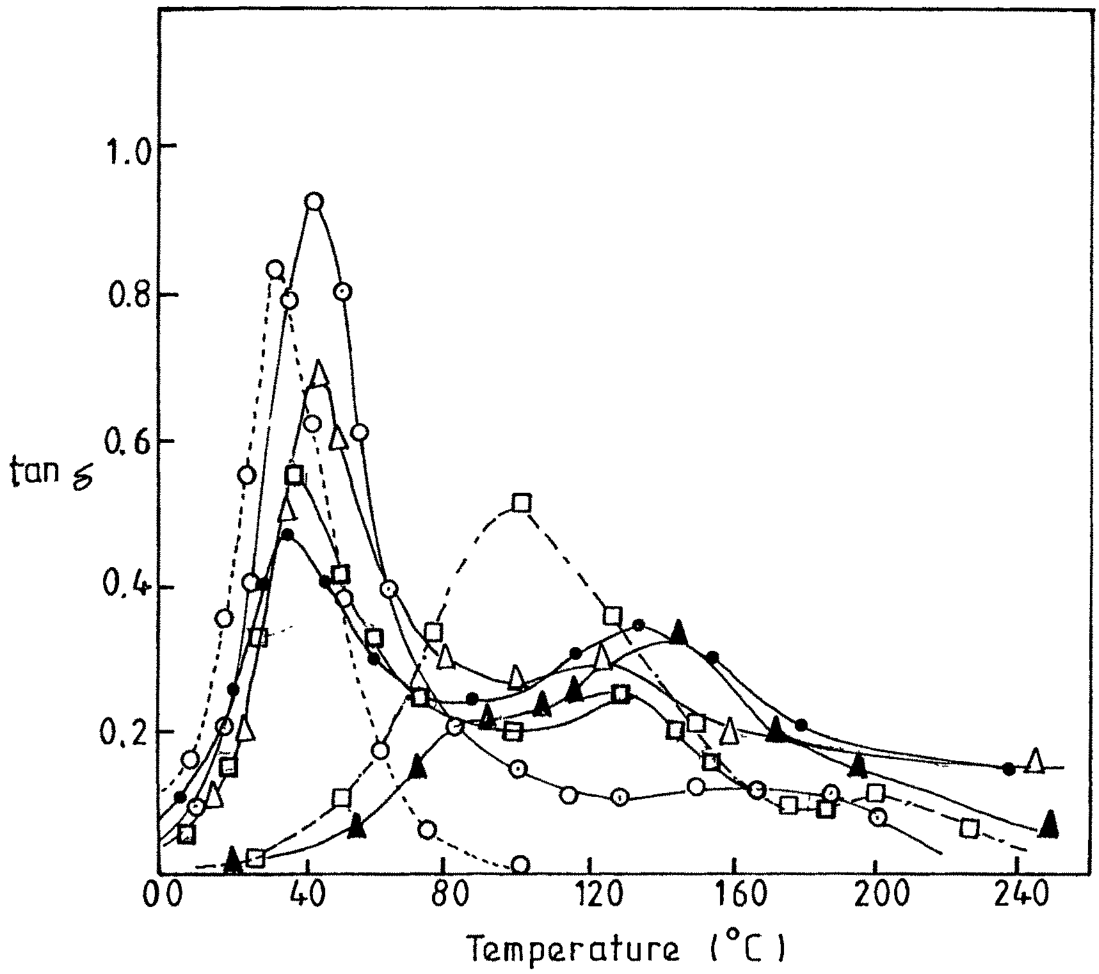

Fig 4.5 tan δ - temperature plots for PUR60 (O), IPE(□) and PUR60(1 2)/IPE IPNs containing 80%(ʘ), 60%(Δ),50%(□),40%(●) and 20%(▲) PUR by weight

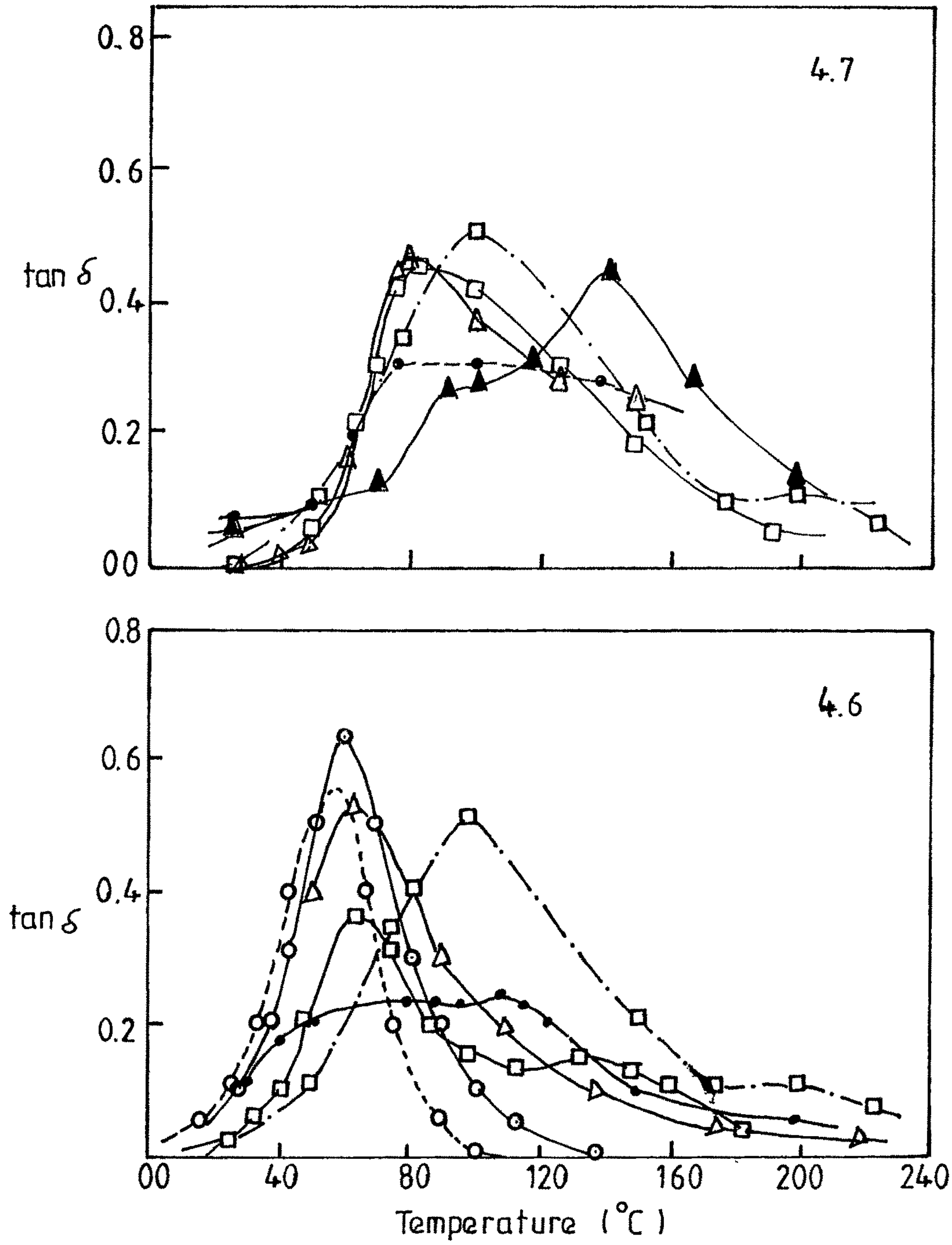

Fig 4.6 tan δ - temperature plots for PUR60 (O), IPE(□) and PUR60(1 5)/IPE IPNs containing 80%(Θ), 60%(Δ),50%(□),40%(●) and 20%(▲) PUR by weight

Fig 4.7 tan δ - temperature plots for IPE(□) and PUR60(2 0)/IPE IPNs containing 60%(Δ),50%(□),40%(●) and 20%(▲) PUR by weight the same figure indicates that the peak at 98°C is disappeared probably because of its merging with PUR phase This is also confirmed by deviation of T_g values of PUR in IPNs

Evidence of mixing can also be seen from the data of half peak width (HPW) (Table 4 4) for IPNs with different weight composition of components Since the solubility parameters of both the components are not very much apart, they form partially miscible networks having micro heterogeneous morphology, which broadens the tan δ peak One striking observation from Fig 4 5 is that, in case of 20 80 IPN, the tan δ_{max} is dramatically shifted to higher temperature from that of pure PUR, and also shows broad transition with PUR peak as shoulder Thus, this composition shows better compatibility compared to the rest of the compositions, which may be assigned to perfect entanglements of both networks leading to decrease in phase separation The reason for the better compatibility are

1) equal rate of crosslinking of IPE and PUR as concentration of polyester phase is higher while that of PUR phase is low

2) higher concentration of polyester provides more terminal hydroxyl groups to react with NCO groups of PUR[29,30]

3) low concentration of PUR network may swell more in polyester to provide uniform phase distribution resulting into uniformly crosslinked network

When PUR content was increased in IPNs, the diffusion of polyester reactants in a high PUR content becomes more difficult due to possibility of less swelling and subsequently phase separation occurs[29]

The glass transition-temperature behavior of IPNs for different compositions of PUR and IPE was also observed at higher NCO/OH ratios of 1 5 and 2 0 Fig 4 6 and Fig. 4.7 show tan δ - temperature plots for PUR60(1.5)/IPE and PUR60 (2 0)/IPE IPN systems respectively of varying compositions and corresponding homopolymers. Comparison of these plots with that of Fig 4 5 and also the data of Table 4 4 reveal that, with increasing NCO/OH ratio of PUR, both the glass transition temperature and half peak width increased On the other hand the tan δ_{max} values decreased The changes are essentially the result of (1)enhanced cross-linking, (2) higher reaction possibility of NCO groups with OH end groups of polyester and (3) more number of H-bonding

To study the effect of cross link density on damping behavior in detail, the tan δ vs temperature plots of PUR60/IPE systems were replotted for a particular composition at various NCO/OH ratios. The plots are shown in Fig 4 8A to 4.8F It can be seen that, IPNs derived from PUR with higher isocyanate content exhibit less phase separation and improved compatibility because of the same reason stated above The tan δ peak of PUR transition decreased with decrease in molecular weight between two

Table 4.4 : Values of T_g, tan δ_{max} and half peak width (HPW) for various IPNs based on IPE and PUR60

PUR:IPE	NCO/OH = 1.2				NCO/OH = 1.5				NCO/OH = 2.0			
	T_g°C		tan δ_{max}	HPW	T_g°C		tan δ_{max}	HPW	T_g°C		tan δ_{max}	HPW
	T_{g1}	T_{g2}			T_{g1}	T_{g2}			T_{g1}	T_{g2}		
100:00	32.6	-	0.83	30	58	-	0.56	34	-	-	-	-
80:20	42	165	0.93	36	59.6	-	0.63	37	-	-	-	-
60:40	44.1	121.5	0.68	46	64.3	-	0.53	52	78.2	-	0.47	78
50:50	37.7	128	0.55	46 (66)	64	135.5	0.36	46 (64)	82.6	-	0.45	80
40:60	36	134	0.47	60 (134)	-	-	0.23	112	74.1	-	0.30	-
20:80	90.7	144.4	0.33	106	-	-	-	-	91	139.3	0.44	96
00:100	98.9	198	0.58	84	98.9	198	0.58	84	98.9	198	0.58	84

Values in parenthesis show the HPW values corresponding to the polyester transition

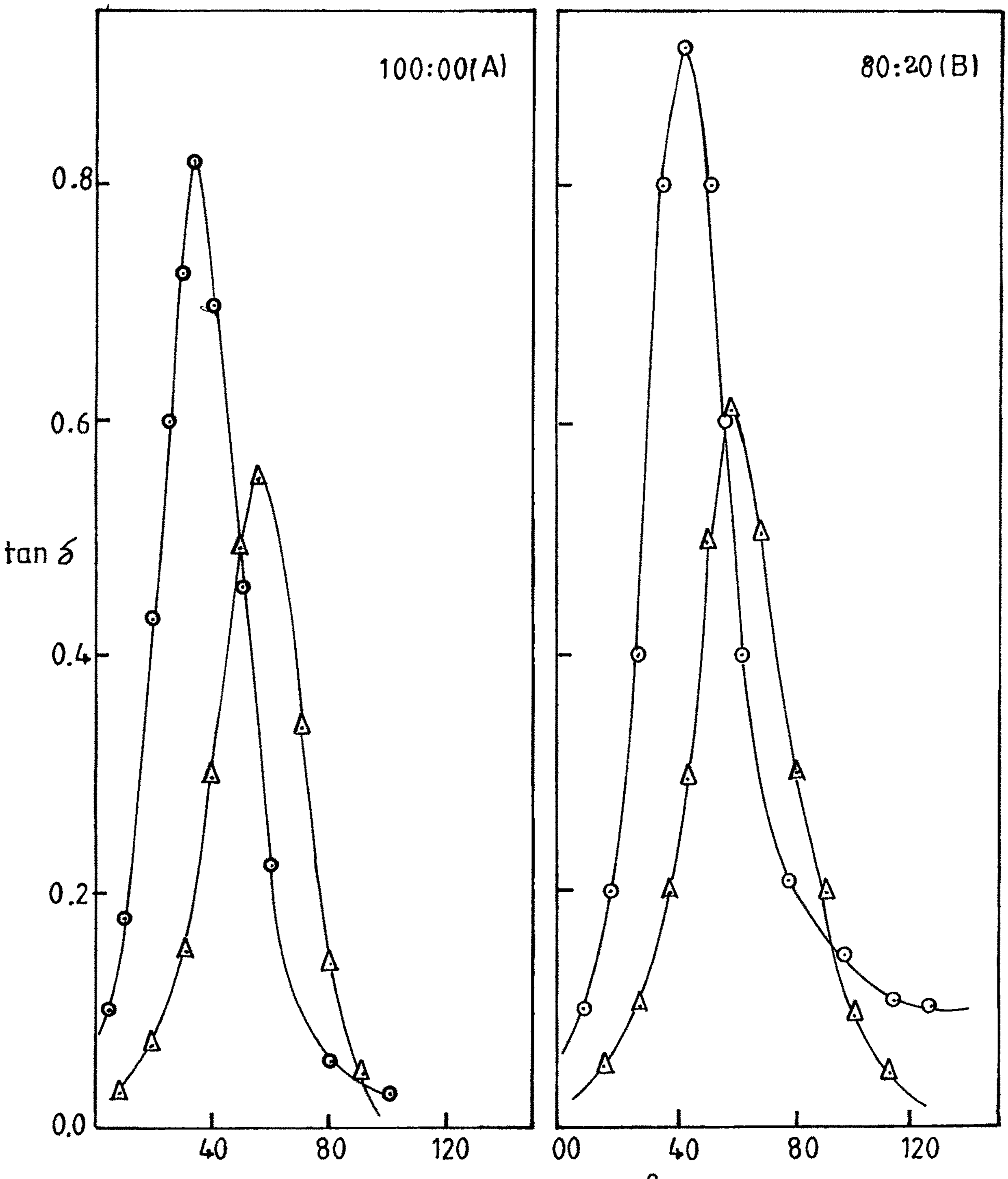

Fig 4.8(A,B) tan δ - temperature plots of PUR60/IPE system for 100.00 (A) and 80 20 (B) samples at various NCO/OH ratios of 1 2 (O) and 1 5 (Δ)

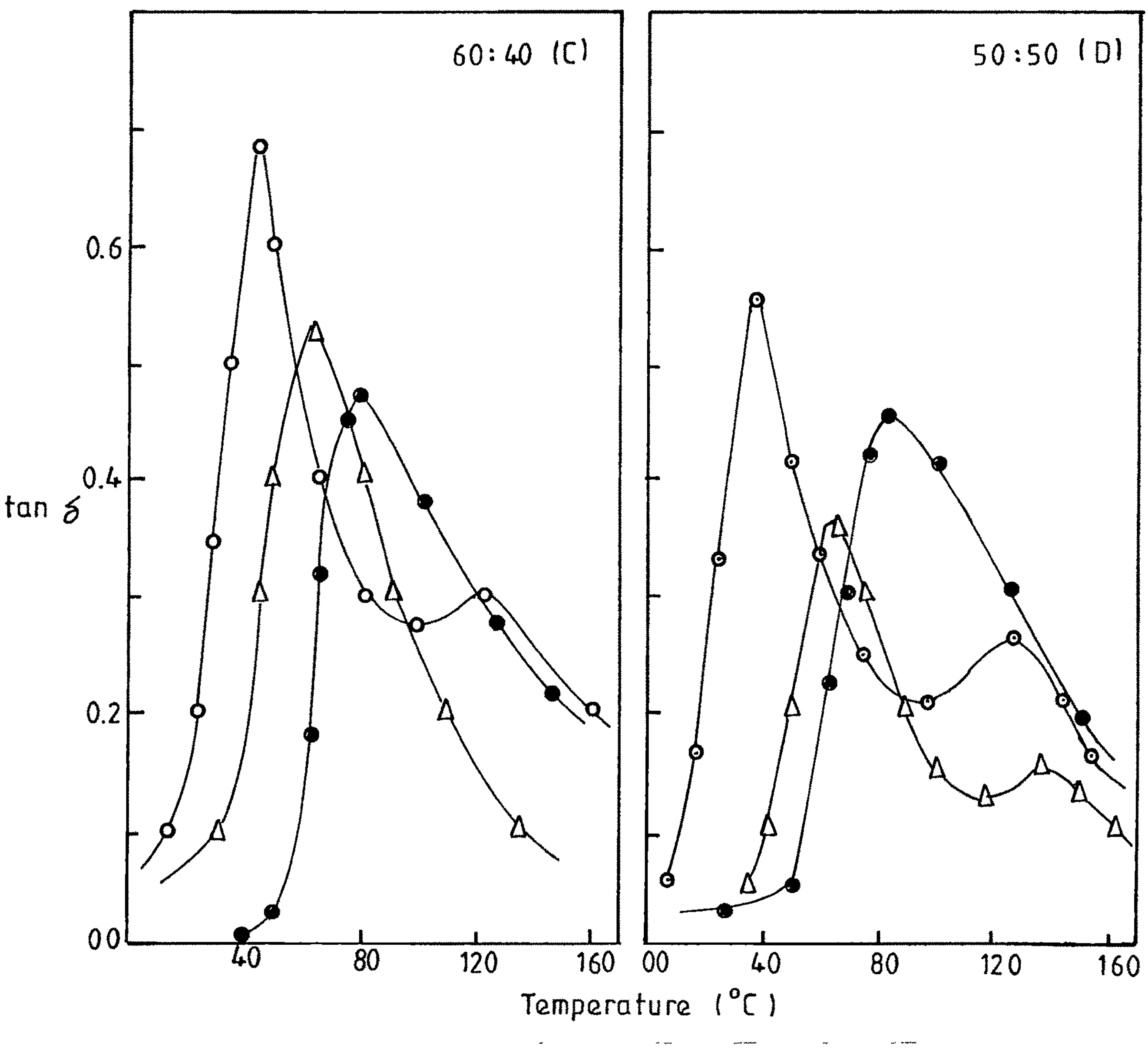

Fig 4.8(C,D) tan δ - temperature plots of PUR60/IPE system for 60 40 (C) and 50 50 (D) samples at various NCO/OH ratios of 1 2(O),1 5(Δ)and2 0 (●)

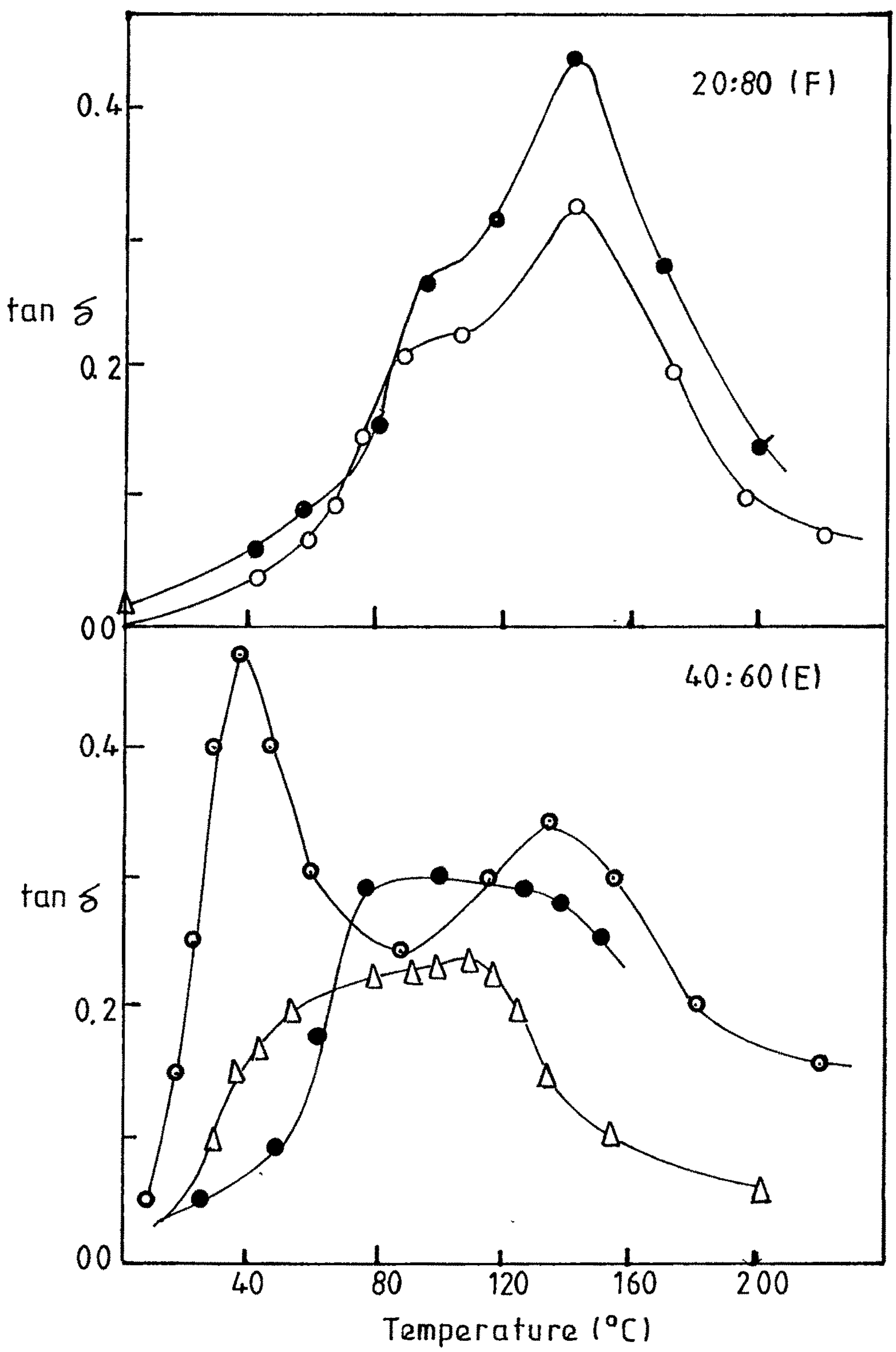

Fig 4.8(E,F) tan δ - temperature plots of PUR60/IPE system for 40 60 (E) and 20 80 (F) samples at various NCO/OH ratios of 1 2 (O), 1 5 (Δ) and 2 0 (●)

crosslinks (M_c) The tan δ peak of polyester transition almost vanished in most of the cases (except few compositions), indicating that PUR component is present as an increasingly continuous phase At this stage it is to be noted that in some IPNs, the transitions corresponding to polyester phase could not be detected due to softening of sample at high temperature during the DMA analysis

The tan δ_{max} values are shifted to higher temperature with increase in NCO/OH ratio, which support the effects caused by higher crosslink density in PUR That is, an increase in number of hard segments as well as decrease in M_c restrict the segmental motion and consequently increases the glass transition temperature From the plots it is also clear that, the tan δ_{max} values decrease with increase in NCO/OH ratio for a particular composition But in IPNs having higher polyester content (> 50%), the change in tan δ_{max} values did not show a regular trend In these samples as NCO/OH ratio increased from1.2 to1.5,tan δ_{max} values decreased, but with further increase in ratio to 2 0, there was an increase in tan δ_{max} The initial decrease in tan δ_{max} value may be due to an optimum extent of incorporation of isocyanate moiety (hard segment) controlling the optimum crosslink density but beyond optimum conditions, the increase in NCO/OH ratio results extensive phase mixing, because of which losses of two individual phases become additive

Out of all the compositions studied, the 40 60 sample (figure 4 8E) in particular showed two different transition temperatures at low NCO/OH ratio of 1 2 while at higher NCO/OH ratios of 1 5 and 2 0, it showed only a single broad dispersion peak over a wide range of temperature IPNs showing such characteristics have good ability for vibration damping Hence 40.60 sample could be a good candidate for such applications The morphology and stress-strain behavior of this IPN also support this characteristic feature

Dynamic Loss Modulus (E^{II})

Fig 4 9 shows the semi-logarithmic plots of loss modulus, E^{II} as a function of temperature with variation in composition for PUR60 (1 2)/IPE IPN system It can be seen from the plots that, for all the IPNs except 20 80 sample, maximum of loss modulus (E^{II}_{max}) appeared at almost the same temperature as that of pure polyurethane The above fact indicates that, the system is considered to be composed of a continuous phase of polyurethane and dispersed phase of IPE[28] In the case of 20 80 sample, transition associated with PUR disappears and results into a broad peak over a wide range of temperature. This is because of the good physical interlocking or molecular network mixing of both the components at this composition

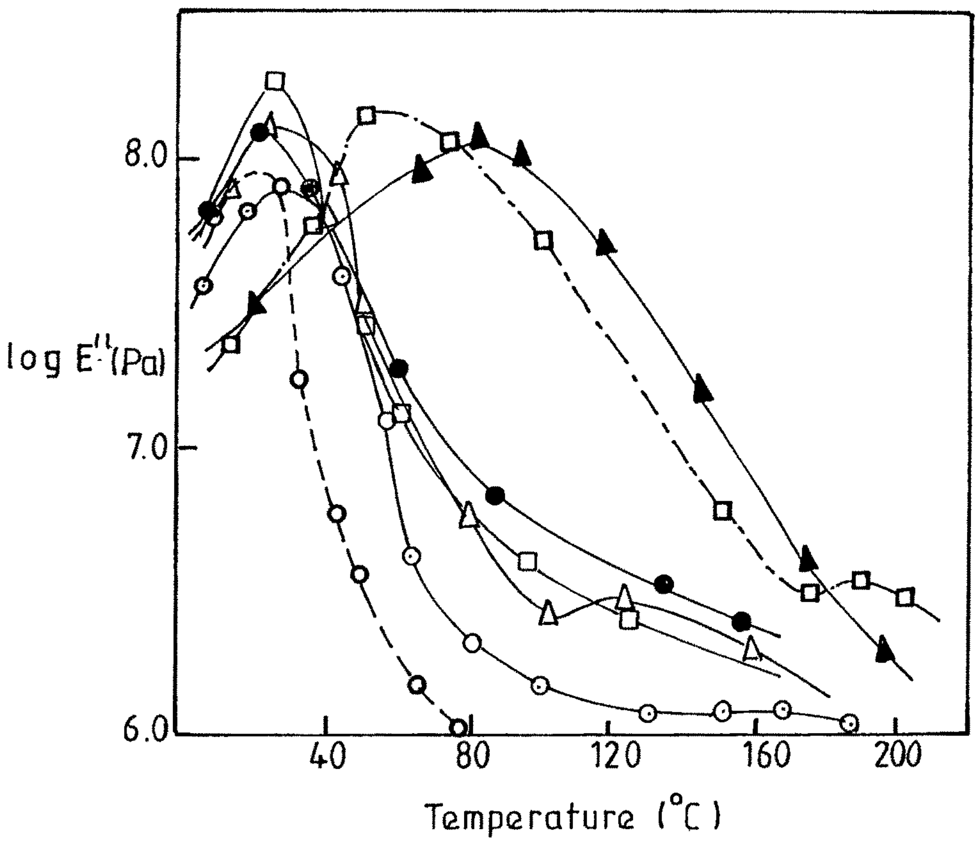

Fig 4.9 log E$^{''}$-temperature plots of PUR60(1 2)/IPE IPNs contaınıng 100%(O), 80%(Θ), 60%(Δ), 50%(□), 40%(●), 20%(▲) and 00%(□) PUR by weıght

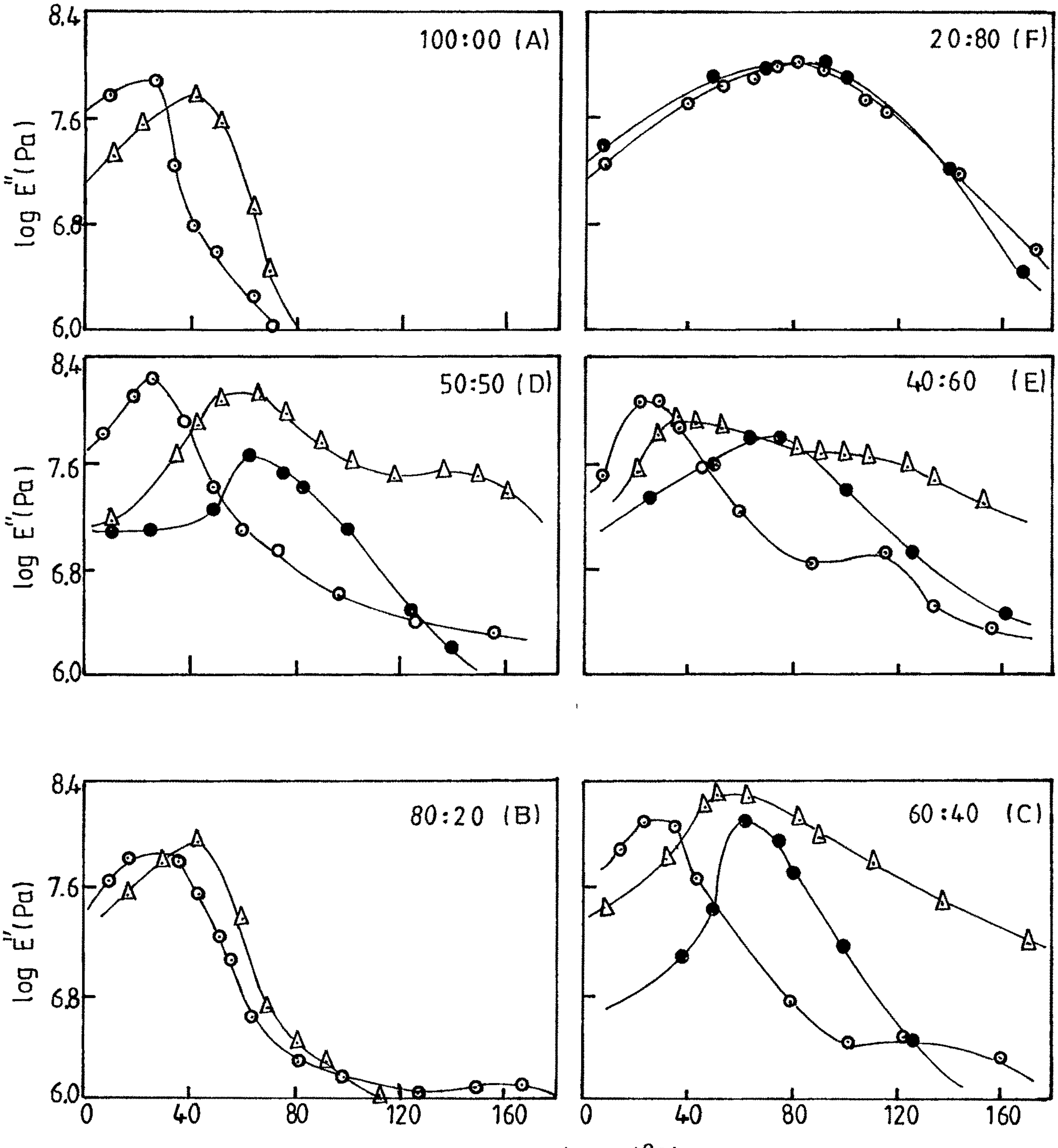

Fig 4.10(A-F) log E^{II} - temperature plots of PUR60/IPE IPNs containing 100%(A),80%(B),60%(C),50%(D),40%(E) and 20%(F) PUR by weight at various NCO/OH ratios of 1 2 (O), 1 5 (Δ) and 2 0 (●)

The effect of crosslink density on the loss modulus behavior as a function of temperature by varying NCO/OH ratio of PUR for different composition is illustrated in Fig 4 10A to 4 10F. When NCO/OH ratio was 1.2, none of the compositions showed a single broad peak (except 20 80 IPN), but rather more or less independent loss modulus peak characteristics of each component were observed However, with increase in ratio to 1.5, the peak maxima are slightly decreased and shifted to higher temperature and also the transition due to polyester gradually disappeared, which supports the reason stated for extensive mixing in the discussion of effects on tan δ

It is noteworthy that, in IPNs, viz 60 40, 50 50 and especially 40·60 having NCO/OH ratio 1 5, broad loss modulus peaks were observed over a wide range of temperature The broadening of peak may be due to the superposition of the different relaxation processes for IPE and PUR in their interpenetrating networks Such large and broad loss modulus in the audio frequency range and in useful temperature ranges is the requirement for a material to show good vibration damping characteristics and thus the above IPNs may find application in vibration damping With further increase in NCO/OH ratio to 2 0, some of the IPNs (60 40 and 50 50) showed narrowing in loss modulus peak and may find their use as narrow band vibration dampers, while 40 60 IPN sample continues to show broad loss modulus peak, even at higher crosslink density

From the above studies it can be inferred that, it is possible to develop vibration damping materials of requisite characteristics by choosing the appropriate composition of both the components and crosslink density of PUR in an IPN

Dynamic Storage Modulus (E^{I})

Fig 4.11 shows the semi-log plot of storage modulus (E^{I}) as a function of temperature with variation in composition for the system, PUR60/IPE at NCO/OH ratio of 1 2 The modulus of pure PUR decreased abruptly at around 30°C, which is the decisive short coming of PUR As shown in the figure, the low modulus of PUR at high temperature can be enhanced significantly by the incorporation of unsaturated polyester On the other hand, when small amount of PUR was added to the IPE, the decrease of storage modulus was not significant This fact is predominant in case of 20.80 system In this particular IPN, the storage modulus plateau region is exceptionally broad and it surpasses that of pure polyester These results suggest the possibility of impact modification of unsaturated polyester by adding rubbery PUR without lowering the modulus seriously due to improvement in rigidity at the cost of brittleness The higher values of E^{I} in glassy region of polyester is due to its brittleness which in turn causes the less possibilities of segmental motion in transition region As a result of which only few segments bare applied load and ultimately break On the other hand in 20·80 sample, the flexibility of PUR part

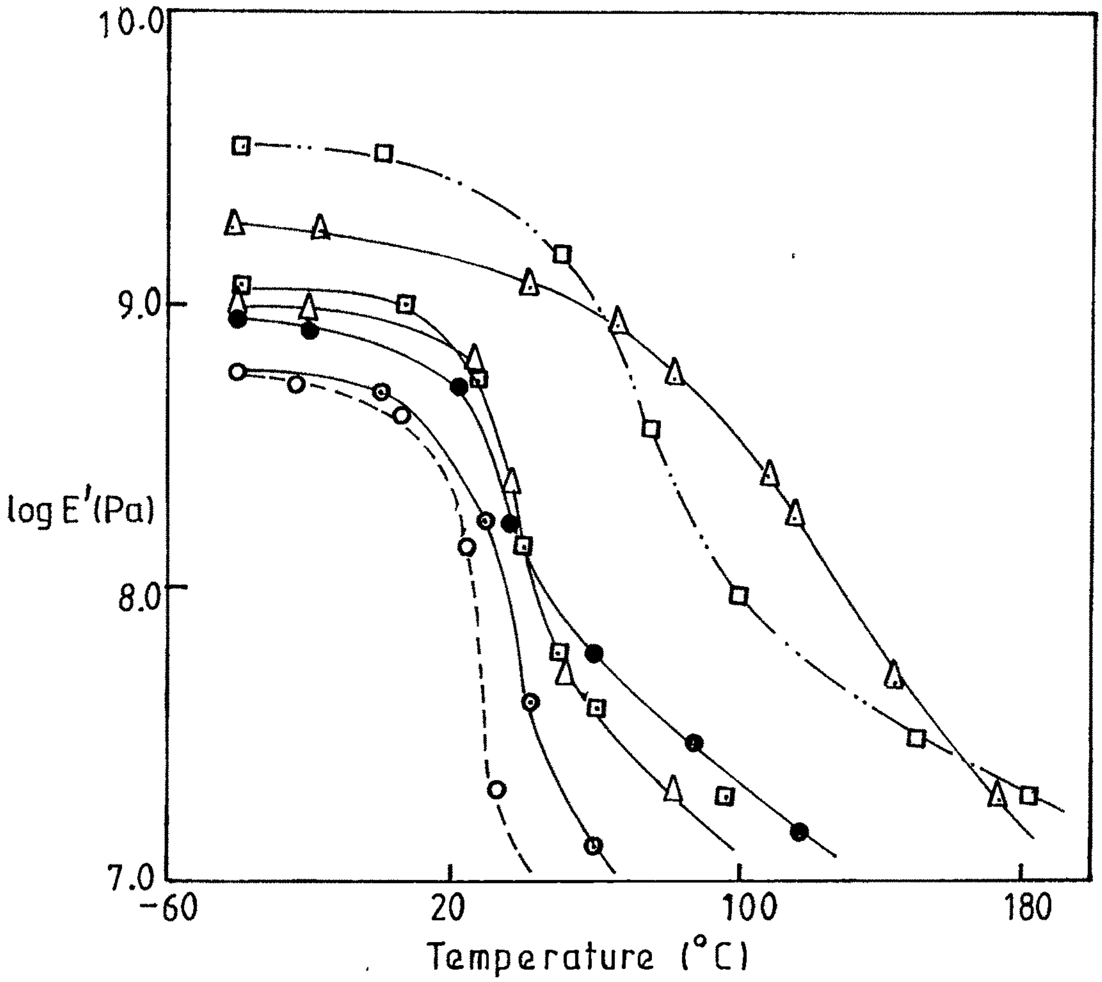

Fig 4.11 log E' - temperature plots of PUR60(1 2)/IPE IPNs containing 100%(O), 80%(Θ), 60%(Δ), 50%(□), 40%(●), 20%(▲) and 00%(□) PUR by weight

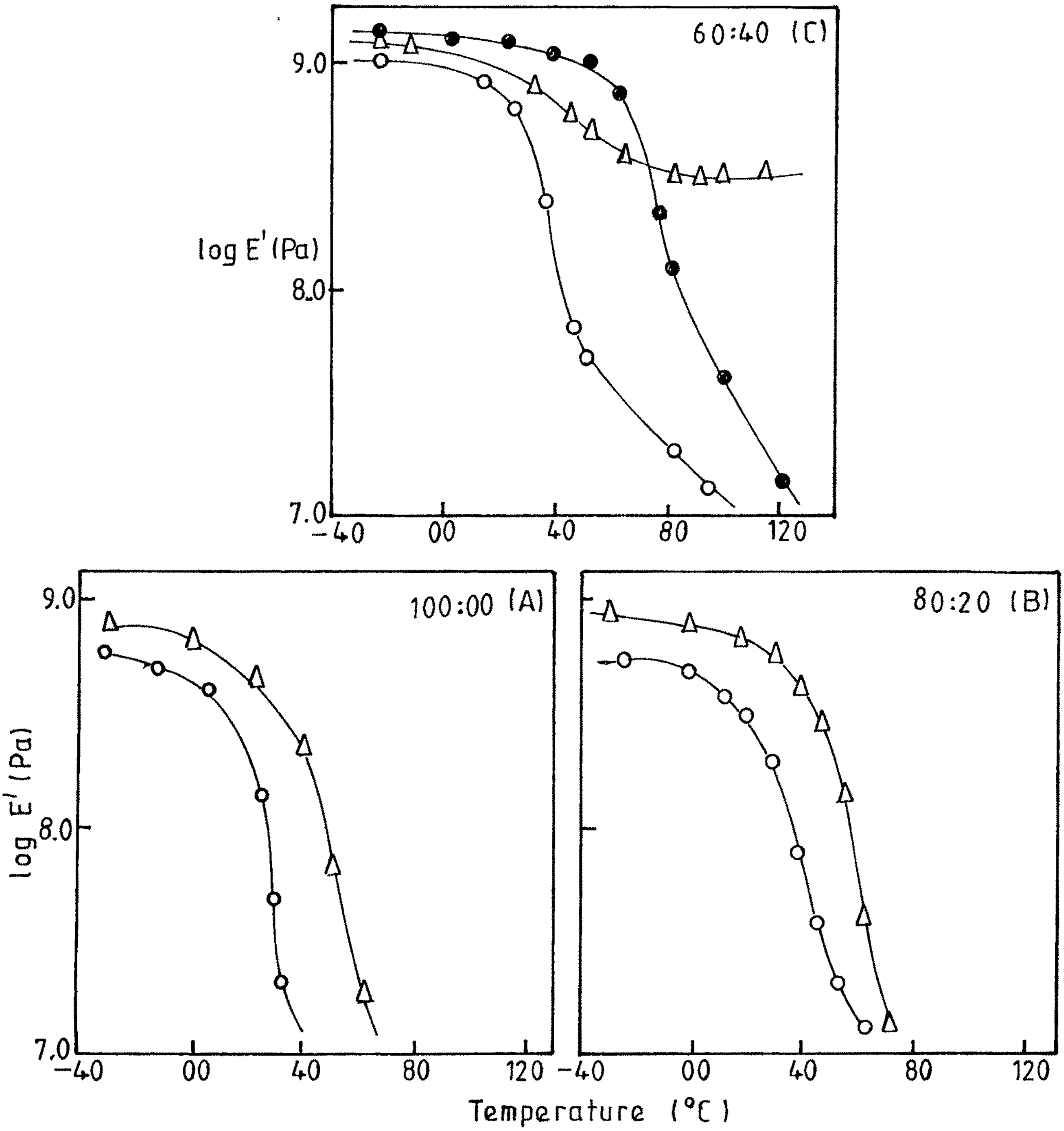

Fig 4.12(A-C) log E' - temperature plots of PUR60/IPE IPNs containing 100%(A), 80%(B) and 60%(C) PUR by weight at various NCO/OH ratios of 1 2 (O), 1 5 (Δ) and 2 0 (●)

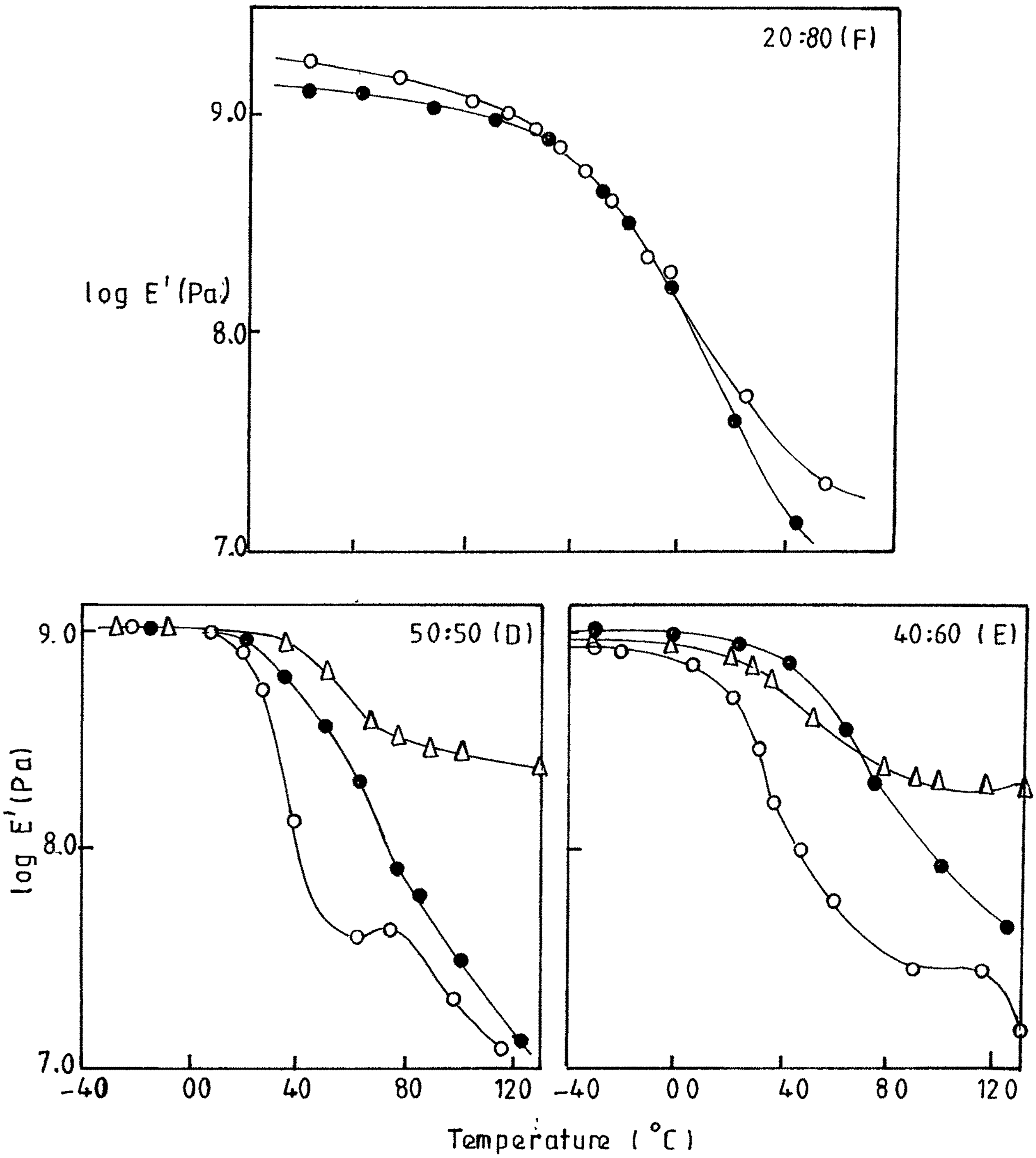

Fig 4.12(D-F) log E' - temperature plots of PUR60/IPE IPNs containing 50%(D), 40%(E) and 20%(F) PUR by weight at various NCO/OH ratios of 1 2 (O), 1 5 (Δ) and 2 0 (●)

provides more possibilities of segmental rearrangement and hence distributes applied load among more molecular network resulting into higher modulus thanthat of pure IPE

The plots of log E^{I} vs temperature of PUR60/IPE IPNs of varying crosslink density at different composition of PUR and IPE are represented in Fig 4 12A to 4 12F From the plots it is clear that, when the NCO/OH ratio was increased from 1 2 to 1 5, initial modulus was not only increased but was maintained up to higher temperature in almost all the samples Moreover, the higher temperature transitions observed as shoulders at low level of corsslinking (1 2) disappeared totally with increase in NCO/OH ratio to 1 5 These observations may be, not only due to the modulus increase of PUR but also due to higher degree of reaction with end groups of IPE at higher NCO/OH ratios of 1 5 and 2 0 DMA analysis also shows that, IPNs having NCO/OH ratio 1 2 had change in modulus value from 10^9 Pa at -50°C to 10^7 Pa at 100°C while those prepared having NCO/OH ratio 1 5 had change in modulus only by a decade i.e. from 10^9 Pa at -50°C to $10^{8 2}$ Pa at 100°C (except 80 20 IPN) Thus the IPNs having 60 40, 50 50, 40 60 and 20 80 compositions and NCO/OH ratio 1 5, show optimum level of composition and crosslink density

Thus by the incorporation of judicious amount of each matrix, and optimum extent of isocyanate moiety, tailor made materials can be prepared by the interpenetration of both components When NCO/OH ratio was increased to 2.0, particularly when polyester content is more, the modulus was decreased significantly at all temperatures, which may be due to brittleness attributed by uneven crosslinks at higher NCO/OH ratio This results high values of E^{I} in glassy state, but at high temperature, segmental motion commences to overload short crosslink points which causes rupture of the same to result rapid loss in modulus

(II) IPNs based on PUR 92 and IPE

Dynamic mechanical properties of PUR and their IPNs were also studied to see the influence of polyol by varying the chain length and number of hydroxyl groups

Glass transition behavior (Dissipation factor)

Fig 4 13 shows the tan δ - temperature plots for PUR92(1 2)/IPE IPN systems having different composition of PUR and IPE and also of the homopolymer networks When R92 was employed as polyol in PUR synthesis, which has less equivalent weight (190 gm equivalent) and more hydroxyl groups (6 per mole) than that of R60 (eq wt. 220 and hydroxyl group/mole = 5), IPNs prepared using PUR92 and IPE at NCO/OH ratio 1 2 follow the similar trend as observed in IPNs based on PUR60 (Fig 4 5) as far as shift to higher T_g, increase in half peak width and reduction in tan δ_{max} with change

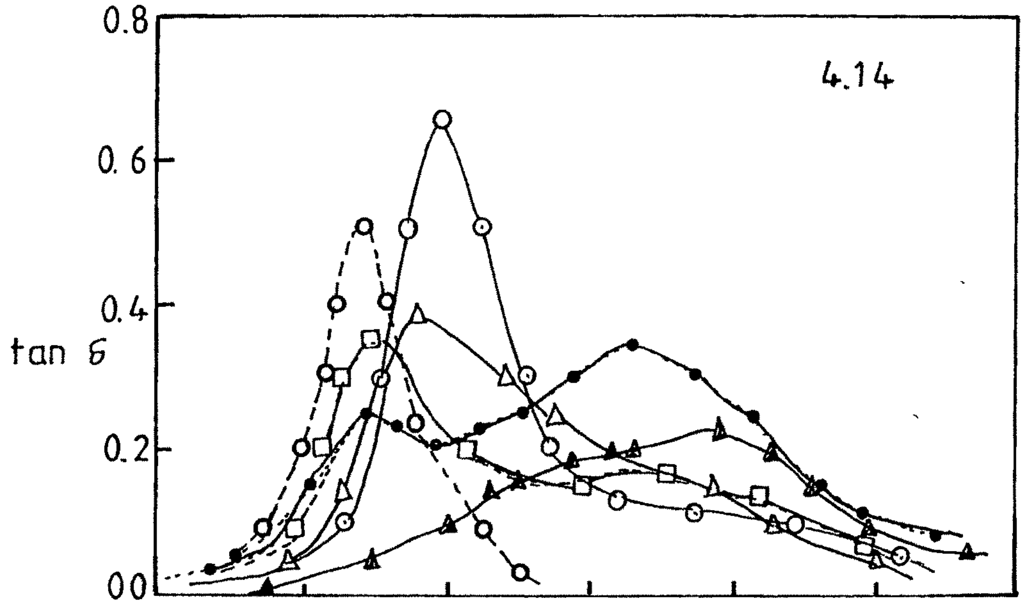

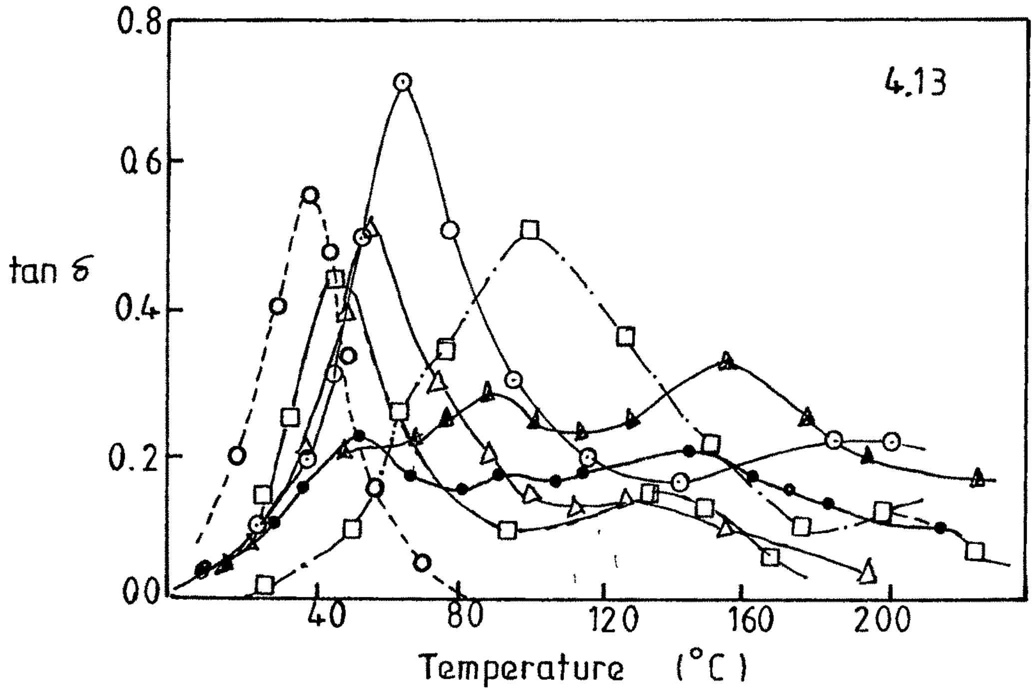

Fig 4.13 tan δ - temperature plots for PUR92 (O), IPE(□) and PUR92(1 2)/IPE IPNs containing 80%(ʘ), 60%(Δ), 50%(□), 40%(●) and 20%(▲) PUR by weight

Fig 4.14 tan δ - temperature plots for PUR92 (O), IPE(□) and PUR92(1 5)/IPE IPNs containing 80%(ʘ), 60%(Δ), 50%(□), 40%(●) and 20%(▲) PUR by weight

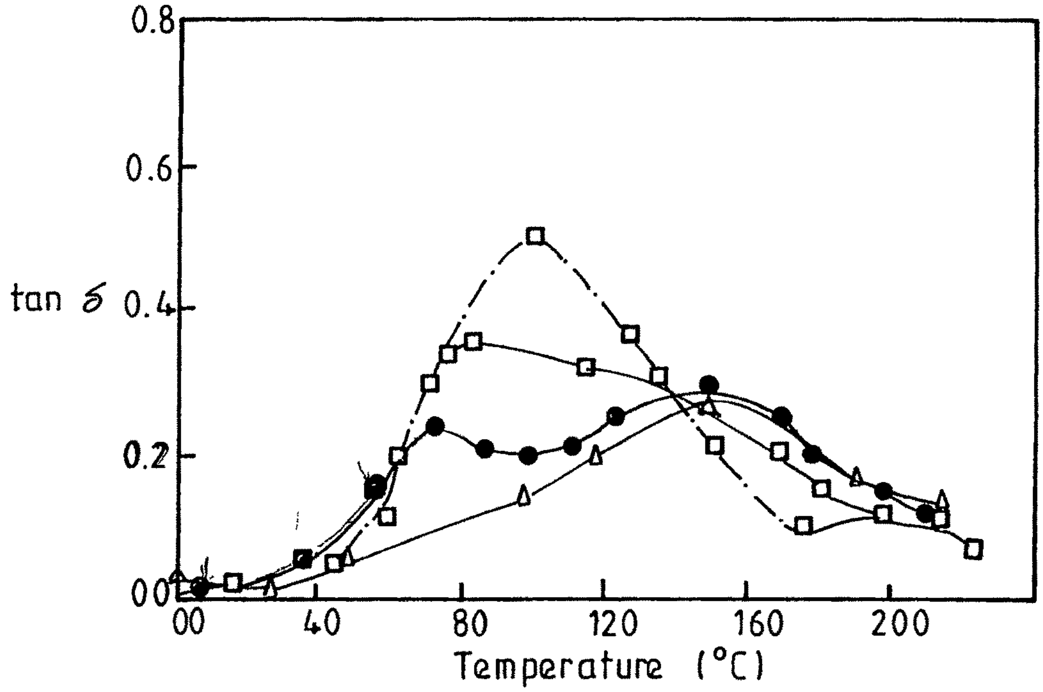

Fig 4.15 tan δ - temperature plots for IPE(□) and PUR92(2.0)/IPE IPNs containing _60%(Δ), 50%(□) and 40%(●) PUR by weight

in percentage of PUR are concerned However, marked difference was observed in tan δ behavior of 40.60 and 20.80 samples

The IPN containing 40% PUR60 at NCO/OH ratio 1.2 (Fig 4.5) showed two separate peaks representing each network, while the IPN containing same amount of PUR92 and having same NCO/OH ratio (Fig 4 13) showed three peaks situated at around 50, 90 and 145°C. These peaks correspond to PUR rich phase, polystyrene (homopolymer and crosslinked) phase and polyester phase respectively, which are more or less superimposed over one another. This is because in case of PUR92 compared to PUR60, higher value of OH causes high crosslinks of PUR network which minimise compatibility with polystyrene part of polyester For the same reason, IPN containing 20% PUR92 (20 80) also showed three different peaks at 59°C (as shoulder), 90°C and 155°C. It is also observed that the transition temperature associated with PUR phase of this IPN is shifted to lower temperature (50°C) compared to that of IPN based on PUR60 of the same composition which is observed at around 80°C This fact is also because of the above mentioned reason. These results indicate that, by increasing the hydroxyl number and decreasing the chain length of polyols, curing reaction of PUR is accelerated and less time would be available for diffusion, which lead to phase separation, when level of crosslinking is not very high (1.2)

The effect of NCO/OH ratio of PUR92 on damping behavior as a function of temperature for various IPNs varying in their compositions are illustrated in Fig 4.14 (NCO/OH=1 5) and Fig 4.15 (NCO/OH=2 0) The values of tan δ_{max}, half peak width (HPW) and glass transition temperature are given in Table 4 5

The glass transition temperatures shifted inward, indicating less phase separation on these samples The values of tan δ_{max} were suppressed and HPW were increased with increasing crosslink density Thus it appears that, incorporation of more isocyanate groups in PUR phase has a positive effect on interpenetration through the reaction of OH groups of polyester with NCO groups.

The behavior of damping factor tan δ as a function of temperature for individual composition at three different NCO/OH ratios are depicted in Fig 4 16A to 4 16F. It can be seen from Fig 4 16B to 4 16D that, with increase in cross link density, tan δ_{max} decreased and glass transitions of PUR phase shifted to higher temperatures It was also observed that transition associated with polyester phase gradually disappears with increase in NCO/OH ratio This shows that, when polyester content is limited up to 50%, PUR network increases and the rigid phase becomes more dispersed In 60.40 and 50·50 IPNs, only broad single tan δ peaks are observed, suggesting less phase separation. This may be due to

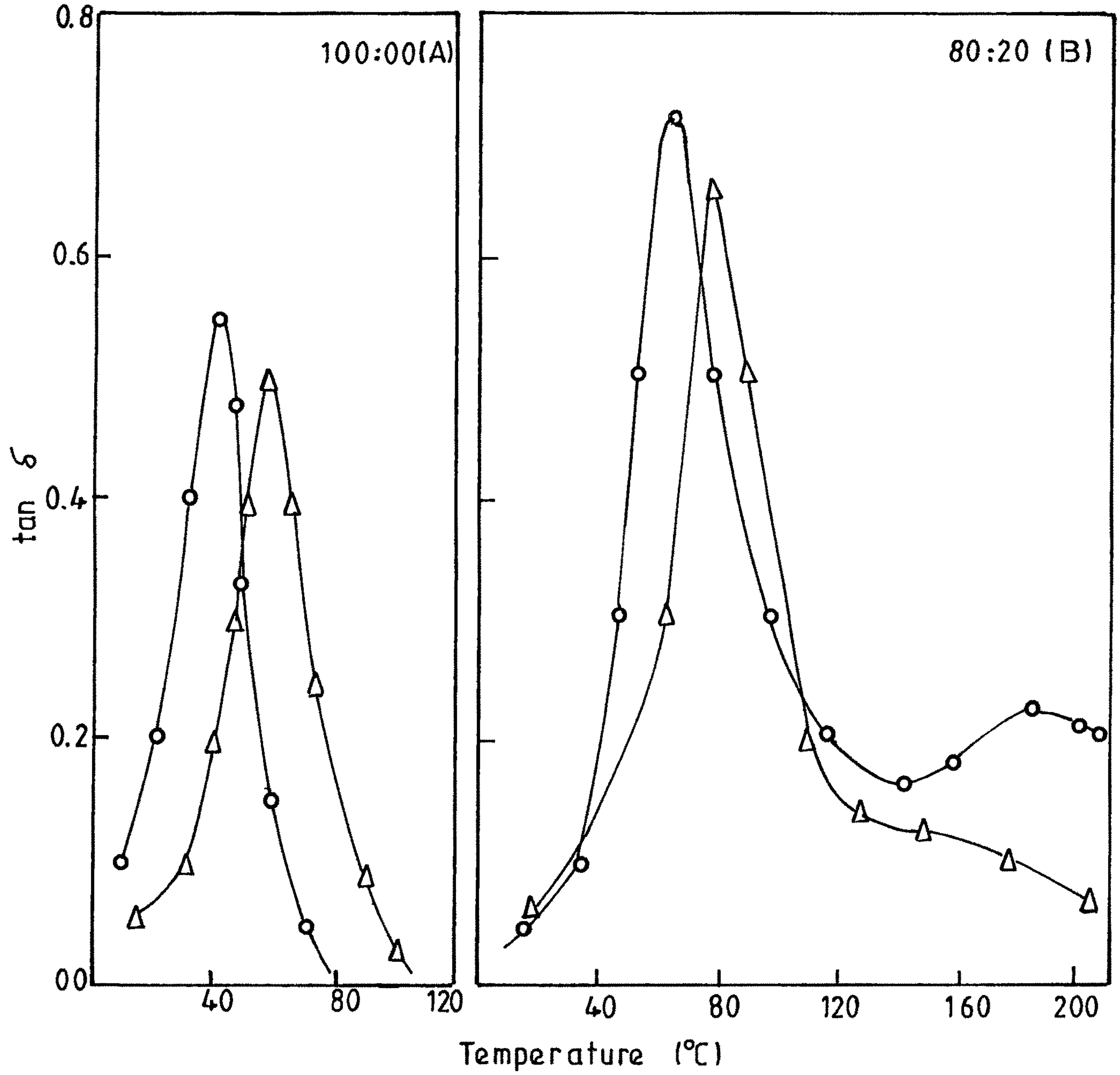

Fig 4.16(A,B) tan δ - temperature plots of PUR92/IPE system for 100 00 (A) and 80 20 (B) samples at various NCO/OH ratios of 1 2 (O) and 1 5 (Δ)

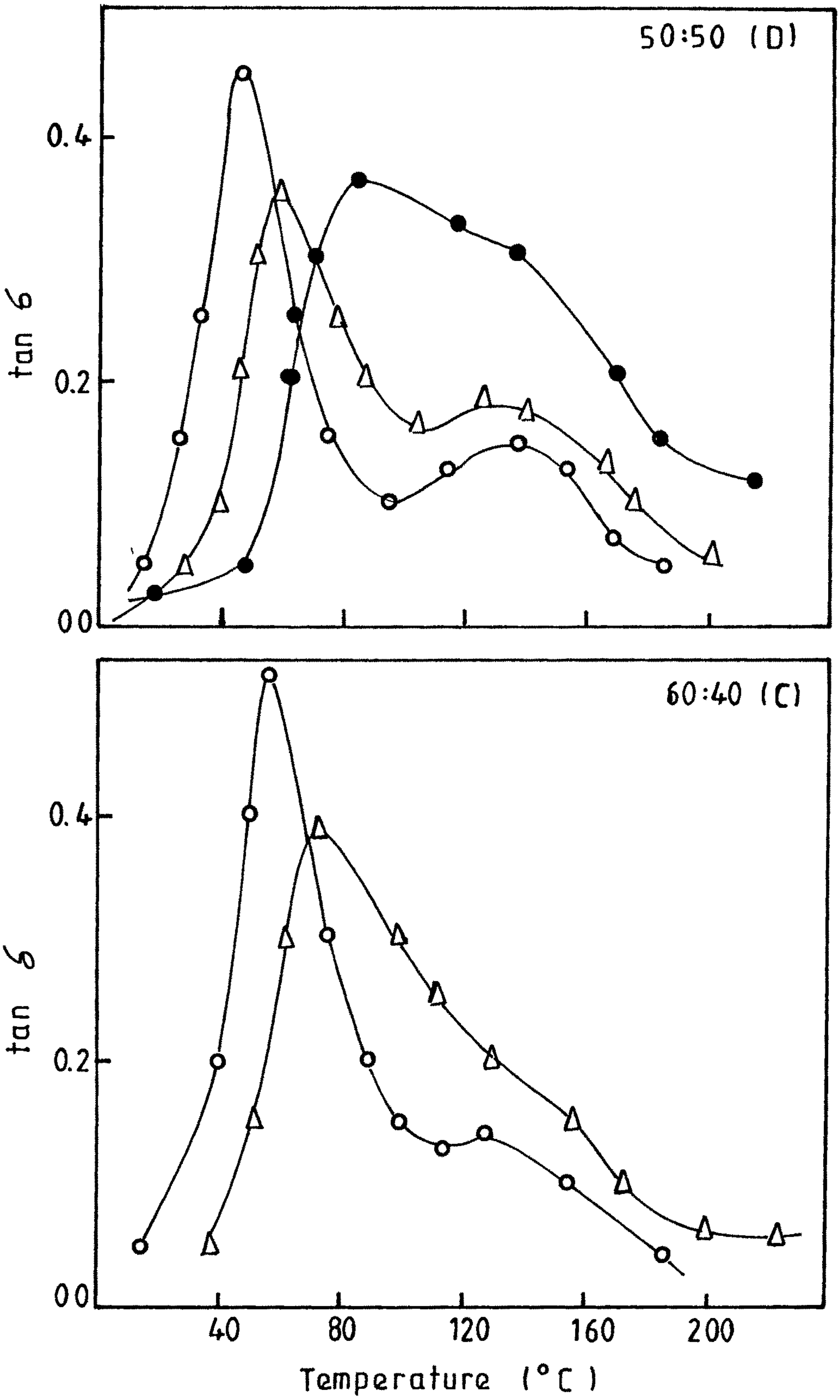

Fig 4.16(C,D) . tan δ-temperature plots of PUR92/IPE system for 60 40 (C) and 50.50 (D) samples at various NCO/OH ratios of 1.2 (O), 1.5 (Δ) and 2.0 (●)

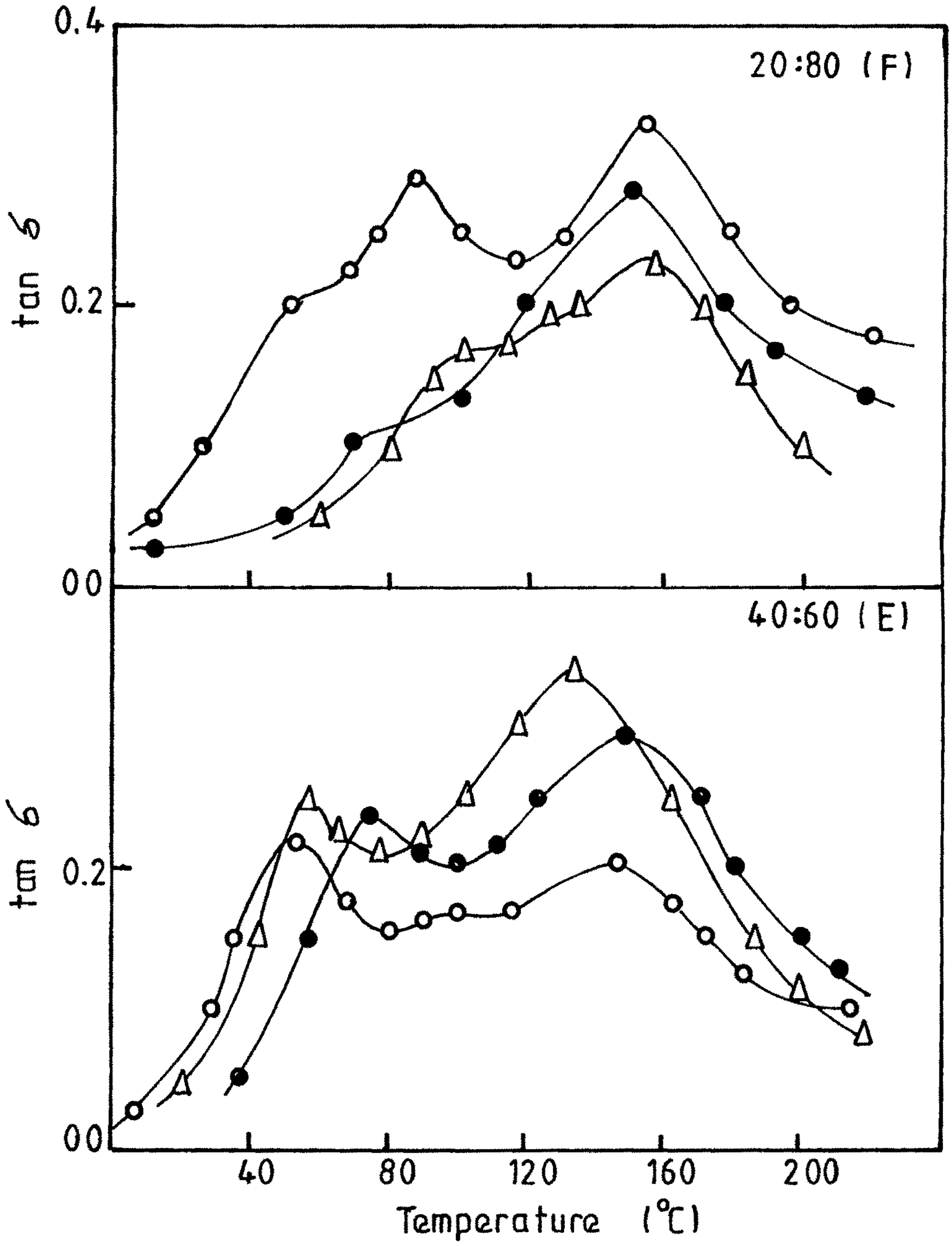

Fig 4.16(E,F) · tan δ -temperature plots of PUR92/IPE system for 40 60 (E) and 20 80 (F) samples at various NCO/OH ratios of 1.2 (O), 1 5 (Δ) and 2 0 (●)

Table 4.5 : Values of T_g, tan δ_{max} and half peak width (HPW) for various IPNs based on IPE and PUR92

PUR:IPE	NCO/OH = 1.2				NCO/OH = 1.5				NCO/OH = 2.0			
	T_g °C		tan δ_{max}	HPW	T_g °C		tan δ_{max}	HPW	T_g °C		tan δ_{max}	HPW
	T_{g1}	T_{g2}			T_{g1}	T_{g2}			T_{g1}	T_{g2}		
100:00	40	-	0.55	28	58	-	0.50	28	-	-	-	-
80:20	65	186	0.71	42 (100)	78	-	0.65	38	-	-	-	-
60:40	57	27	0.51	39 (86)	71	-	0.39	76	-	-	-	-
50:50	47	137	0.45	36 (74)	58.5	125	0.35	50	82.2	-	0.36	112
40:60	53.5	147	0.204	60 (120)	57.5	133	0.34	36 (106)	74	148	0.29	50 (108)
20:80	87.5	154	0.33	- (100)	-	158	0.235	106	-	150	0.28	110
00:100	98.9	198	0.58	84	98.9	198	0.58	84	98.9	198	0.58	84

Values in parenthesis show the HPW values corresponding to the polyester transition increase in crosslinking, additional crosslinks through allophanate linkages and enhanced H-bonding at higher NCO/OH ratio[31] and interaction of terminal OH groups with NCO groups

The damping characteristics of IPNs containing 20% PUR (20 80) and 40% PUR (40.60) were found to be different than those having higher percentage of PUR As can be seen from Fig. 4.16E (40·60 IPN), the peak height of transition of rubbery phase was greatly suppressed (tan δ_{max} 0 7 to tan δ_{max} 0.25) (Table 4.5) compared to that in polyester phase. This indicates that polyester network in this present IPN may be regarded as continuous phase and PUR as dispersed phase consisting of interconnected microgels of various sizes and representing the heterogeneity of the materials This is further supported by scanning electron microscopy which is discussed later. From the above behavior, it seems that phase inversion takes place at this composition.

The damping behavior of 20·80 IPN (Fig 4.16F) is entirely reverse as that of 80:20 IPN (Fig. 4 16B). In the latter case transition associated with polyester gradually decreases, while in former system transition due to PUR phase disappears and also shifts to lower temperature as isocyanate content (crosslink density) increases. In case of 80.20 IPN, the two phases become compatible due to which the rigidity of flexible PUR network increases and shows shifts in T_g towards high temperature This is also evident from high E^{I} values of this IPN in rubbery region (Fig 4 19) When the composition is reversed (20.80 IPN), the more amount of polyester provides more number of OH groups and particularly at higher NCO/OH ratio, NCO groups are free to interact with these OH groups resulting into compatibility of two phases. However, in this case increase in compatibility increases flexibility of polyester which is reflected by decrease in T_g of polyester and disappearance of PUR transition. From the above results it follows that at NCO/OH ratio 1.5 and 2 0, when amount of polyester is increased beyond 60%, phase inversion takes place and polyester becomes the continuous phase

Dynamic Loss Modulus (E^{II})

The loss modulus vs temperature plots of PUR92(1 2)/IPE, IPNs were also plotted to see the effect of change in composition The plots are shown in Fig 4 17. As seen from the figure, E^{II}_{max} appeared at almost the same temperature as that of pure PUR-92 in IPNs having composition 60·40 and 50:50. The above fact indicates that, the system is considered to be composed of a continuous phase of PUR and dispersed phase of IPE. However, samples 80 20, 40.60 and 20:80 showed relatively broad transitions and E^{II}_{max} shifted to higher temperatures. The influence of NCO/OH ratio on loss modulus is presented in Fig 4.18A to 4 18F for various compositions. As the tan δ and loss modulus carry the same meaning, the effect of composition and crosslink density on loss modulus behavior can be explained on the same basis as that of tan δ - temperature behavior Thus explanation given for tan δ - temperature

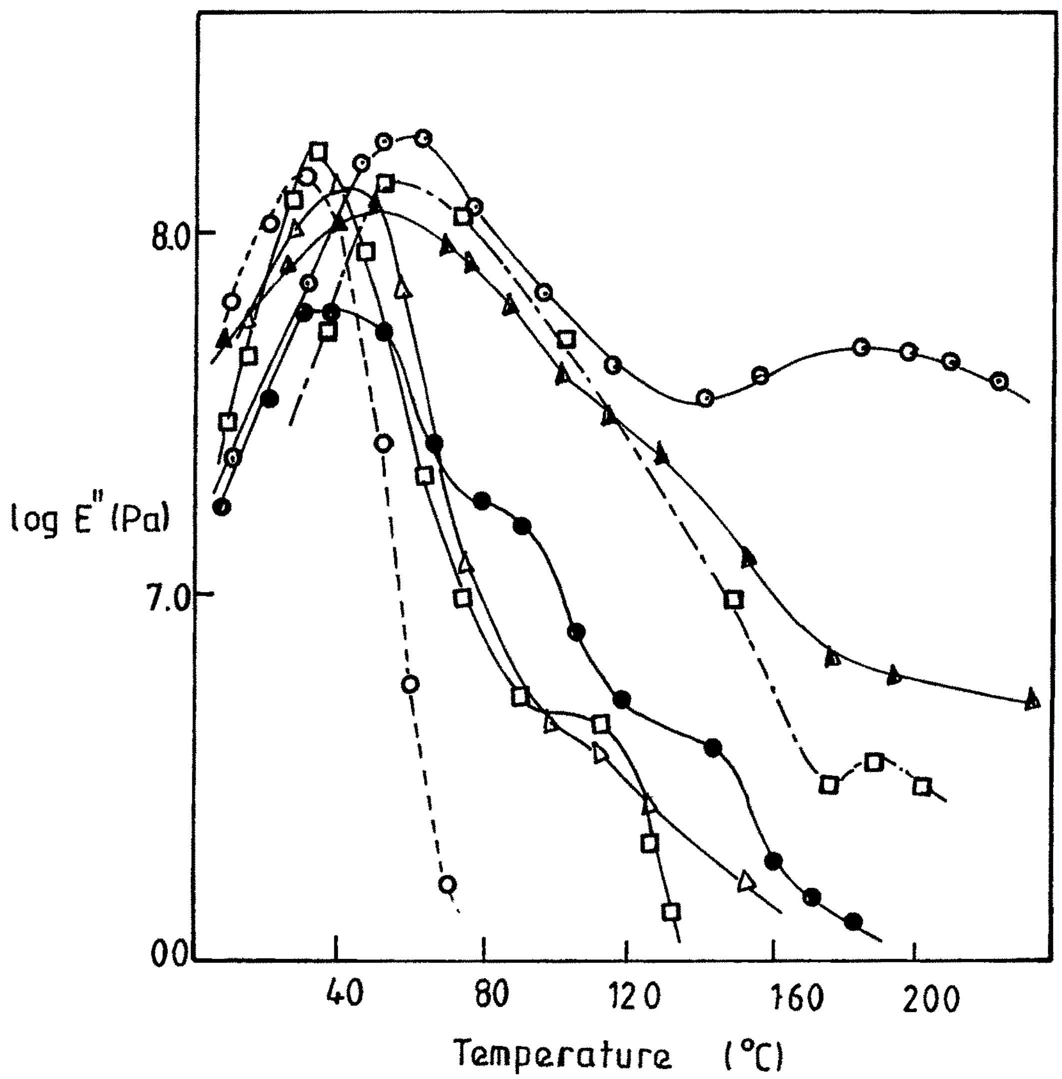

Fig 4.17 . log E'' - temperature plots for PUR92(1 2)/IPE IPNs containing 100%(O), 80%(Θ), 60%(Δ), 50%(□), 40%(●), 20%(▲) and 00%(□) PUR by weight

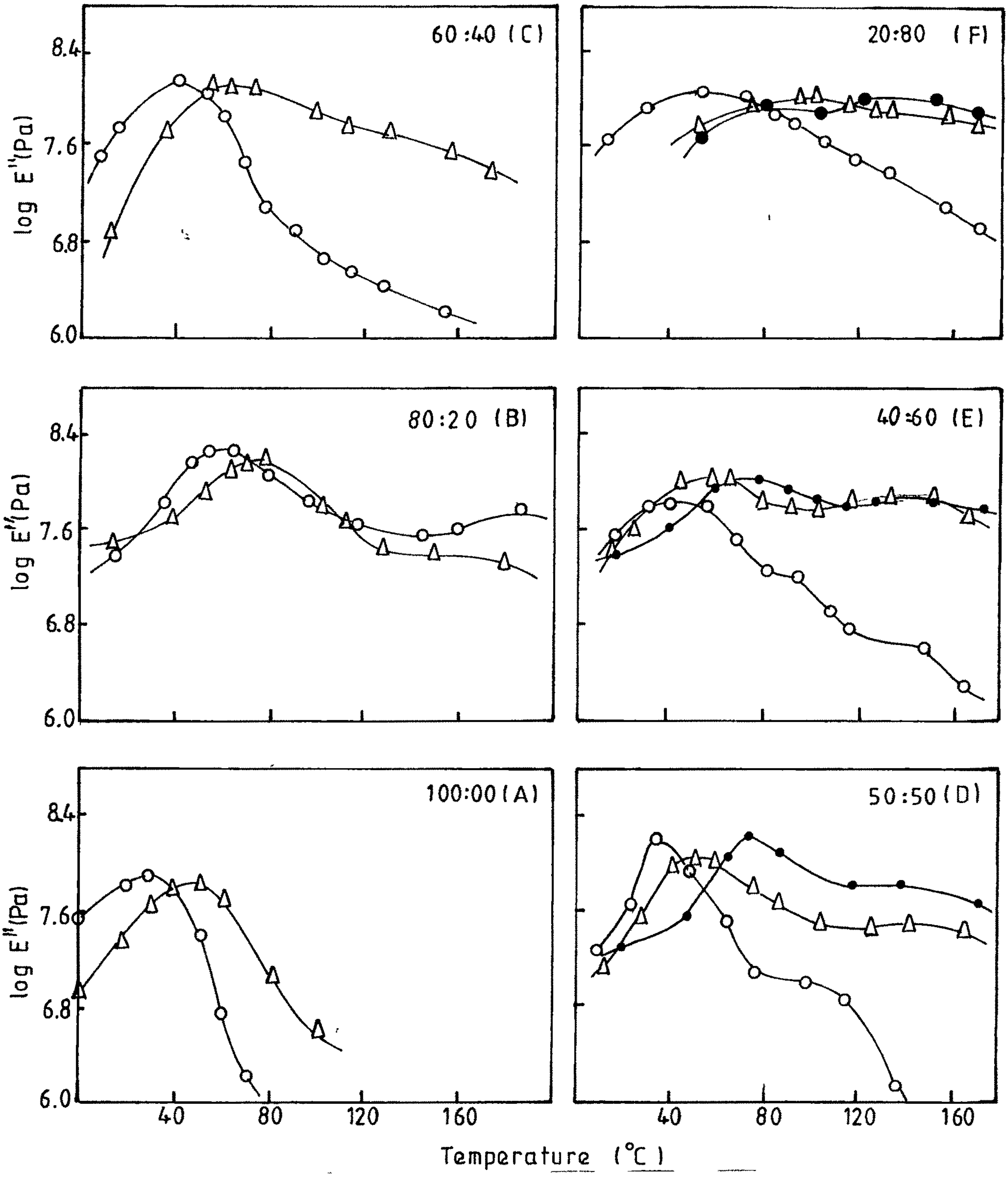

Fig 4.18(A-F) log E'' - temperature plots of PUR92/IPE IPNs ontaining100%(A), 80%(B),60%(C),50%(D),40%(E) and 20%(F) PUR by weight at various NCO/OH ratios of 1 2 (O), 1 5 (Δ) and 2 0 (●)

characteristics of IPNs by varying composition and crosslink density also hold true for loss modulus - temperature behavior of these IPNs

It is interesting to note that unlike IPNs based on PUR60 (Fig. 4 10A to 4.10F), PUR92/IPE IPNs at NCO/OH ratio 1 5 and 2 0 show broadening of loss modulus peak for almost all compositions. Thus introduction of shorter chain length and incorporation of more hydroxyl groups in polyurethane moiety has widened the possibility of variation of composition in IPNs for their use as vibration damping materials

Dynamic Storage Modulus (E^{I})

The effect of concentration of PUR92 and IPE at NCO/OH ratio of 1.2 on dynamic storage modulus of IPNs is shown in Fig 4.19. Although all IPNs showed broad transitions compared to that of pure PUR, 80 20 and 20:80 compositions showed exceptionally broad transitions This suggests enhanced mixing of the constituted polymers at these compositions

It can be seen from the storage modulus curves of IPNs differing in their compositions at various level of crosslinking that (Fig 4 20A to 4 20 F), for all compositions (except 80:20), higher temperature transitions were present as shoulders at low level of crosslinking But when NCO/OH ratio was increased to 1 5 and 2.0, there was a dramatic change in the behavior of storage modulus as can be seen from the following few observations. The high temperature transitions almost disappeared and the plateau region of E^{I} not only broadened but also maintained to almost constant value in temperature ranges below and above T_g. Moreover, when NCO/OH ratio was 1.2 the magnitude of E^{I} decreased by two decade while for higher NCO/OH ratios, it decreased only by less than one decade over the temperature range studied i e from -120 to 250°C. These observations could be due to the combined effect of (i) increase in concentration of hard segment of PUR and enhanced H-bonding, (ii) high degree of interpenetration of both constituents at higher crosslink density and (iii) possibility of reaction between terminal OH groups of polyester and NCO groups of PUR.

4.3.1 COMPOSITE MODELS FOR DMA

The variation of dynamic mechanical modulus with composition in polyblends have been represented through several mathematical relations One of the simplest among them is the logarithmic additivity rule of mixtures[32,33] i e

$$\log E^{I} = \phi_1 \log E_1^{I} + \phi_2 \log E_2^{I}$$

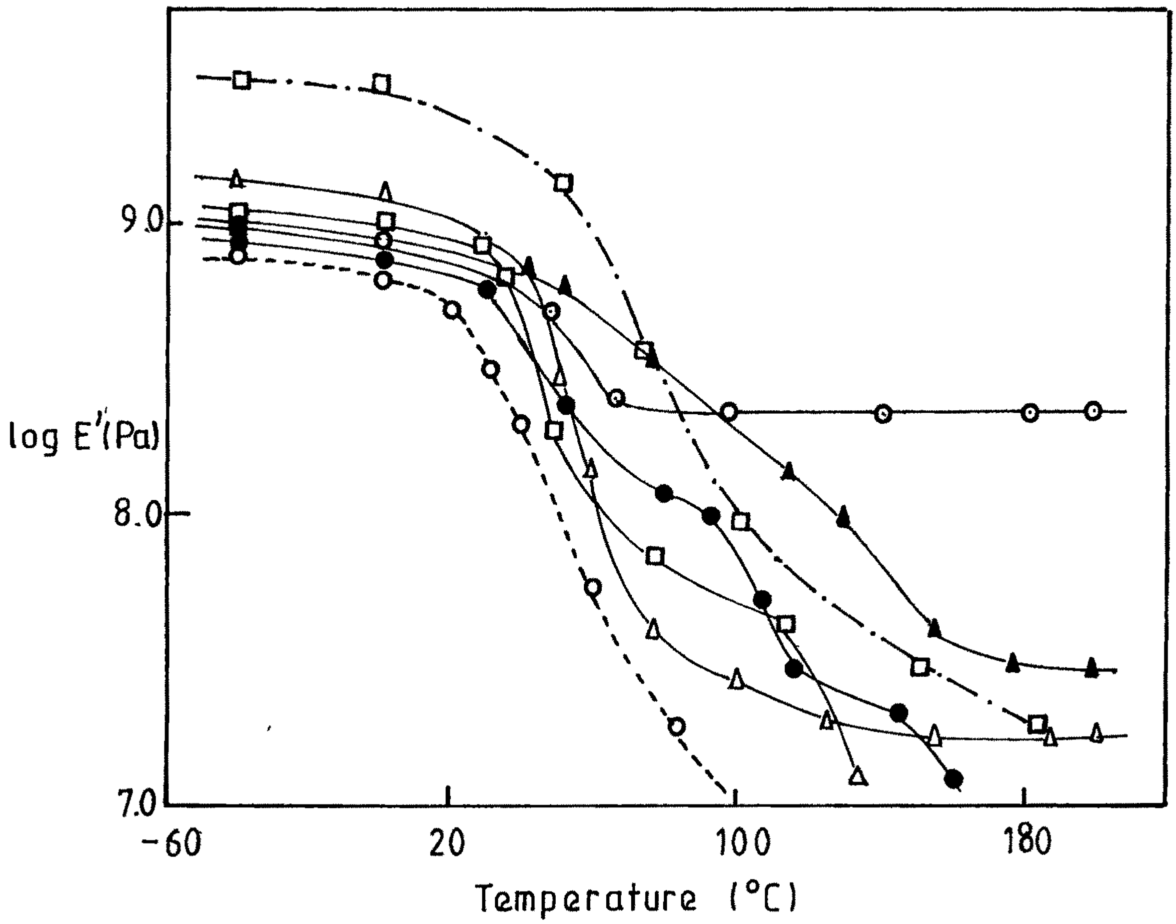

Fig 4.19 log E^{l} - temperature plots of PUR92(1 2)/IPE IPNs contaımng 100%(O), 80%(ʘ), 60%(Δ),50%(□), 40%(●), 20%(▲) and 00%(□) PUR by weight

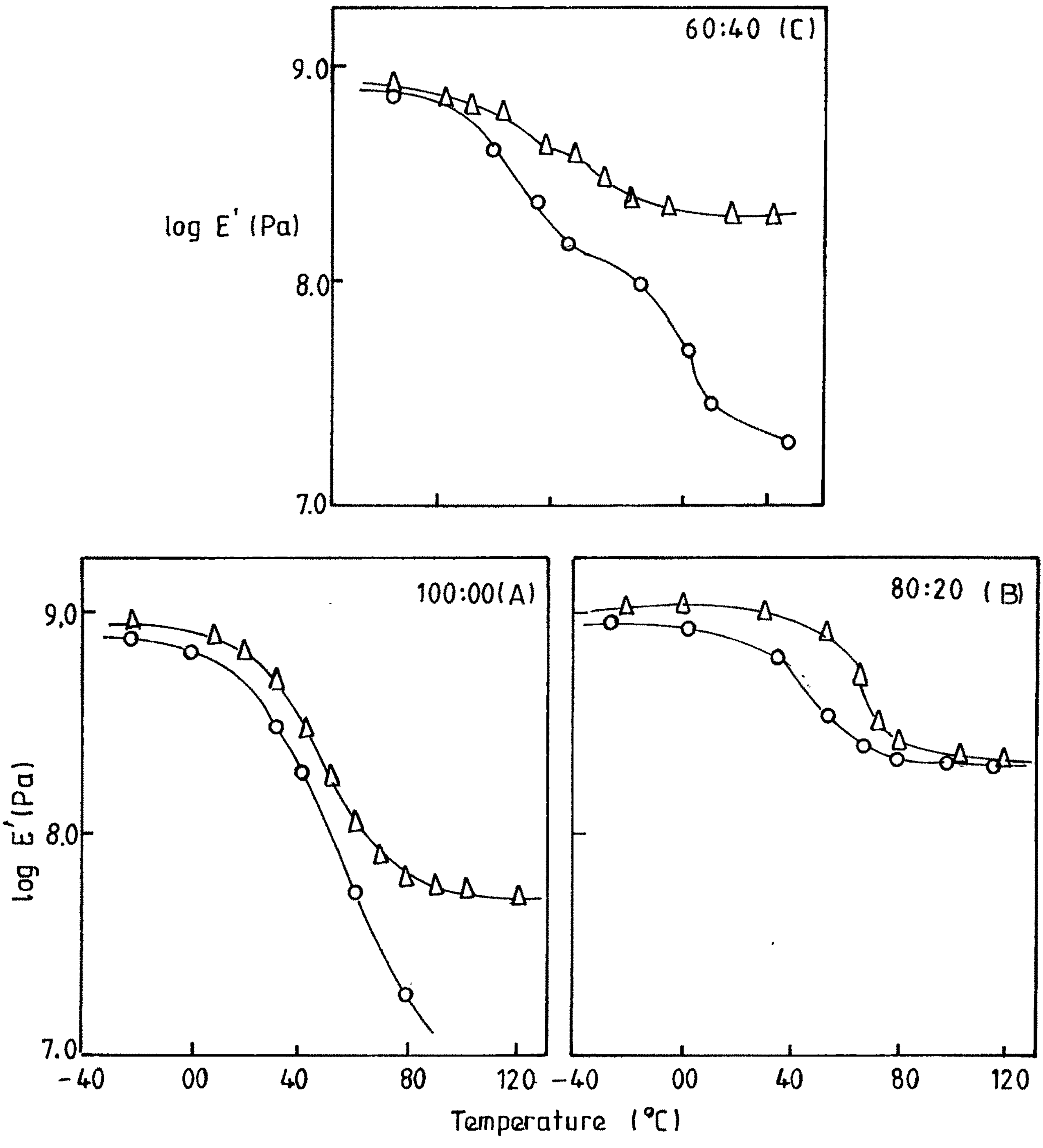

Fig 4.20(A-C) : log E' - temperature plots of PUR92/IPE IPNs containing 100%(A), 80%(B) and 60%(C) PUR by weight at various NCO/OH ratios of 1 2 (O), 1 5 (Δ) and 2.0 (●)

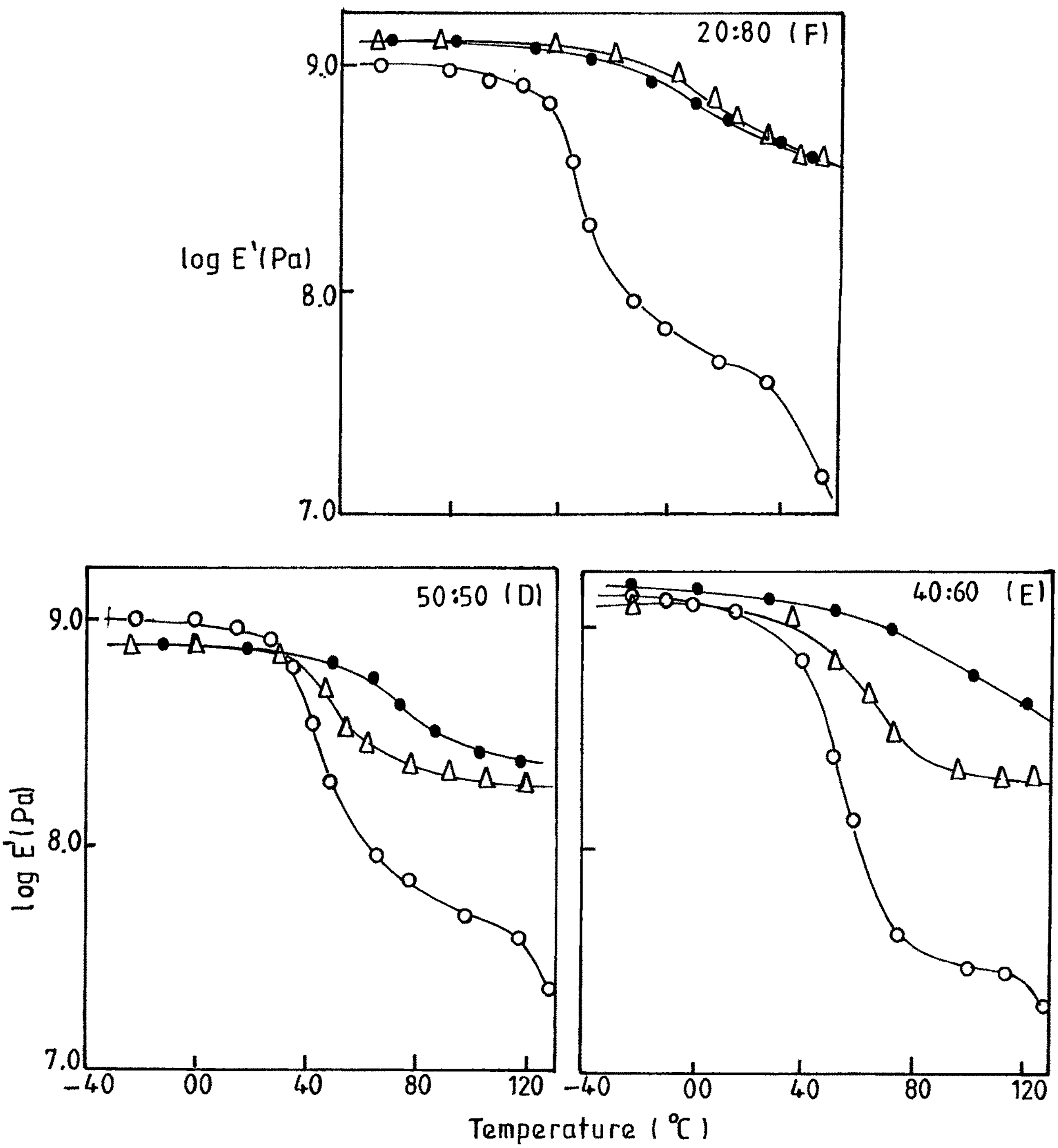

Fig 4.20(D-F) . log E^{I} - temperature plots of PUR92/IPE IPNs containing50%(D),40%(E) and 20%(F) PUR by weight at various NCO/OH ratios of 1.2 (O), 1 5 (Δ) and 2 0 (●)

where ϕ_1 and ϕ_2 are the volume fraction of component 1 and 2 respectively and E_1^{I} and E_2^{I} are the storage modulus of each component

If the glassy component, polyester is the continuous phase, a plot of storage modulus vs volume fraction at a fixed temperature show positive deviation from the logarithmic additivity rule, based on Takayanagi's parallel model[34] i e

$$E^{I} = (1-\phi_2) E_1^{I} + \phi_2 E_2^{I}$$

If the elastomeric component, polyurethane is the continuous phase, a similar plot would show a negative deviation from logarithmic addtivity rule according to Takayanagi's series model[34] i.e.

$$E^{I} = \left[(1-\phi_2)/E_1^{I} + \phi_2/E_2^{I}\right]^{-1}$$

When both the components form a two-continuous phase, Davie's model[35] can be used to calculate storage modulus as a function of sample volume fraction, i e

$$E^{I\,1/5} = (1-\phi_2) E_1^{I\,1/5} + \phi_2 E_2^{I\,1/5}$$

Fig 4.21A and 4 21B show such plots of PUR60(1 2)/IPE and PUR60(1.5)/IPE IPNs at 30°C Line 1 is the modulus - composition relation according to linear logarithmic rule, and line 2 is according to Davie's equation. The experimental points are located between these two lines (except 40:60 sample), which implies that the components in the IPNs are mixed extensively, and show dual phase continuity of both the components irrespective of the NCO/OH ratio of PUR

The modulus-temperature plots of PUR92(1.2)/IPE and PUR92(1 5)/IPE using various theories with the experimental results are shown in Fig 4.22A and 4 22B respectively. When NCO/OH ratio is 1.2, compositions 60·40 and 50.50 either show complete mixing or co-continuity of the two phases But polyester is not forming the continuous phase even when its concentration is high in the IPNs, which is clear from their experimental values of modulus lying on line 4 (Takayanagi's series model). In 20·80 sample at both NCO/OH ratios of 1.2 and 1.5 the experimental values of modulus lie on line 4 (Takayanagi's series model), which indicates that PUR is the continuous phase. However the SEM microgra showed a single phase morphology for this sample which could not be explained by this

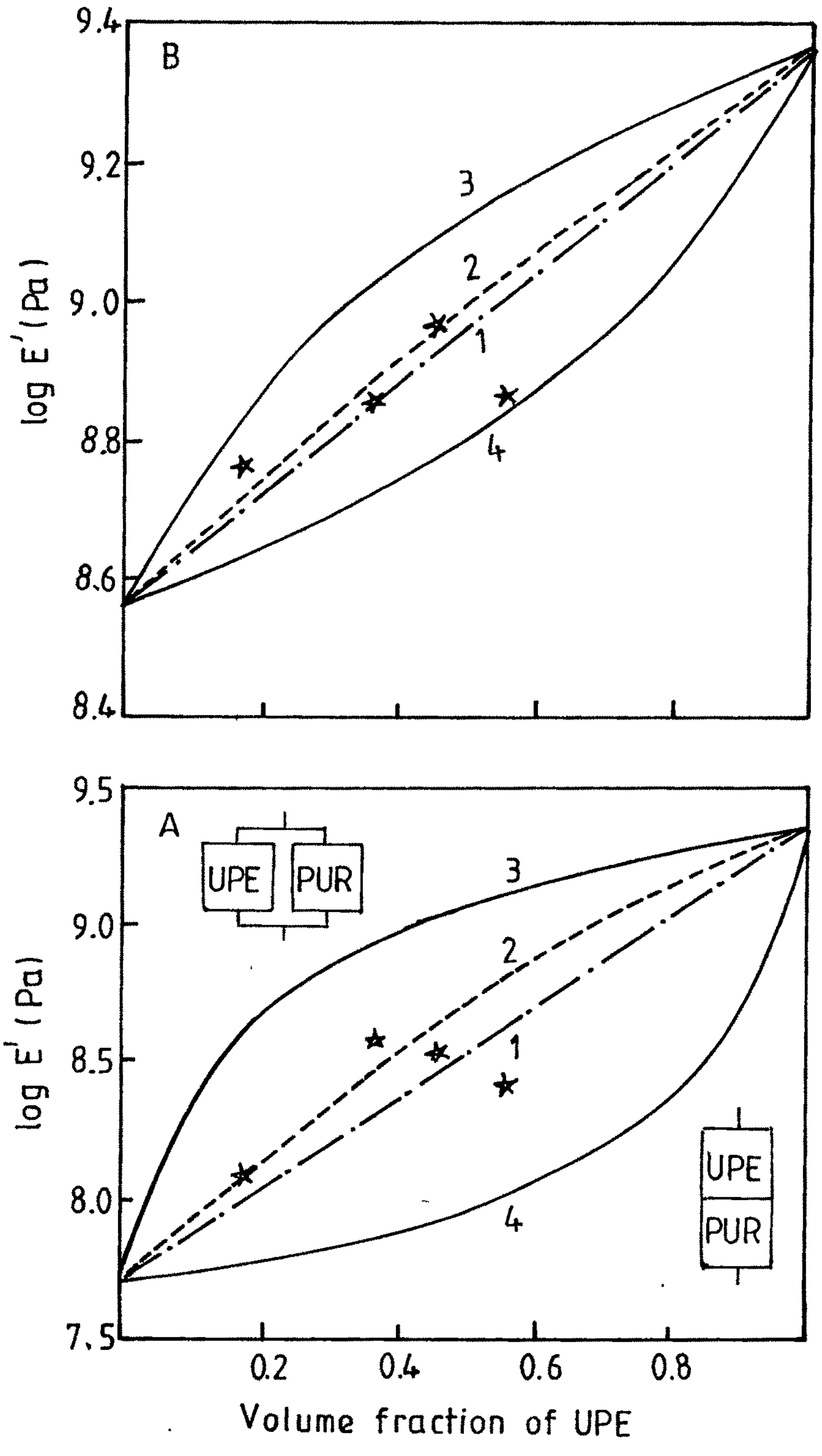

Fig 4.21 log E' - volume fraction(δ) of IPE plots of PUR60(1 2)/IPE (A) and PUR60(1 5)/IPE (B) IPNs at 30°C, Additivity rule(line 1), Davy's model (line 2), Takayanagi's series model (line 3) and Takayanagi's parallel model(line 4) Experimental points (✳)

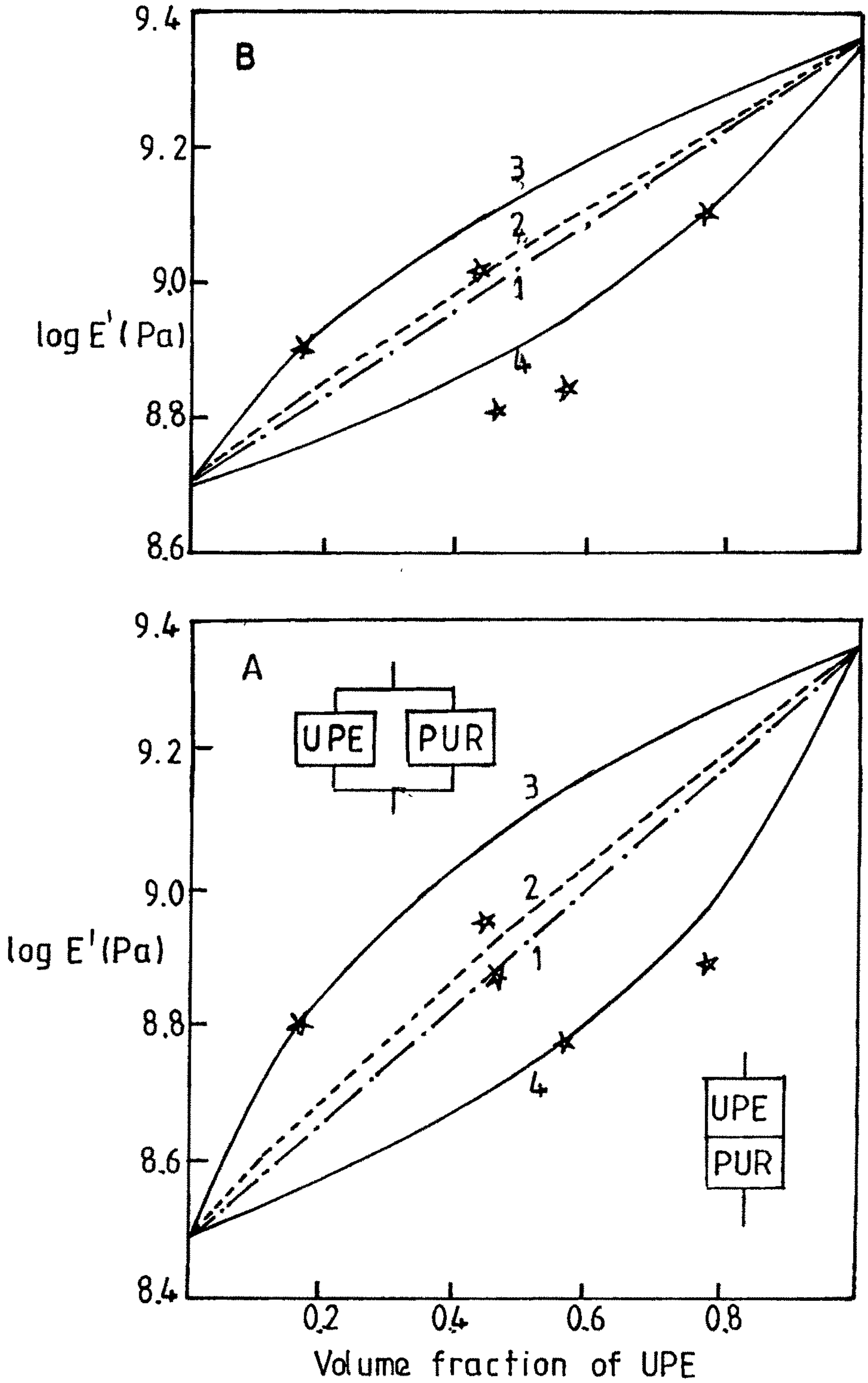

Fig 4.22 : log E^I - volume fraction (δ) of IPE plots of PUR92(1 2)/IPE (A) and PUR92(1.5)/IPE (B) IPNs at 30°C, Additivity rule(line 1), Davy's model (line 2), Takayanagi's series model (line 3) and Takayanagi's parallel model(line 4) Experimental points (✳)

model The IPN having 50 50 composition at NCO/OH ratio of 1.5 also show similar discrepancy between micrographs and models as that of 20·80 sample

As discussed above, the SEM micrographs agree with the models in general, although morphology of some samples predicted based on these models were not identified clearly in the micrographs

4.4 SCANNING ELECTRON MICROSCOPY (SEM)

Direct visual confirmation of the presence of two phases has been used more often than any other method as a preliminary indication of the degree of miscibility in polymer-polymer blend systems The technique of Scanning electron microscopy (SEM) has found a niche in phase studies Morphology and microstructure of polyblends and IPNs can be investigated directly by means of this technique.

Experimental technique

The phase composition of some of the IPNs are determined using a S-4000 series scanning electron microscope (Hitachi co ltd , Japan) with an acceleration voltage of 10 kV and a working distance of 15mm First, the cross section of the films were prepared by freeze fracturing them in liquid nitrogen and osmium tetroxide,OsO_4 coating was carried out using an APC 120 plazma multi coater unit (Meiwa Shoji co ltd., Japan) before scanning it using SEM. Therefore in analysing the micrographs of IPNs, dark areas (OsO_4 stained) represent the urethane phase and the bright areas represent the polyester phase, in general

Results and Discussion

The morphologies of PUR60(1 2)/IPE, IPNs at different compositions are represented in Fig 4.23 (A-D) The studies clearly show variations in morphology in all the four stages. It is evident from micrograph 4.23A that, polyester up to a concentration of 20 wt % (80 20), shows almost single phase morphology At higher NCO/OH ratio of 1 5 also this composition exhibit a single phase morphology as can be seen from the micrograph (Fig. 4.24A) The difference in morphology between 80 20 and 60 40 composition is apparent from their respective micrographs. In the case of 60 40 composition having NCO/OH ratio 1.2 (Fig 4 23B), the IPNs become macroheterogenous and tiny globules of polyester of about (1-1 3 μm) diameter appear largely interlinked with one another and fairly uniformly dispersed in polyurethane matrix, effectively forming a co-continuous phase morphology Similar trend was observed for 50:50 sample having NCO/OH ratio 1.5 (domain size 1-1 5 μm, Fig 4 24B) .

When the IPE content is increased to 60% (40.60) at NCO/OH ratio 1 2, phase transformation takes place and one can see several large PUR domains of about 40-80 μm diameter dispersed in PE matrix (Fig 4.23C) In the same sample, when the NCO/OH ratio is increased to 1.5 (Fig. 4 24C), the size of the PUR domains did not change significantly (37-80 μm), the dispersed sub domains of IPE with in the large PUR domains were observed It seems that, the sub domains captured within the PUR domain are the polymerization product of residual styrene monomer which cannot diffuse out of the PUR domain because of the high medium viscosity[30,31] Thus the complex morphology of 40.60 sample at NCO/OH ratio 1.5 is favourable for impact modification

As IPE content is further increased to 80% (20 80) at NCO/OH ratio 1 2, micrograph (Fig. 4.23D) showed a particular morphology where, both the phases assume total continuity with no resolved domain of either component This behavior would suggest that, the relative rates of polymerization of the two components would be almost same at this particular composition This fact is also reflected in the results of DMA and stress-strain behavior of this IPN.

Fig 4 25 (A-C) shows SEM photographs of PUR92(1 2)/IPE system There seems to be hardly any difference in the morphology when these samples are compared with that of IPNs based on R60 having NCO/OH ratio 1 2 and 1 5 at various compositions In the case of PUR92(1 2)/IPE IPNs containing 80% PUR (80·20) having NCO/OH ratio 1 2 (Fig 4 25A), the continuous phase is relatively bright indicating a high level of polyester. There are also some dispersed domains of PUR, of about 5 μm diameter (not clearly visible in the micrograph) formed in the sample. Similar morphology is shown by 80 20 sample at higher NCO/OH ratio of 1.5 also (Fig 4 26A)

With increase in IPE content to 40% (60:40) at NCO/OH ratio 1.2 (Fig 4 25B), the IPN became macroheterogenous and showed a morphology similar to 60 40 sample of PUR60(1.2)/IPE system, that is, the globules (~1.0 μm diameter) of IPE phase seem to be interconnected in PUR matrix Here it is very difficult to identify the continuous and dispersed phase and hence can be viewed as co-continuous The 50·50 sample at NCO/OH ratio 1 5 and 2.0 (Fig 4 26B and 4 27A) show a similar morphology as that of 60:40 sample at NCO/OH ratio of 1.2 This shows that, 10% increase in IPE content as well as increase in crosslink density of PUR does not contribute significantly in controlling the morphology of these IPNs However the 50 50 sample with higher crosslink density (2 0) showed more miscibility compared to the one having NCO/OH ratio 1 5

With further increase in IPE content to 80% (20 80) at NCO/OH ratio of 1.2 (Fig 4.25C), the micrograph showed a river like pattern and produced a finer morphology with greater regularity The same composition at higher NCO/OH ratio of 1.5 and 2.0, show enhanced miscibility which is evident from the more homogenous arrangement of the two phases (Fig. 4.26C and Fig. 4 27C).

The sample with 60% IPE (40 60) at NCO/OH ratio of 2.0 (Fig. 4.27B) showed a similar behavior as that of 50.50 sample at the same crosslink density Unfortunately the SEM analysis of the 40 60 sample

Fig 4.23 : Scanning electron micrographs of PUR60(1.2)/IPE IPNs containing 80%(A), 60%(B), 40%(C) and 20%(D) PUR by weight

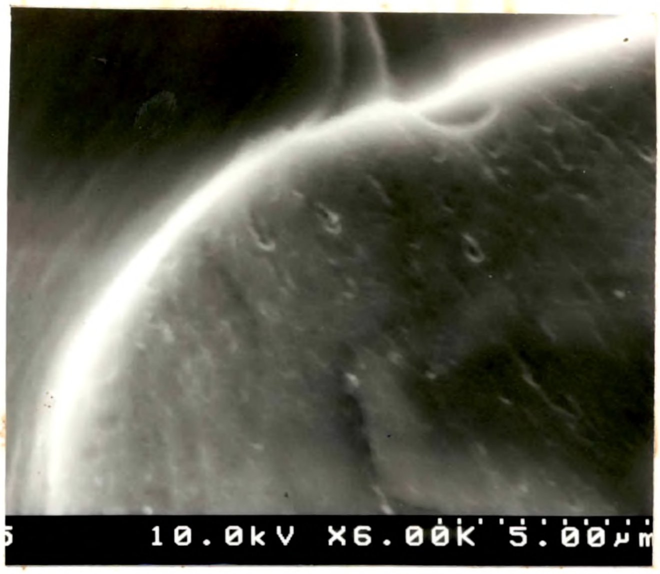
10.0kV X6.00K 5.00µm

A

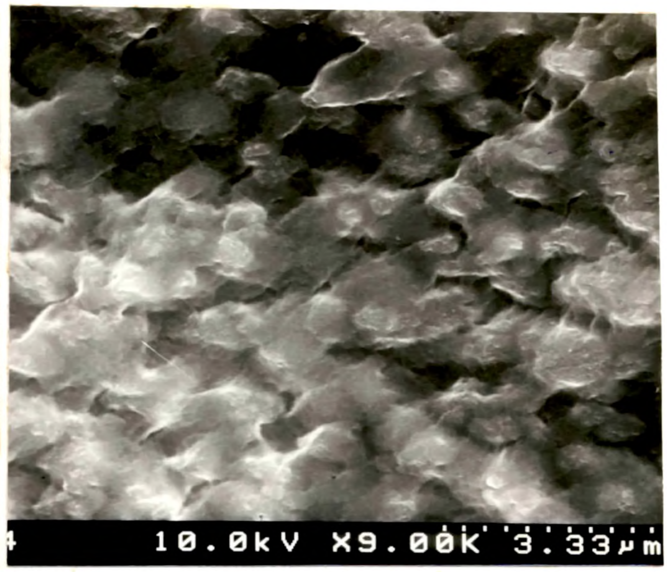
10.0kV X9.00K 3.33µm

B

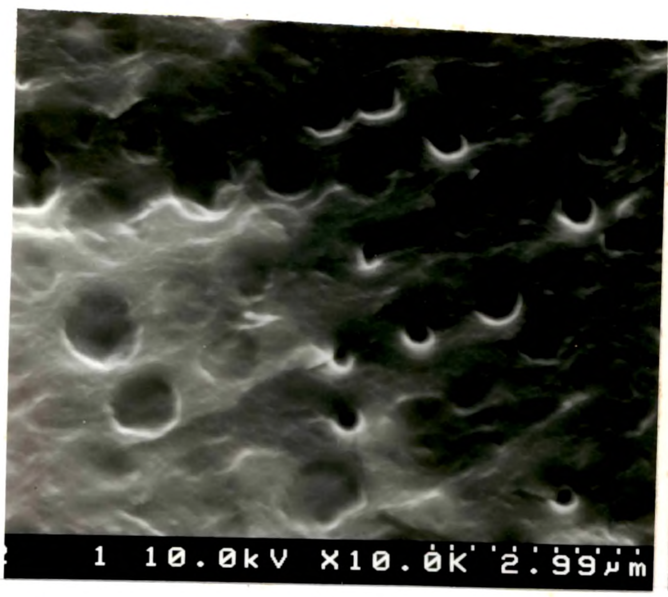
1 10.0kV X10.0K 2.99µm

C

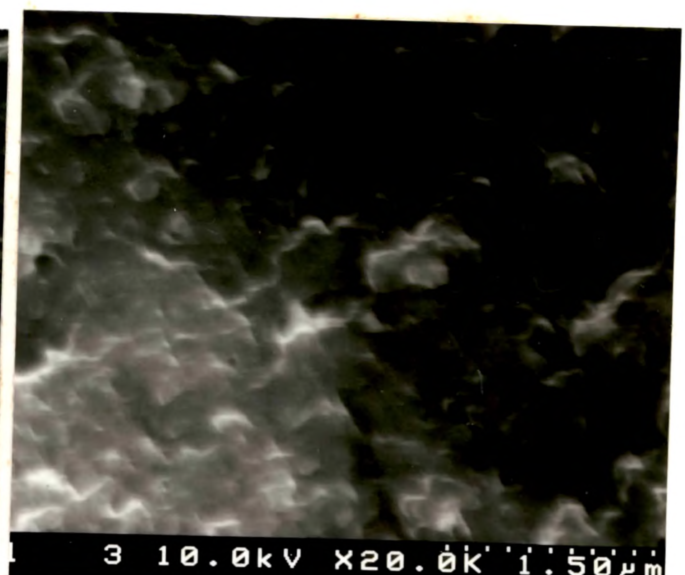
3 10.0kV X20.0K 1.50µm

D

Fig 4.24 : Scanning electron micrographs of PUR60(1.5)/IPE IPNs containing 80%(A), 50%(B), and 40%(C) PUR by weight

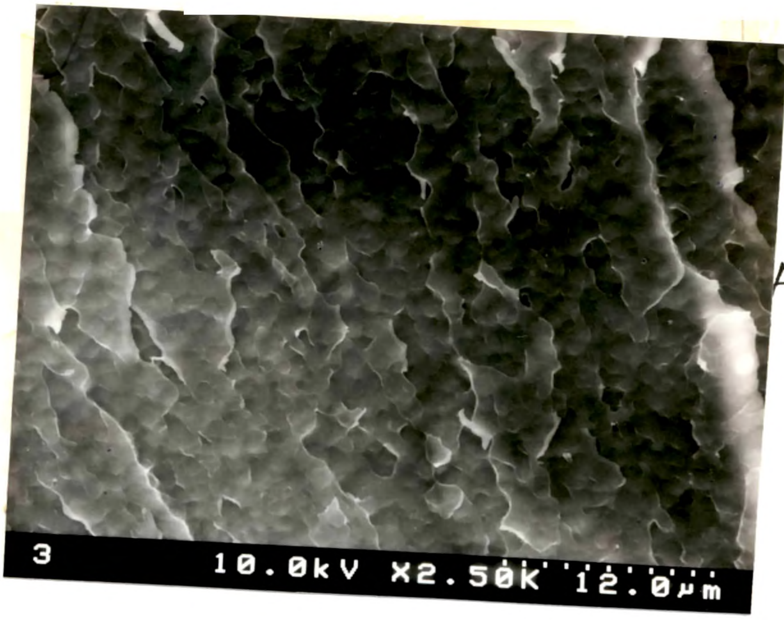

A

B

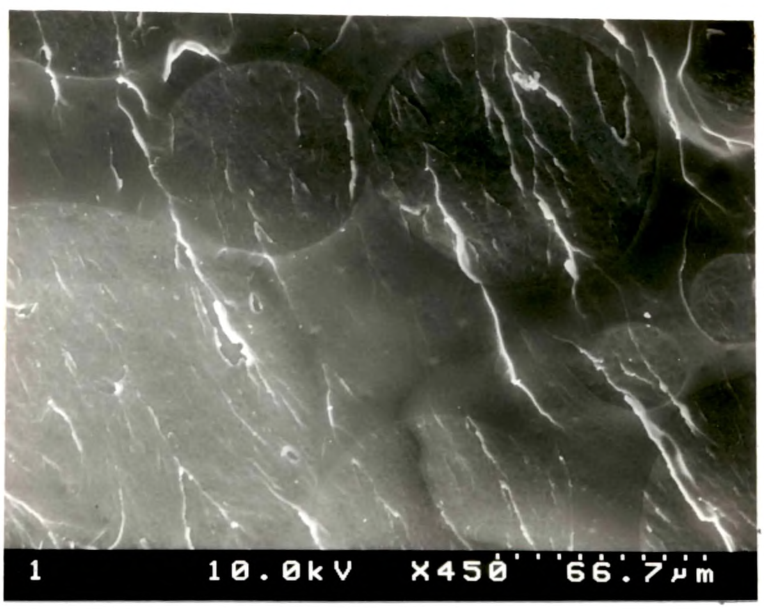

C

Fig 4.25 : Scanning electron micrographs of PUR92(1.2)/IPE IPNs containing 80%(A), 60%(B) and 20%(C) PUR by weight

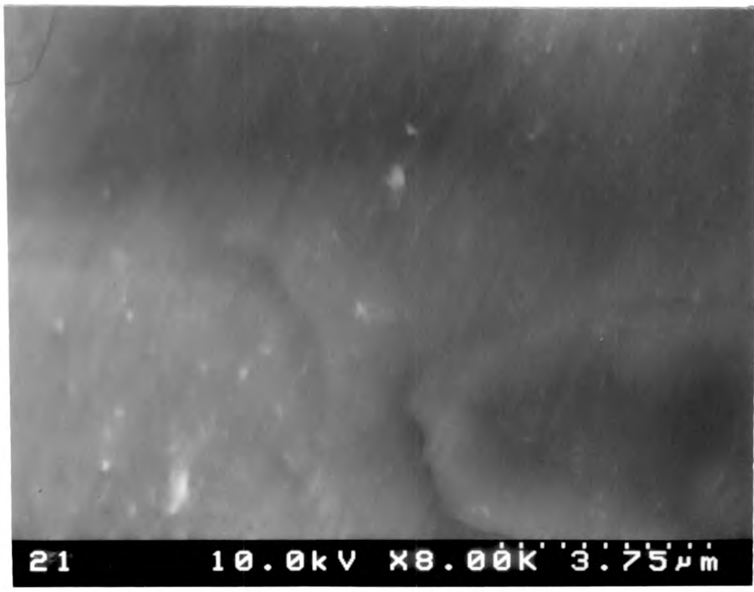
21 10.0kV X8.00K 3.75µm

A

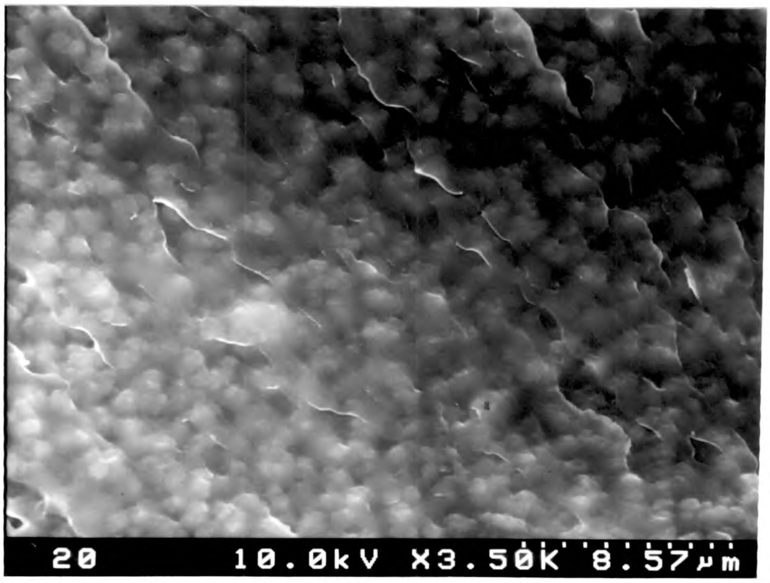
20 10.0kV X3.50K 8.57µm

B

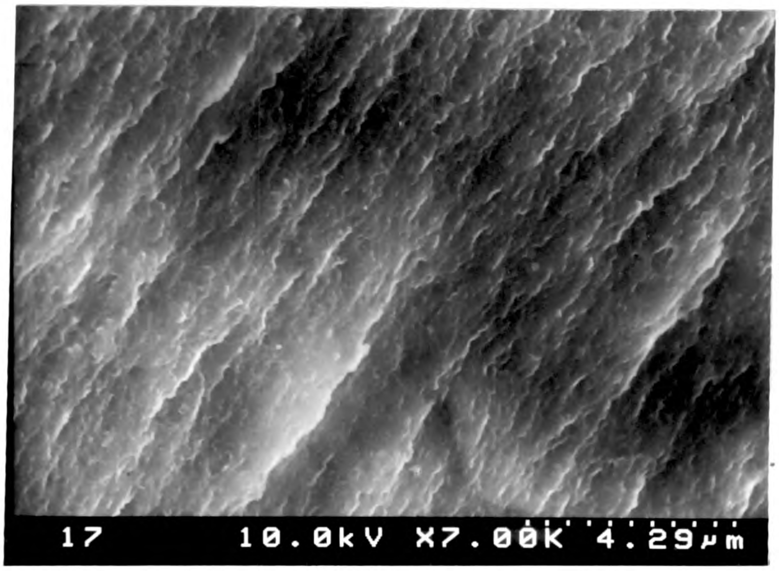
17 10.0kV X7.00K 4.29µm

C

Fig 4.26 : Scanning electron micrographs of PUR92(1.5)/IPE IPNs containing 80%(A), 50%(B), 20%(C) PUR by weight

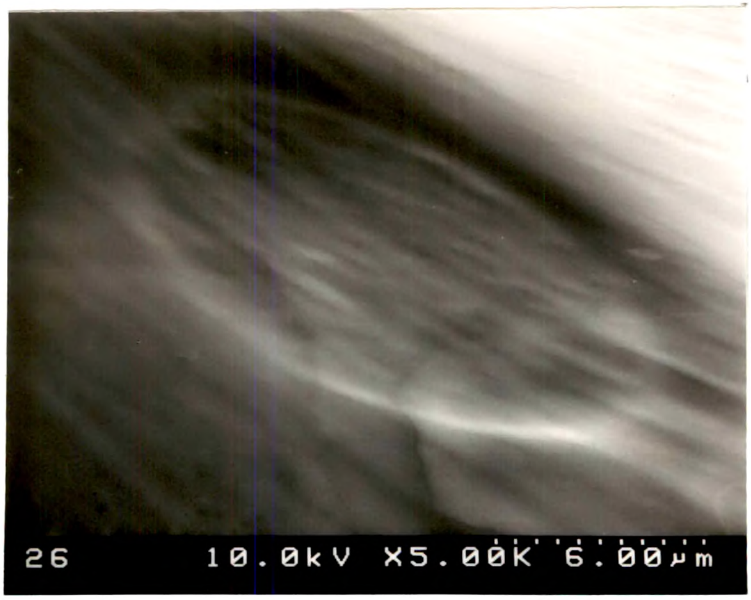
26 10.0kV X5.00K 6.00µm

A

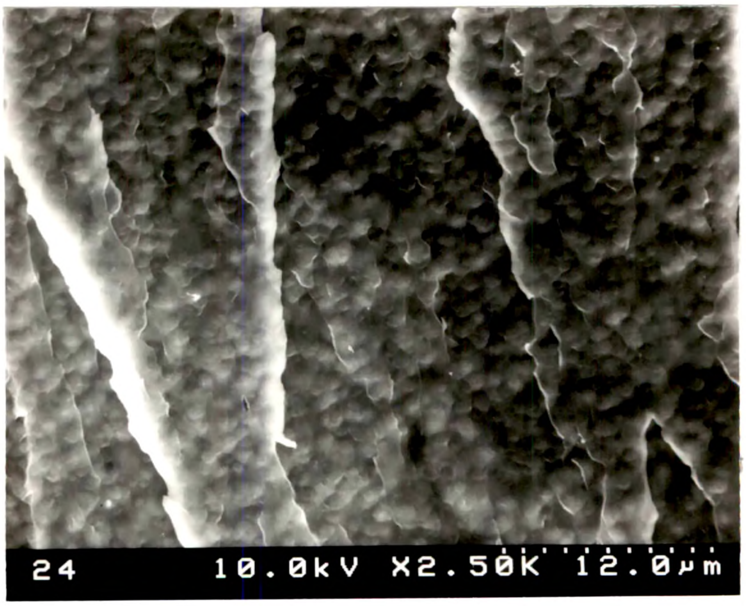
24 10.0kV X2.50K 12.0µm

B

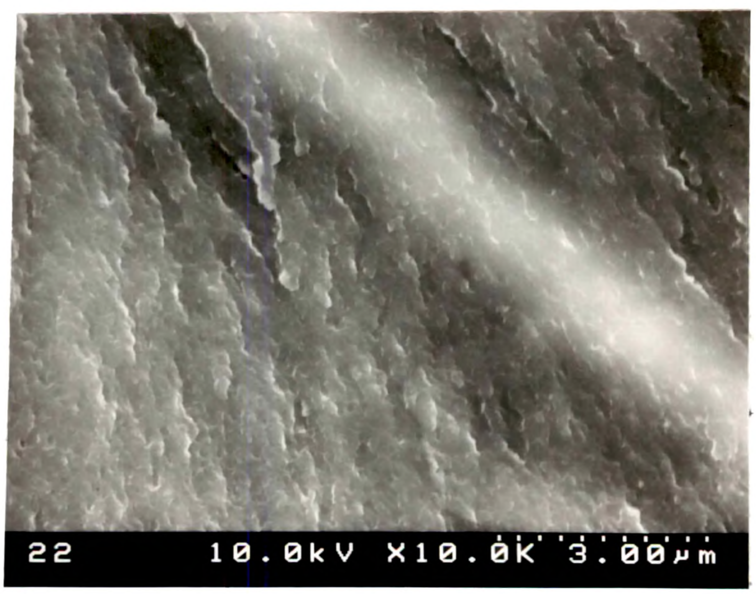
22 10.0kV X10.0K 3.00µm

C

Fig 4.27 : Scanning electron micrographs of PUR92(2.0)/IPE IPNs containing 50%(A), 40%(B) and 20%(C) PUR by weight

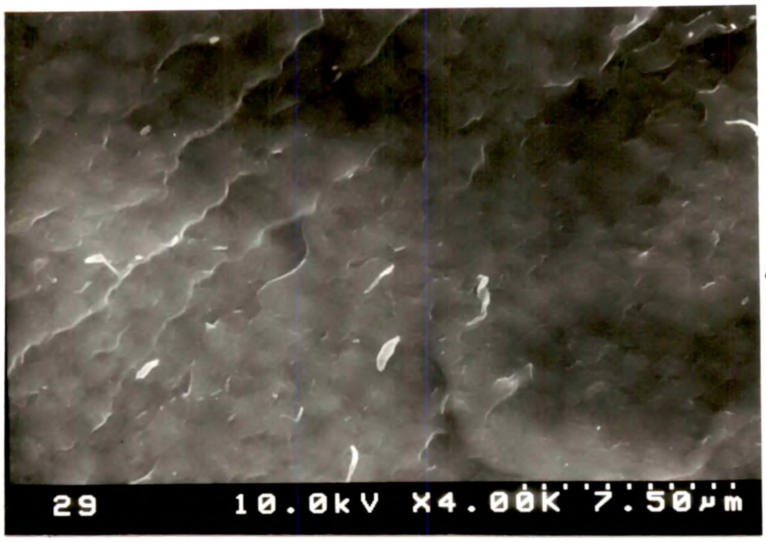
29 10.0kV X4.00K 7.50μm

A

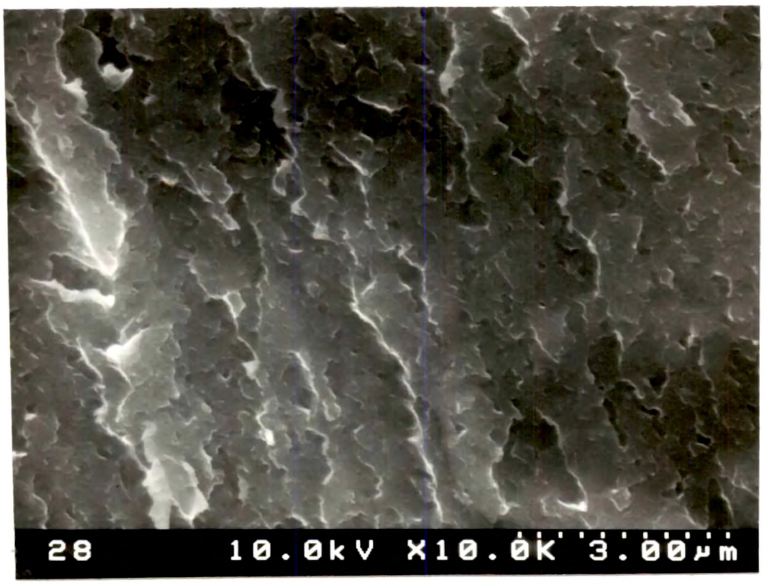
28 10.0kV X10.0K 3.00μm

B

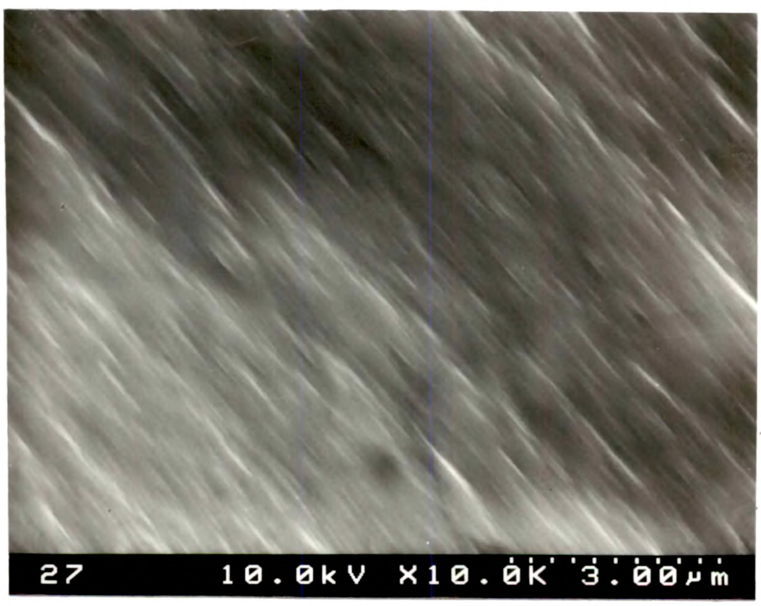
27 10.0kV X10.0K 3.00μm

C

at NCO/OH ratio of 1 2 and 1 5 could not be carried out and hence the changes in morphology of these IPNs with variation in crosslink density and nature of polyol could not be predicted.

From the SEM studies it is revealed that, both corsslink density (NCO/OH ratio) and composition of components play their role in deciding the final morphology of the IPNs Increasing the amount of polyester and/or corsslink density, the IPNs show enhanced miscibility The effect is found to be maximum in 20:80 sample at all levels of crosslinking However, the domain distribution and the phase morphology from Transmission electron microscopy (TEM) could not be studied because of the difficulty in getting ultra thin sections required for this study

4.5 MECHANICAL PROPERTIES

One of the most informative mechanical experiments for any engineering material is the determination of its stress- strain curve in tension which brings out basic characteristics of mechanical properties such as stiffness, elasticity, strength, elongation at break and yield stress.

Experimental

Tensile properties were measured on Instron tensile testing machine. Tensile data were obtained by elongating the samples held between two compression jaws initially 5.0 cm apart. Measurements were carried out with strain rate 0.5 cm/min at room temperature.

The stress - strain data were obtained from the following relations

$$\text{Stress } (\sigma) = \frac{\text{Load}}{\text{Cross sectional area}} = \frac{\text{Load}}{\text{breadth x thickness}}$$

$$\text{Strain (e)} = \frac{\text{Elongation } (\Delta L)}{\text{Original gage length } (L_o)}$$

The surface hardness was measured by means of a type A Shore Durometer at room temperature according to ASTM A2240.

Results and discussion

Stress - strain behavior of PUR60(1.2)/IPE IPNs having different compositions of PUR and IPE matrix is shown in Fig 4.28. The behavior ranges from rubbery characteristics of PUR to the stiff polyester. Depending on the percentage of both components, the IPNs behave like reinforced elastomer or toughened plastic.

By examining the mechanical characteristics of these IPNs (Table 4.6) it is seen that there is an increase in tensile strength (T.S) with increase in polyester content up to 40% IPE. In other words, at PUR rich region, IPNs behaved as plastic reinforced elastomers. The enhancement in T.S is most likely due to enhanced coexistence of two networks caused by (i) reaction of end groups of polyester and NCO groups of PUR (ii) H-bond formation and (iii) perfect interpenetration of both phases.

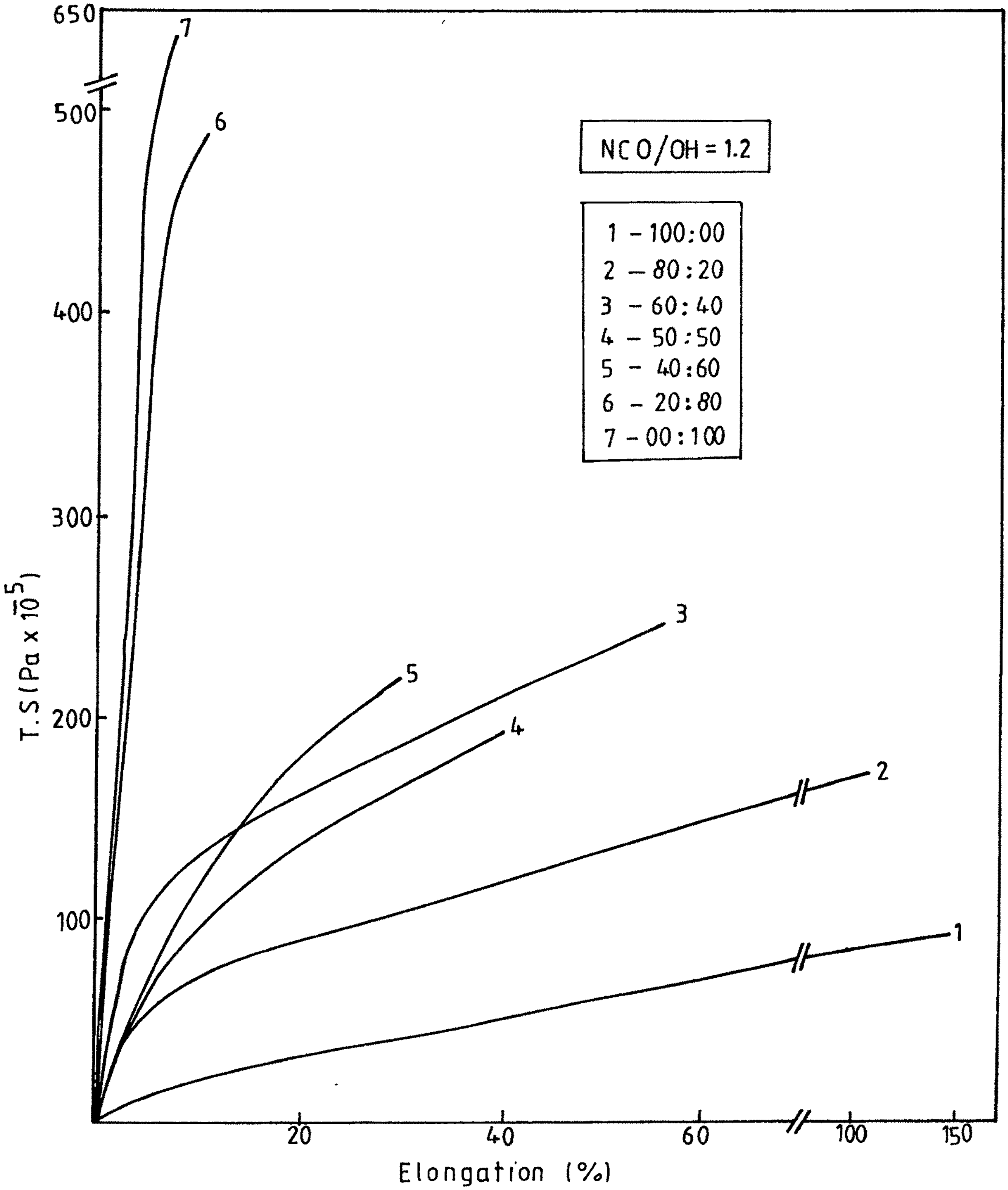

Fig 4.28 . Stress strain curves of various IPNs based on PUR60(1 2)/IPE system

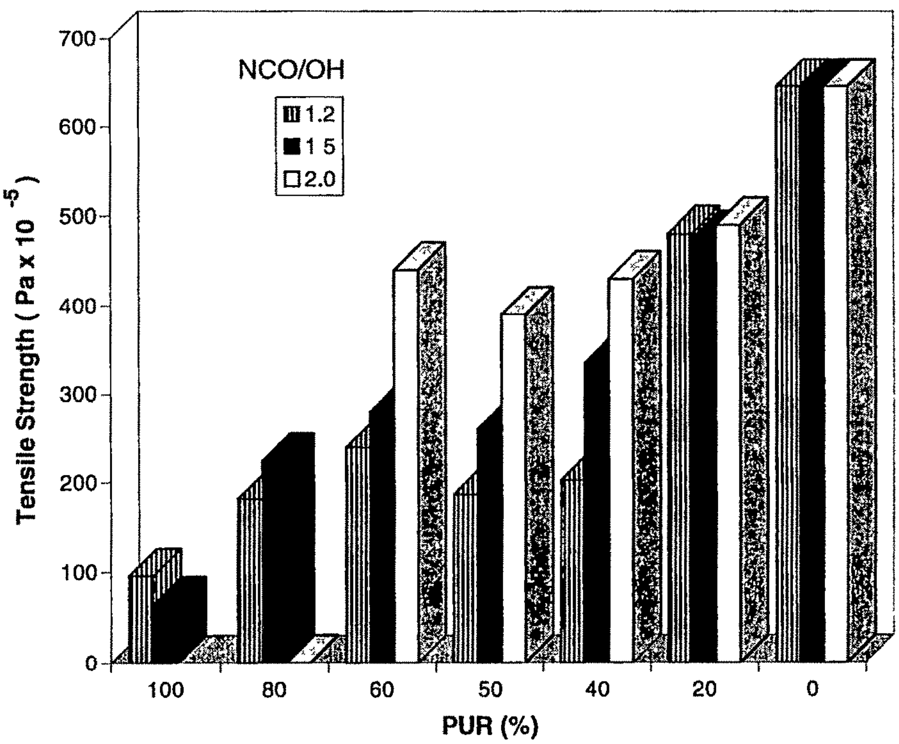

Fig 4.29 Variation in tensile strength with change in composition of PUR60/IPE IPNs at various NCO/OH ratios

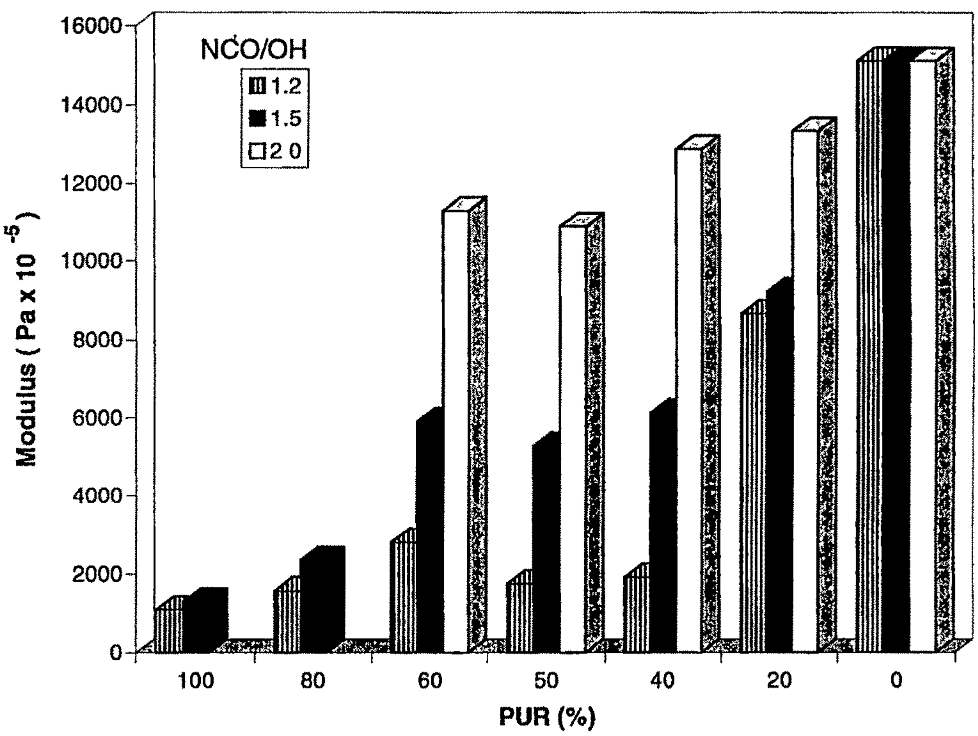

Fig 4.30 Variation in modulus with change in composition of PUR60/IPE IPNs at various NCO/OH ratios

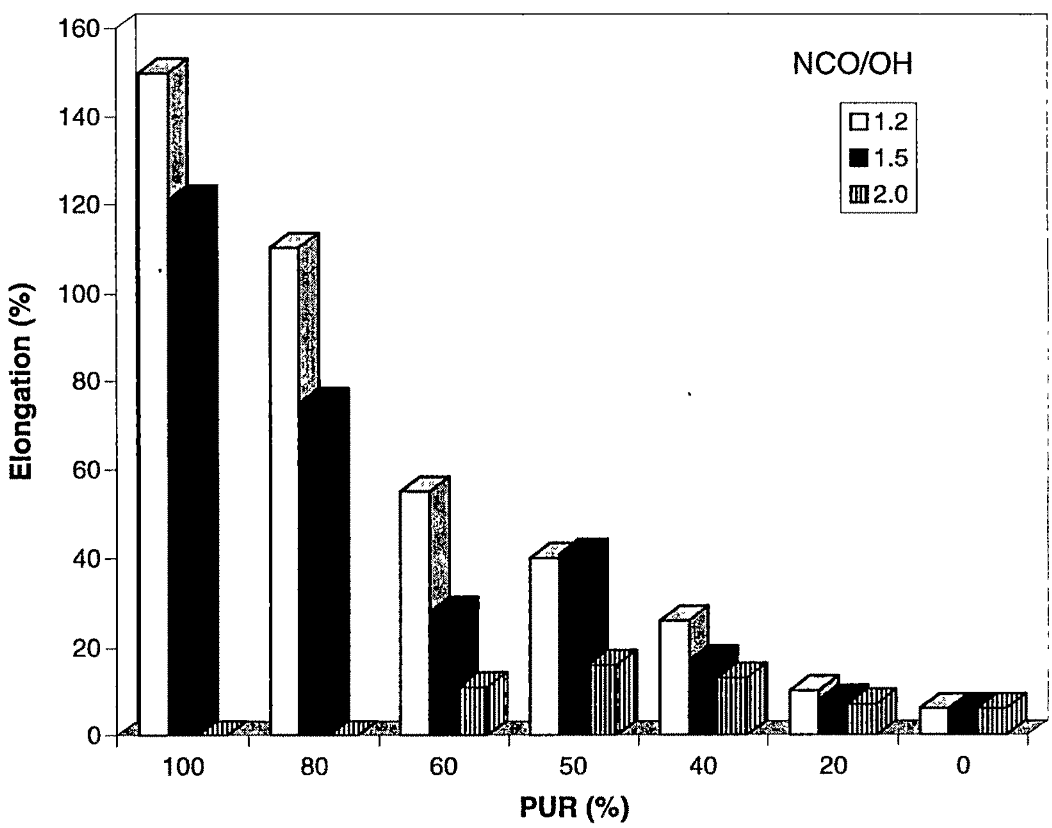

Fig 4.31 Variation in elongation with change in composition of PUR60/IPE IPNs at various NCO/OH ratios

With the incorporation of 50% IPE, the IPN showed minima in T.S and modulus as shown in the bar diagram (Fig 4.29 and 4.30). This may be due to poor interpenetration of networks resulted because of the difference in crosslinking rate and swelling of PUR network already formed, which weakens their coexistence and decreases reinforcing effect. The drastic reduction in T.S and modulus for -
40 : 60 IPN (Table 4.6) could be due to an onset of phase inversion as proposed by Kim and others[38-39] where PUR acts as impact modifier and IPE as continuous matrix.

When PUR content incorporated in brittle polyester is 20%, the tensile modulus and T S were decreased and elongation at break increased (Table 4.6, Fig 4.29 - 4.31), but changes in properties at low PUR content were insignificant. It is desirable that tensile properties and hardness are not changed greatly when UPE is modified by adding small amount of rubbery PUR. This is because, when PUR content is less, it can't congregate to have its identity as separate phase and shows complete molecular mixing. This effect is similar to copolymerization rather than partially compatible blends like High Impact Polystyrene[40] (HIPS) . This is also supported by data of percentage elongation Vs percentage PUR shown in Fig 4.31, indicating smooth decrease in elongation up to 60% IPE, beyond which it levels off.

Fig 4.32 shows the stress- strain curves of PUR60(1.5)/IPE IPN system at various composition of PUR and IPE. The tensile properties of resulting IPNs are shown in Table 4.6. It can be seen from the data that, trend in the results remain same even at high NCO/OH ratio, but the T.S modulus and surface appearance are improved considerably with increase in isocyanate content. The samples become stiffer and stronger. This could be due to increase in crosslink density, additional crosslinks through allophanate linkages, enhanced H- bonding at high NCO/OH ratio and reaction possibility of terminal OH groups and NCO groups of respective matrix. The IPNs derived from PUR with high isocyanate content exhibit less phase separation and improved compatibility caused by shorter chain length of PUR. The results are in agreement with others[41]

The effect of crosslink density can be seen significantly from the stress- strain curve of 60:40 IPN. This IPN did not show yield point at low NCO/OH ratio (Fig.4.28), but exhibited yield point at high NCO/OH ratio of 1.5. (Figure 4.32). This suggests considerable toughness of the sample, as the area under the stress- strain curve being large compared to that of polyester which normally fails at 5-6% extension. In this respect 60:40 IPN at NCO/OH ratio 1.5, resembles high impact polystyrene. With further increase in NCO/OH ratio to 2.0 (Tab. 4.6 and Fig. 4.33), the strength and hardness are augmented due to increased crosslink density. The elongation at break is reduced considerably(Fig.4.31). At this ratio, the IPNs varying their composition from 40 to 60% PUR display yield point and yield drop (Fig.4.33). This is probably because of compensation effects. That is, the increase in T.S with increase in NCO/OH ratio because of high crosslink density and other reasons stated earlier compensate the decrease in T.S due to decrease in IPE content. Thus

Table 4.6 : Mechanical properties of PUR60/IPE IPNs at various NCO/OH ratios

NCO/OH=1.2

PUR:IPE	T. S x 10^{-5} (Pa)	e (%)	Modulus x 10^{-5} (Pa)	Hardness (Shore A)
100:00	96.0	150.2	1078	63
80:20	178.4	110.4	1821	72
60.40	235.8	55.1	2750	83
50:50	183.7	40.8	1715	81
40:60	199.1	26.7	1882	84
20:80	470.6	10.5	8487	86
00:100	645.0	6.0	14918	91

NCO/OH=1.5

100.00	120.0	121.4	1274	65
80:20	220.8	75.3	2313	80
60:40	274.5	28.1	5786	84
50:50	256.3	41.6	5177	83
40:60	328.4	17.0	5978	86
20:80	465.4	8.5	9045	87
00:100	645.0	6.0	14918	91

NCO/OH=2.0

100:00	-	-	-	-
80:20	3631	28.1	9585	84
60:40	431.4	11.1	11074	87
50:50	382.2	16.5	10672	85
40:60	421.2	13.6	12612	87
20:80	480.7	7.6	13063	88
00:100	645.0	6.0	14918	91

Table 4.7 : Mechanical properties of PUR92/IPE IPNs at various NCO/OH ratios

NCO/OH=1.2

PUR:IPE	T. S x 10^{-5} (Pa)	e (%)	Modulus x 10^{-5} (Pa)	Hardness (Shore A)
100:00	113.0	120.0	1000	62
80:20	273.2	86.7	4571	74
60:40	302.6	69.2	3802	81
50:50	295.1	63.6	4648	84
40:60	250.6	33.3	2422	85
00:100	645.0	6.0	14918	91

NCO/OH=1.5

100:00	135.7	91.0	1272	65
80:20	322.8	56.6	4900	80
60:40	351.4	46.4	4875	82
50:50	300.0	31.3	3504	86
40:60	349.8	26.8	4614	87
20:80	402.6	5.3	8697	89
00:100	645.0	6.0	14918	91

NCO/OH=2.0

100:00	-	-	-	-
60:40	432.3	20.5	10758	82
40:60	570.0	15.1	10789	88
20:80	631.2	6.5	11989	88
00:100	645.0	6.0	14918	91

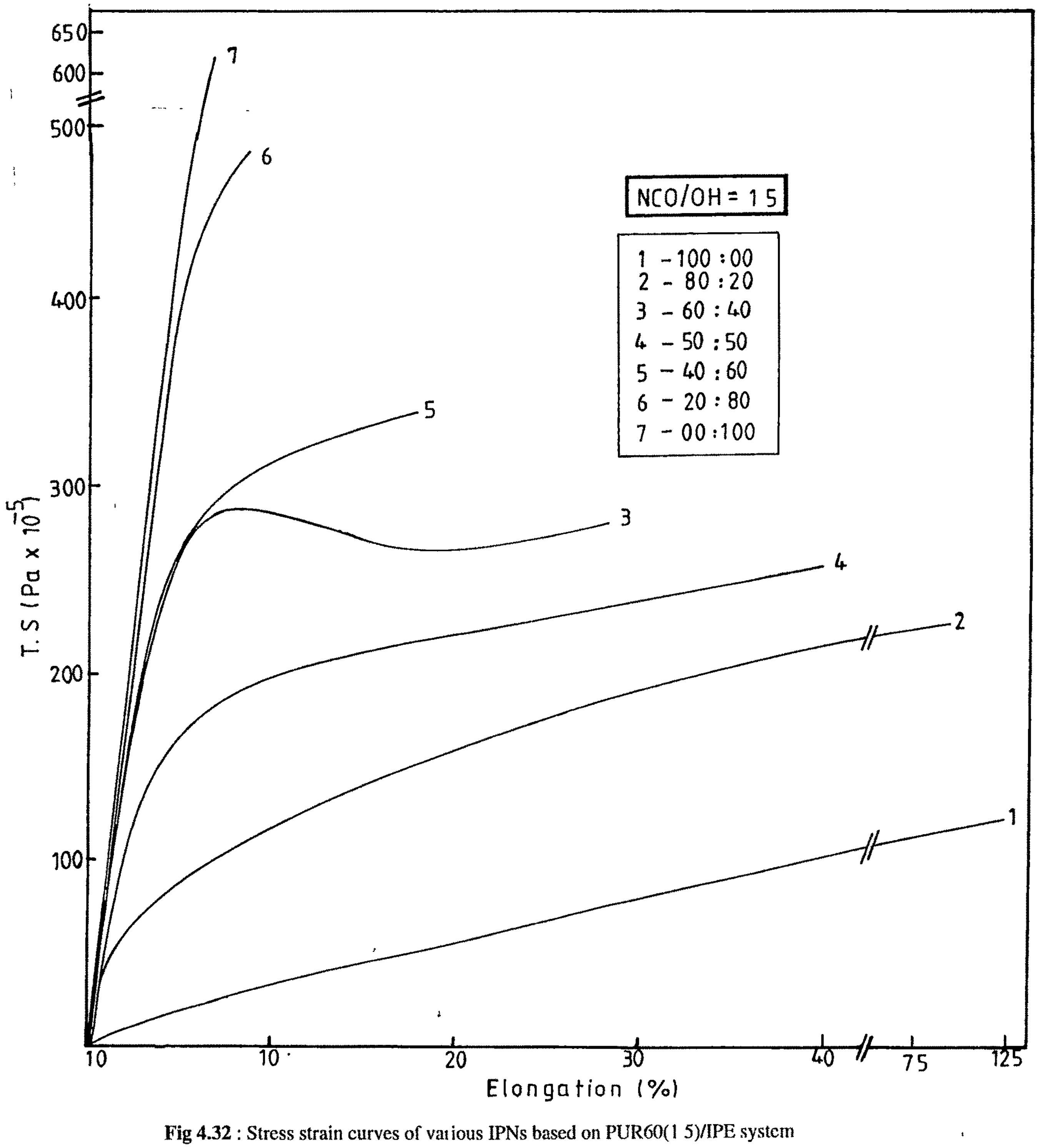

Fig 4.32 : Stress strain curves of vaiious IPNs based on PUR60(1 5)/IPE system

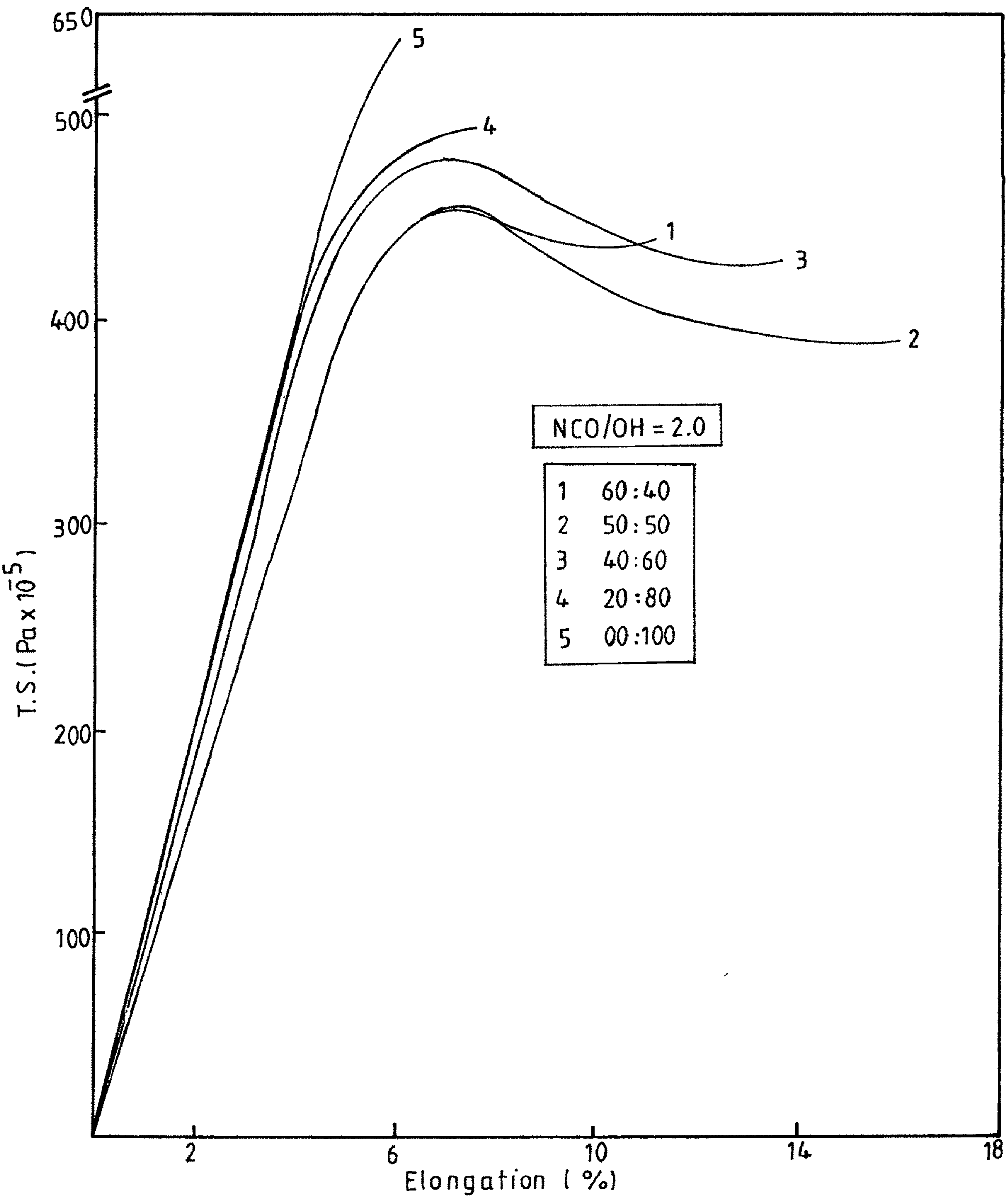

Fig 4.33 . Stress strain curves of various IPNs based on PUR60(2.0)/IPE system

these compositions show yield point rather than rubbery behavior observed at low NCO/OH ratio. These IPNs can act as toughened plastics.

Data of Tab.4.6 also revealed that effect of composition on tensile properties and hardness are not significant when crosslinking level was kept too high (NCO/OH ratio=2.0)

The tensile strength and percentage elongation (% e) data of PUR92/IPE IPN system for different compositions and at three different NCO/OH ratios are given in Tab. 4.7. The results clearly indicate that, as NCO/OH ratio increases from 1.2 to 2.0 (for a given composition), T.S and hardness increases and % e decreases. This is because of the increase in crosslink density provided by reaction of excess NCO groups of polyols as well as terminal OH groups of polyester. It is also evident from the comparison of data of PUR60 based IPNs (Tab.4.6) and PUR92 based IPNs that, the strength is higher in case of latter because of the same reason stated above. R92 having more hydroxyl values provide higher crosslink points and thus form IPNs having more dense structure.

When NCO/OH ratio is maintained same the trend in the results of T.S, hardness and % e as a function of composition is as expected except for 80 :20 IPN (Tab. 4.7). The unexpected results along with yield characteristics in stress-strain behavior indicate that, at this composition there is an enhanced and uniform coexistence of both phases (synergistic effect). This is also supported by results of DMA, as this IPN showed marked shift in T_g to high temperature in tan δ temperature plot (Fig. 4.13). On the other hand, for 50:50 IPN tensile properties are poor as two networks show poor coexistence because of the difference in crosslinking rates of both networks. However, at this composition reduction in T.S of IPN is not very high when compared to that observed in IPNs based on PUR60 at a given NCO/OH ratio. This is because of the high crosslink density of the former which is resulted form the employment of R92 polyol.

The results of tensile properties for PUR60/OPE and PUR92/OPE IPNs are shown in Tab. 4.8 and Tab.4.9 respectively. The values of T.S, hardness and % e follow more or less similar trend as that of IPE based IPNs. The basic difference in their results reflects the low strength of OPE based IPNs than that of IPE based IPNs. This is mainly attributed to the brittle nature and low molecular weight of OPE. Orthophthalic anhydride has a tendency to reform and sublime from its half esters during polymer preparation which renders the preparation of high molecular weighty polymers difficult to accomplish. Another limitation of phthalic anhydride is its tendency to form low molecular weight cyclic products because of the proximity of the acid groups[42].

The comparison of data of Tab. 4.8 and 4.9 with that of Tab.4.6 and 4.7 shows that the incorporation of PUR improves flexibility of OPE resin to a greater extent than that of IPE resin IPNs having equal composition of both components (50:50) show lowering in T.S which may be

Table 4.8 : Mechanical properties of PUR60/OPE IPNs at various NCO/OH ratios

NCO/OH=1.2

PUR:OPE	T. S x 10^{-5} (Pa)	e (%)	Hardness (Shore A)
100:00	96.0	150.0	63
80:20	26.8	62.5	70
50:50	35.3	12.5	82
40:60	202.4	11.6	85
20:80	286.8	9.0	87
00:100	598.0	2.1	94

NCO/OH=1.5

100:00	120.0	121.0	65
80:20	179.8	30.0	82
60:40	199.1	15.0	83
50:50	151.2	10.1	84
40:60	192.7	8.9	88
20:80	388.2	6.8	89
00:100	598.0	2.1	94

NCO/OH=2.0

100:00	-	-	-
50.50	278.4	7.9	87
40:60	345.5	7.1	88
20:80	394.6	5.2	90
00:100	598.0	2.1	94

Table 4.9 : Mechanical properties of PUR92/OPE IPNs at various NCO/OH ratios

NCO/OH=1.2

PUR:OPE	T. S x 10^{-5} (Pa)	e (%)	Hardness (Shore A)
100:00	115	120.0	61
80:20	116.8	30.0	77
60:40	205.0	15.0	82
50:50	97.4	12.2	86
40:60	225.4	9.8	87
20:80	303.9	4.9	88
00:100	598.0	2.1	94

NCO/OH=1.5

100:00	135.7	91.0	-
50:50	248.4	8.8	89
40:60	440.2	10.0	88
20:80	438.8	7.6	91
00:100	598.0	2.1	94

NCO/OH=2.0

100:00	-	-	-
50:50	358.2	7.8	88
40:60	353.7	8.1	90
20:80	405.4	5.0	92
00:100	598.0	2.1	94

due to phase separation. With the increase in NCO/OH ratio from 1.2 to 2.0 in both sets of IPNs (PUR60 and PUR92 based), the T.S improves and approaches to that of pure polyester. However, the improvement in elongation is found to be more in comparison to loss in T.S. This is predominant when PUR is prepared from polyols having more OH values (R92) and also when NCO/OH ratio is high.

As polyurethane percentage increases, T.S decreases drastically particularly for IPNs prepared from R60 polyols and having low NCO/OH ratio. The exponential decrease in T.S clearly indicates that, brittle network of polyester and highly flexible PUR network under this condition cannot behave cooperatively and show antagonism effect. However, with the lower percentage of PUR, the flexible PUR network may get distributed more or less uniformly and improves flexibility without deteriorating tensile strength to a greater extent.

4.6 THERMOGRAVIMETRY (TG)

As the name implies, this method involves monitoring continuously the weight of a sample at a constant rate of change of temperature or with time isothermally. Thermogravimetry has been used widely to study all physical processes involving weight changes. The most common use for TG is in measuring the thermal and oxidative stability of polymers under working conditions. The two most important information that can be extracted out of thermograms are

1. The onset temperature, which provides indication of the thermal stability of the specimen.
2. The percentage weight loss of the component(s) present which enables quantification of degradation characteristics of polymers like activation energy, order of reaction etc.

Experimental

Thermogravimetric analysis of pure polyurethanes, pure polyesters and their IPNs were carried out using Shimadzu TG-30 thermal analyzer at a heating rate of 10°C/min in air.

Results and discussion

Thermal studies of IPNs were carried out in air up to 700°C to see the effect of

i) Weight composition of components
ii) Cross-link density of PUR
iii) Types of polyols used in PUR and
iv) Types of polyester moiety

on their thermal stability. Initial degradation temperature (IDT) and other thermal characteristics determined from the analysis of thermograms are given in Table 4.10 and 4.11.

Thermograms of pure polyesters (IPE & OPE) exhibit two distinct portions of degradation (Fig. 4.34 & 4.35). These crosslinked resins, regardless of the type of saturated acid used, undergo spontaneous decomposition at ~330°C. Once the degradation has started, weight loss is rapid up to 60% weight loss. This is a characteristic of vinyl copolymers which are degraded into monomeric units at high temperatures unlike nonvinyl crosslinked thermosets such as phenolic and epoxy resins[43-44]. It is proposed that, styrene-styrene linkage in the crosslinked polyester system is subjected to breakdown in much the same fashion as straight polystyrene[45] The second stage decomposition starts at around 500°C and seem to follow different pattern of degradation than that of polystyrene cleavage. This higher temperature degradation may be due to the fragmentation reaction of ester groups with the elimination of carbon monoxide[46].

Polyurethanes, on the other hand, are found to be less stable compared to UPE (Fig.4.34 & 4.36). Here also degradation takes place in two stages, however they are not well-distinct. Stage I may correspond to the urethane bond breaking which starts at 250°C (low NCO/OH ratio) leading to formation of carbon dioxide, alcohols, amines, aldehydes, carbon monoxide etc[47,48], and stage II

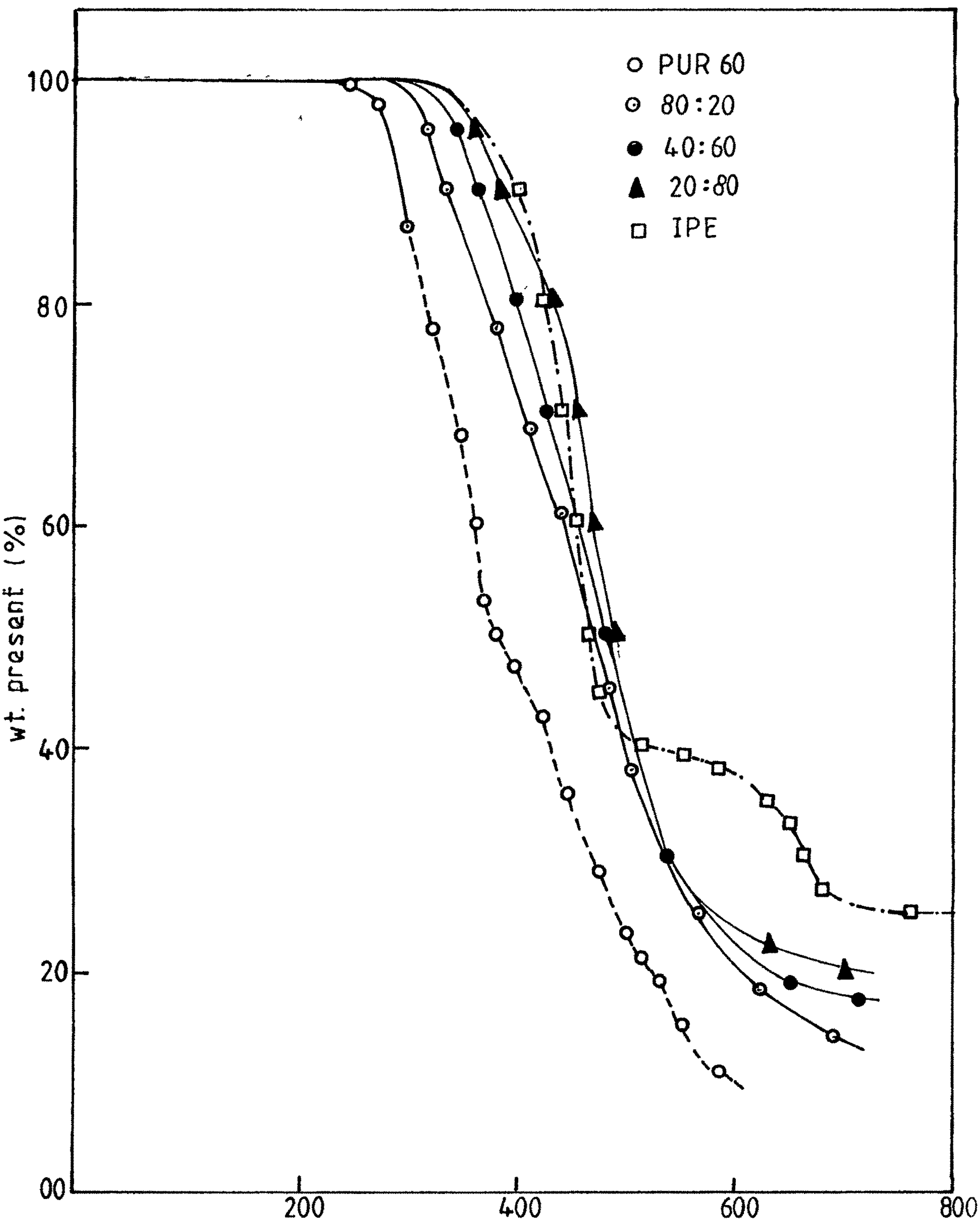

Fig 4.34 : TGA thermograms of PUR60(1.2)/IPE IPNs

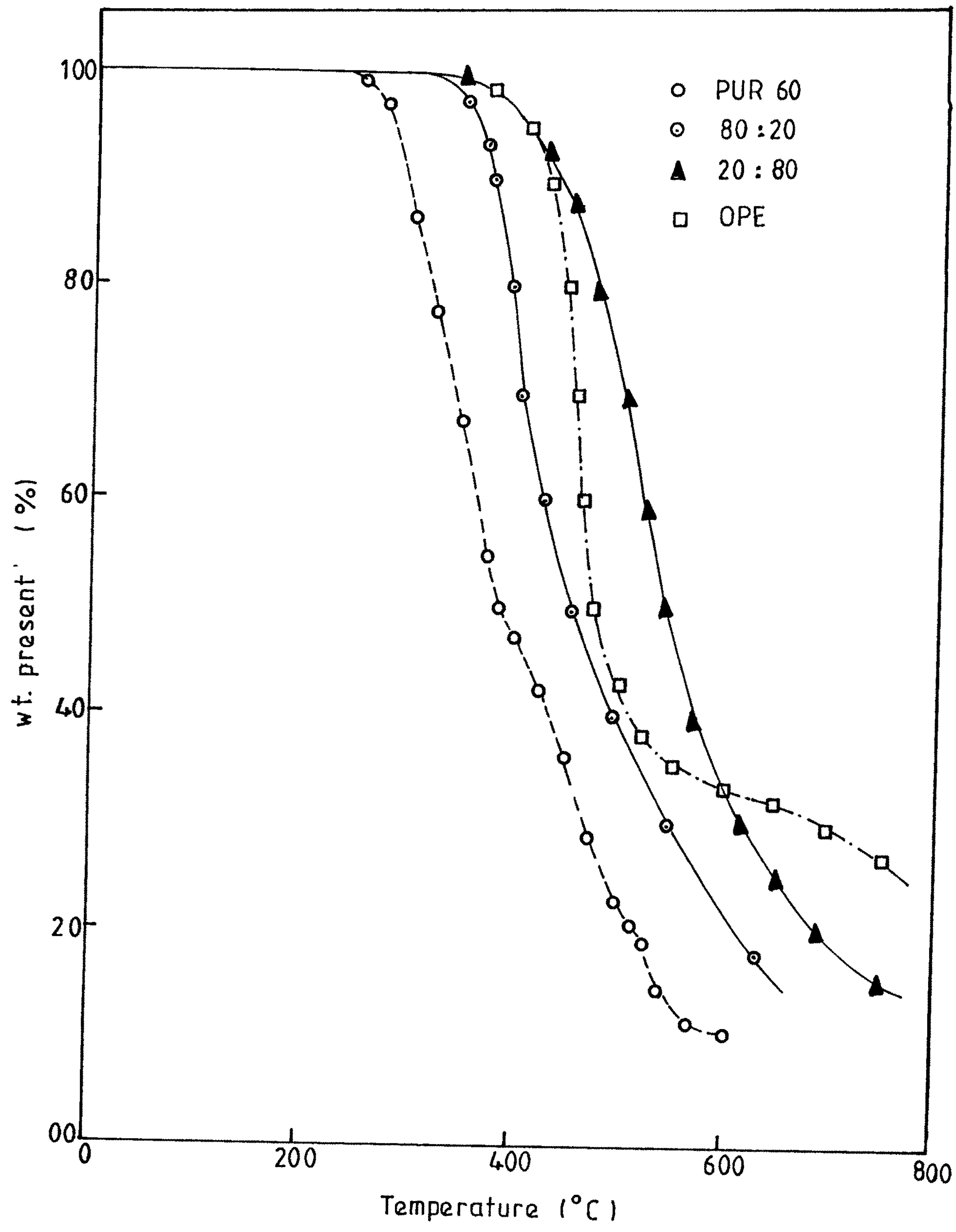

Fig 4.35 : TGA thermograms of PUR60(1.2)/OPE IPNs

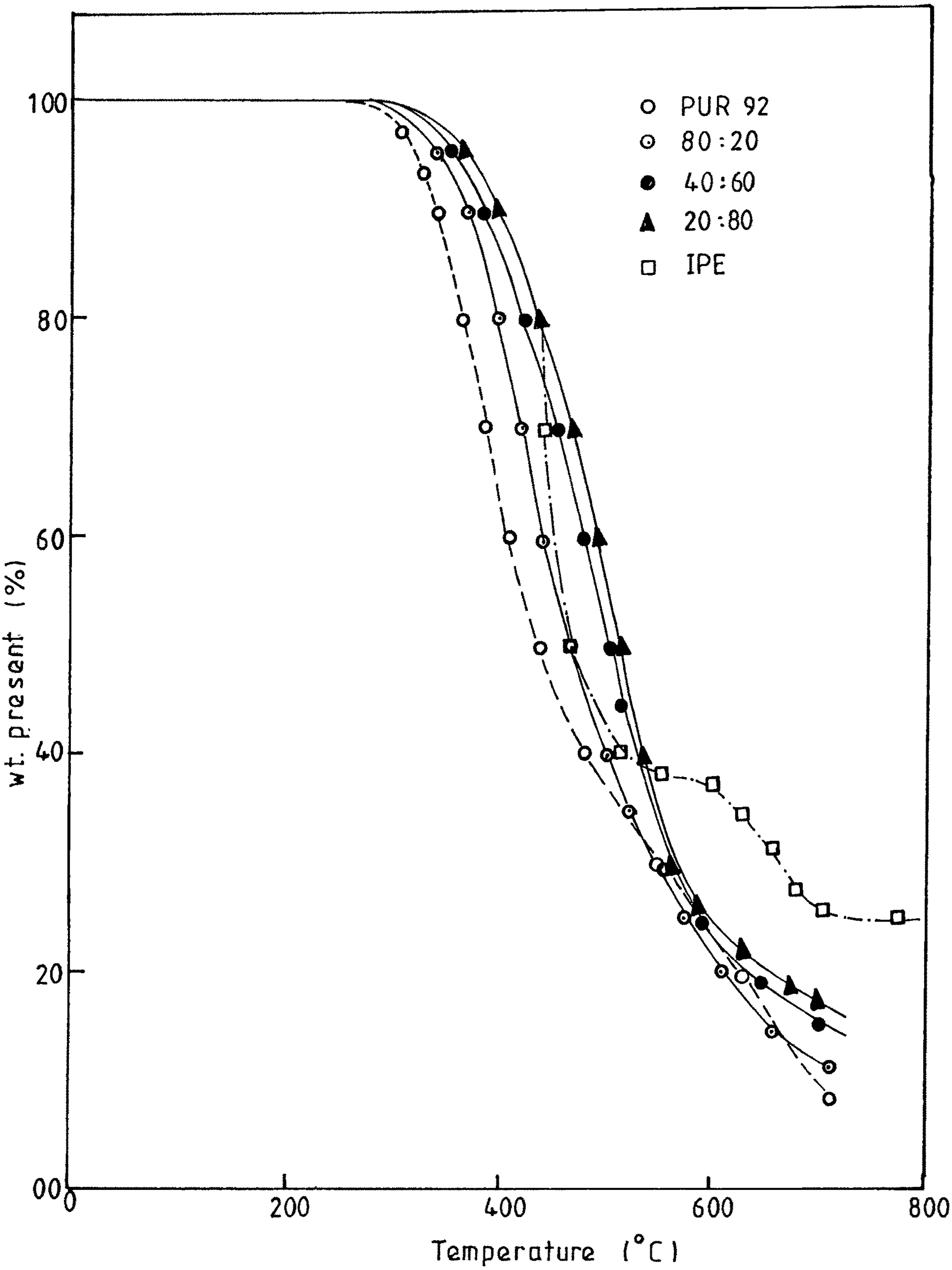

Fig 4.36 : TGA thermograms of PUR92(1.2)/IPE IPNs

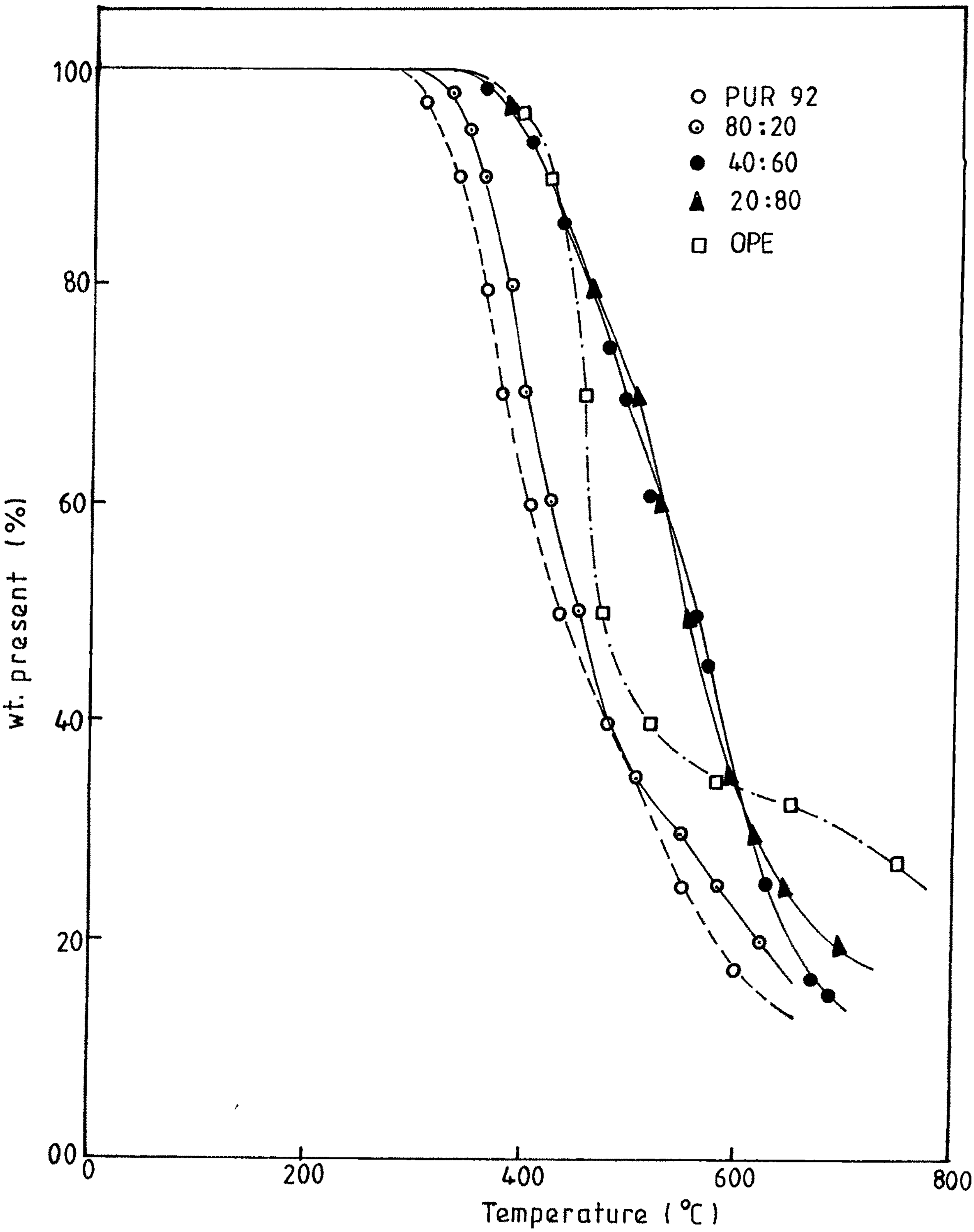

Fig 4.37 : TGA thermograms of PUR92(1.2)/OPE IPNs

may be due to the polyol decomposition which occurred at ~375°C. Since polyols used in this study are based on castor-oil, the main chain scission may occur with the formation of 10-undecanoic acid and heptanal as evidenced by the thermal degradation of ricinoleic acid[49]

The thermal stability of IPNs fall in between that of homopolymer networks and all of them show a single stage degradation pattern in TG curves (Fig. 4.34 - 4.37).

Figure 4.34 depicts the representative thermograms of various IPNs prepared from PUR60 at NCO/OH ratio 1.2 and IPE in various proportions. The pure PUR60 exhibits an IDT of around 250°C which increases with increase in the concentration of IPE in the IPNs. It can also be seen from Table that, incorporation of 20% PUR60 not only retain the IDT values but also showed a considerable increase in T_{50} values compared to that of pure IPE. Moreover all IPNs irrespective of their compositions also show higher T_{50} values than that of pure IPE. The whole phenomena can be explained primarily on the basis of degradation pattern of IPNs. They showed a single stage degradation unlike that of UPE, which is a clear indication of mixing of the two components. Also the close juxtaposition of the IPNs allow polystyrene and its degradation products to act as free-radical scavengers for PUR thereby retarding its further degradation[50]. Similar results were observed for IPNs at higher NCO/OH ratios of 1.5 and 2.0 also.

Increase in crosslink density of PUR60 at a given composition did not improve the thermal stability of IPNs significantly (Table 4.10). On the contrary in certain IPNs, IDT and T_{50} values were decreased with increase in isocyanate content of PUR60. This may be because of the higher concentration of urethane linkages beyond optimum level, which become susceptible to oxidative degradation.

The substitution of orthophthalic acid in place of isophthalic acid in polyester backbone increased the thermal stability of pure polyester network and its IPNs at a given composition and NCO/OH ratio by marginal value (Table 4.10). The reason for higher thermal stability of OPE containing IPNs is not known.

Thermal characteristics of IPNs based on PUR92 (PUR92/IPE & PUR92/OPE) are shown in Table 4.11. The representative thermograms of various IPNs at NCO/OH ratio 1.2 are shown in Fig. 4.36 &.4.37 respectively. From the values of decomposition temperatures it is clear that, these IPNs are thermally more stable than IPNs where PUR60 was employed. This could be due to shorter chain length of R92 polyol than R60 polyol.

It can be inferred from the results of TG analysis that, irrespective of the type of polyol, type of polyester and NCO/OH ratio, the 20:80 IPN showed a synergistic behavior in the thermal stability.

Table 4.10 : The thermogravimetric data of IPNs based on PUR60 with IPE and OPE

PUR60/IPE

NCO/OH	1.2				1.5				2.0			
PUR:PE	IDT	T_{10}	T_{50}	E(KJ/mol)	IDT	T_{10}	T_{50}	E(KJ/mol)	IDT	T_{10}	T_{50}	E (KJ/mol)
100:00	250	330	440	43.7	292	340	450	49.6	288	330	450	45.7
80:20	310	330	470	55.6	300	335	470	65.5	310	320	448	55.6
40:60	315	365	480	79.4	340	385	500	71.5	320	350	470	68.3
20:80	330	390	490	85.4	340	370	485	87.4	320	380	515	75.5
00:100	330	400	465	91.4	330	400	465	91.4	330	400	465	91.4

PUR60/OPE

100:00	250	330	440	43.7	292	340	450	49.6	288	330	450	45.7
80:20	300	372	456	67.5	306	381	448	59.6	303	381	456	63.1
40:60	300	401	530	74.3	330	410	520	74.1	300	430	560	77.2
20:80	345	430	545	87.4	340	440	520	81.4	343	440	536	81.4
00:100	339	432	473	93.4	339	432	473	93.4	339	432	473	93.4

Table 4.11 : The thermogravimetric data of IPNs based on PUR92 with IPE and OPE

PUR92/IPE

NCO/OH	1.2				1.5				2.0			
PUR/PE	IDT	T_{10}	T_{50}	E(kJ/mol)	IDT	T_{10}	T_{50}	E(kJ/mol)	IDT	T_{10}	T_{50}	E(kJ/mol)
100:00	285	340	442	49.6	280	340	440	45.7	280	336	442	47.6
80:20	300	370	470	63.5	300	370	460	59.6	316	380	455	61.6
40:60	320	380	510	75.5	340	385	500	71.5	320	350	470	68.3
20:80	320	400	508	87.4	330	410	520	83.4	332	400	440	77.5
00:100	330	400	465	91.4	330	400	465	91.4	330	400	465	91.4

PUR92/OPE

100:00	285	340	442	49.6	280	340	440	45.7	280	336	442	47.6
80:20	310	363	461	69.5	321	371	458	66.1	318	374	450	65.3
40:60	344	421	567	83.4	340	425	549	85.4	344	420	540	79.4
20:80	347	420	560	83.2	345	408	558	81.4	340	410	520	80.4
00:100	339	432	473	93.4	339	432	473	93.4	339	432	473	93.4

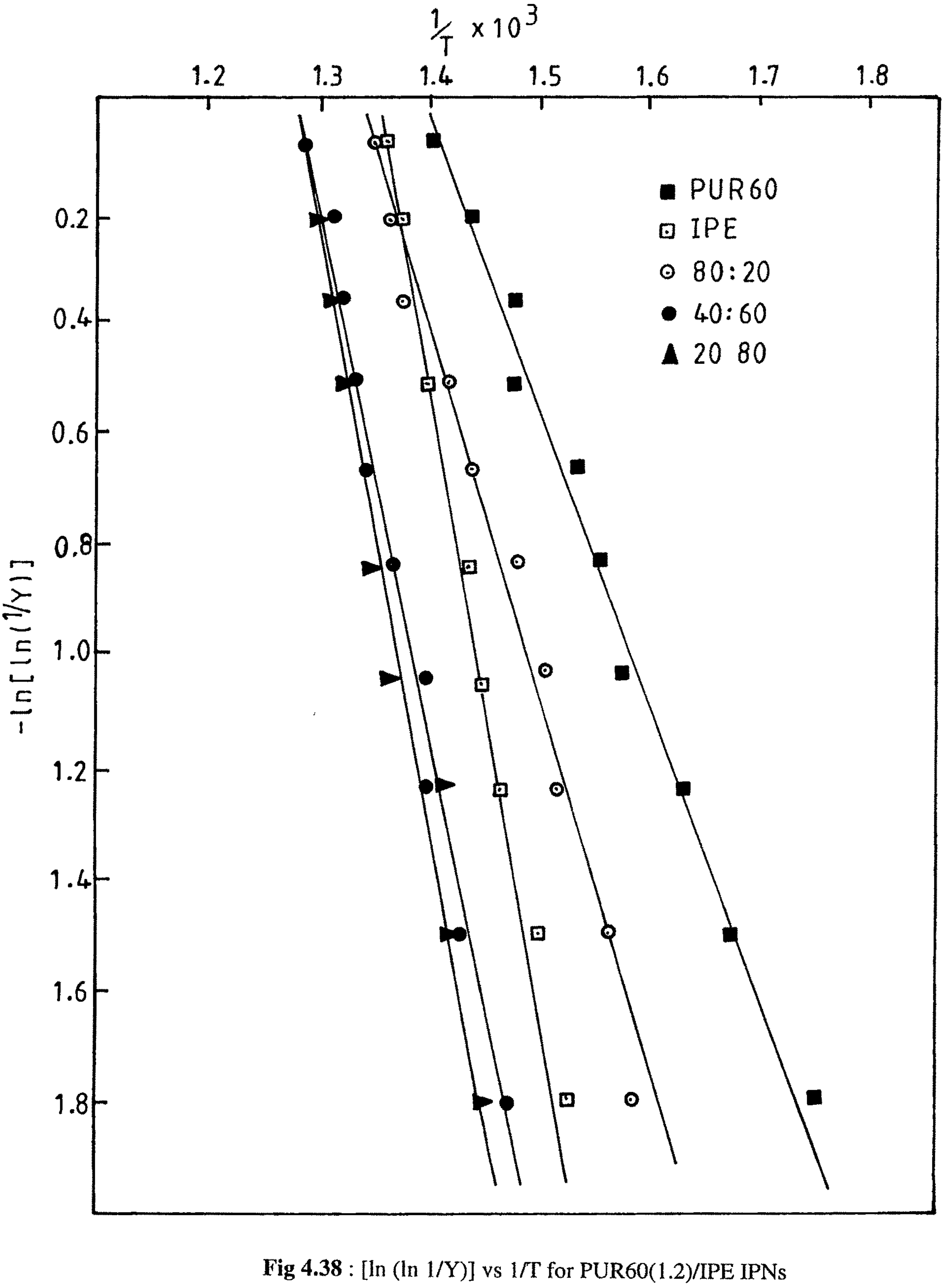

Fig 4.38 : [ln (ln 1/Y)] vs 1/T for PUR60(1.2)/IPE IPNs

Activation energy (E) which is a quantitative measure of thermal stability was determined for all IPNs by Broido method[51]. The integrated Broido equation used to calculate E is of the form

$$\ln [\ln (1/Y)] = -(E/R)(1/T) + \text{constant}$$

where Y is the weight of the original material taking part in a given reaction step. E is the activation energy of thermal decomposition, R is the gas constant and T is the absolute temperature. A plot of $\ln [\ln (1/Y)]$ against $1/T$ should yield a straight line of slope $-E/R$ for a first order reaction. Representative plots of homopolymer and PUR60(1.2)/IPE IPNs are shown in Fig.4.38. The values of activation energy for thermal degradation of various IPNs are given in Table 4.10 & 4.11 . The values of activation energy of pure PUR60 and PUR92 at NCO/OH ratio 1.2 are 43.7 and 49.6 kJ/mole respectively. The higher values of E observed in IPNs indicate that polyester makes a positive contribution towards thermal stability of PUR. This is more significant at low level of polyurethane.

4.7 DIFFERENTIAL SCANNING CALORIMETRY (DSC)

Although DMA method is more sensitive to heterogeneity of phases in polymer systems than DSC method, the latter one also provide evidence for the compatibility of blends and IPNs.

Experimental

The DSC analysis of some selected IPNs were carried out on a Perkin Elmer 7- series thermal analysis system at a heating rate of 10°C/min from -50 to 250°C.

Results and discussion

The DSC curves of some of the IPNs are presented in Fig.4.39 and their glass transition temperatures (T_g) along with that of the polyurethane network are given in Table 4.12. The T_g corresponding to polyester part was not clearly obtained in DSC thermograms which might be due to its highly crosslinked nature.

Pure PUR60 showed a T_g of 44.1°C at an NCO/OH ratio of 1.5 . With the incorporation of polyester, T_g values are shifted to higher temperatures indicating the formation of more rigid networks. Sample 40:60 showed a deviation from the normal behavior, which showed a low T_g compared to the samples with low IPE content. This could be due to toughening effect of polyester matrix by PUR elastomers which is evident from the SEM photograph showing dispersion of PUR domains of large dimension in polyester matrix. From the table it is also evident that, 80:20 and 60:40 samples showed only a single transition corresponding to the urethane phase, where as in samples with higher IPE content (50:50 and 40:60), a second transition at higher temperatures of 142 and 121.6°C is also observed, corresponding to the glassy phase. Similar was the observation with these samples in the DMA analysis also, where a single tan δ peak was obtained for 80:20 and 60:40 samples and two distinct tan δ peaks for 50:50 and 40:60 samples at NCO/OH ratio of 1.5.

The transition temperatures of homopolymer networks, PUR60 and PUR92 along with their IPN (40:60) with orthophthalic based polyester (OPE) are also given in Table 4.12. The values of transition temperature with change in crosslink density (NCO/OH ratio) is clear from this table. In the case of PUR60 and PUR92, the T_g values are shifted to higher temperatures with increase in NCO/OH ratio from 1.2 to 1.5. The 40:60 IPN also showed an increase in T_g from 63.3 to 68.6°C and 65.0°C to 68.7°C in the case of PUR60/OPE and PUR92/OPE systems respectively. This could be due to the stiffening effect of the aromatic ring and increase in H-bonding with increase in isocyanate content in the samples[52].

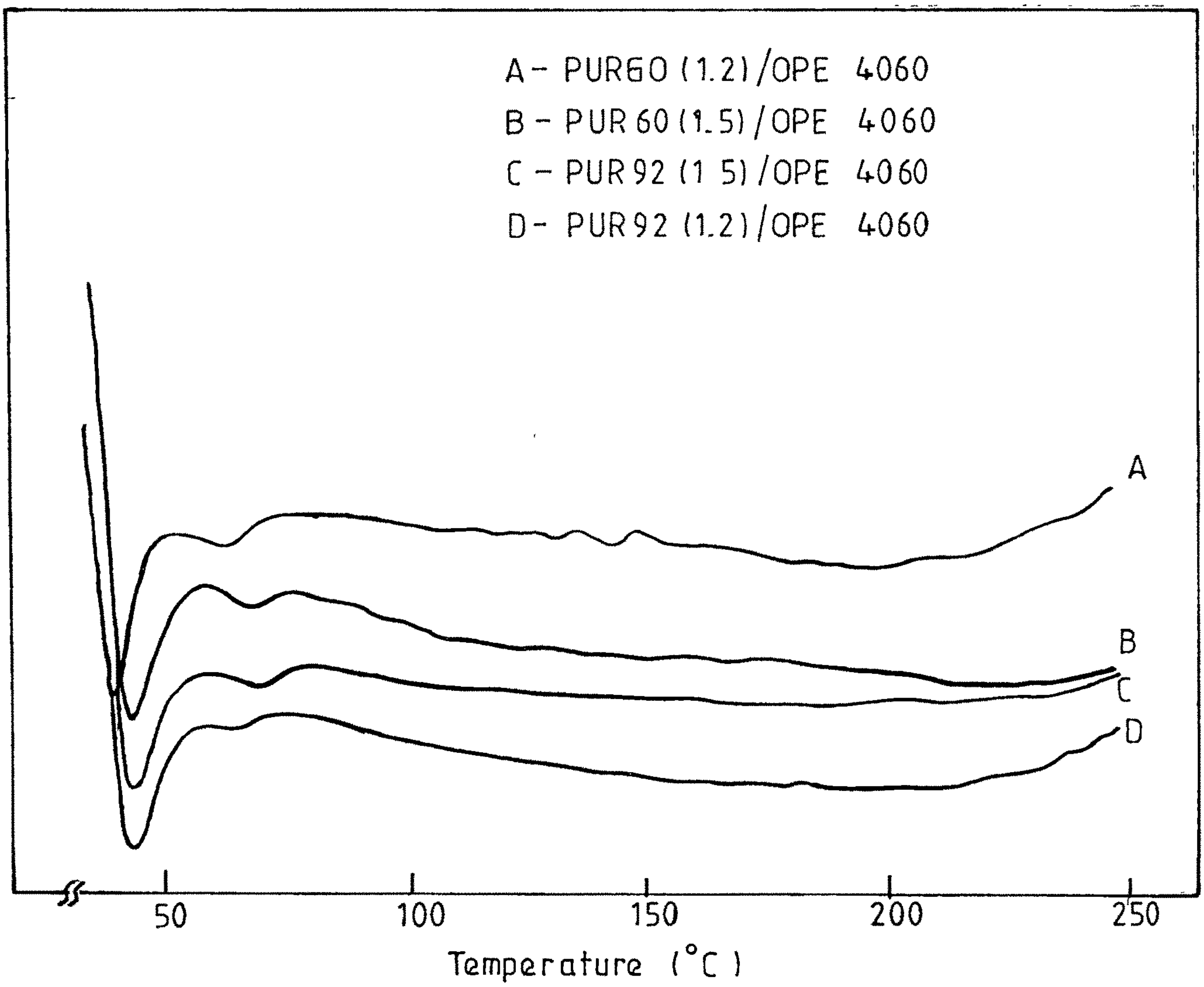

Fig 4.39 · DSC curves of various IPNs

From the table it is also clear that, IPNs based on PUR92 showed slightly higher T_g compared to that based on PUR60, irrespective of the NCO/OH ratio. This could be attributed to the higher content of hydroxyl groups in the former (R92) which lead to enhanced crosslinking and thus a more stiff network. The DMA result also support the above reasoning.

When T_g's of 40:60 sample based on IPE and OPE were compared with each other, it was clear that, sample based on OPE showed a higher T_g (68.6°C) than that based on IPE (38.1°C) at an NCO/OH ratio of 1.5. But before concluding anything, it is necessary to compare the DSC results of OPE based IPNs with DMA and SEM results, which could not be carried out unfortunately.

Table 4.12 : Glass transition temperature of various IPNs obtained from DSC analyses

PUR60/IPE (1.5)

PUR:IPE	T_{g1}°C	T_{g2}°C
100:00	44.1	-
80:20	47.0	-
60: 0	48.9	-
50:50	55.0	142.0
40:60	38.1	121.6

PUR:OPE	**PUR60/OPE**		**PUR92/OPE**	
	NCO/OH		NCO/OH	
	1.2	1.5	1.2	1.5
100:00	38.7	44.1	48.2	54.8
40:60	63.3	68.6	65.0	68.7

REFERENCES

1. P. Flory and J. Rehner, J. Chem. Phys., **11**, 521, 1943.
2. H. Hiaw, Z.H. Ping, J.W. Xie and T.Y. Yu, J. Polym. Sci Part A, Polym. Chem , **28**, 585, 1990.
3. A. P. Mathew, S. Packirisamy and S. Thomas, Polymer, **36(26)**, 4935, 1995.
4. C. Saikumar, S. Rajadurai and G. Thyagarajan, J. Polym. Mater., **4**, 139, 1987.
5. U. A. Santhamurthy and T. M. Aminabhavi, Polymer, **31**, 1757, 1990.
6. V. Vittoria and A. Ruvolo Filho, J. Appl. Polym Sci., **44**, 2127, 1992.
7. S. B. Aarogoppad, T. M. Aminabhavi and R H Balundgi, J. Appl. Polym. Sci., **44**, 1687, 1992.
8. S.B. Harogoppad and T. M. Aminabhavi, Polymer, **31**, 2346, 1990.
9. H. L. Frisch and K.C. Frisch, Prog. Org. Coat., **7**, 105, 1979.
10. H. L. Frisch, J. Cifarathi, R. Palma, R. Foreman, H. Yoon, D. Klempner and K.C. Frisch, Polymer alloys, Eds. D. Klempner and K.C.Frisch, Plenum, New York, 1977.
11. L. H. Sperling, Interpenetrating Polymer Networks and related materials, Plenum Press, New York, 1981.
12. B.M. Kolarz., Angew Makromol. Chem., **90**, 167, 1980.
13. G. Pozniak and W. Trochimczuk., Angew Makromol. Chem., **104**, 01, 1982.
14. G. C. Martin, E. Enssani and M. Shen., J. Appl. Polym. Sci., **26**, 1465, 1981.
15. G.T. Fieldson and T. A. Barbari., Polymer , **34**, 1146, 1993.
16. T Tetsuya, Y. Keiko, Y. Kazuo and M.Shuji., Polymer, **36(15)**, 2941, 1995.
17. A. R. Berens and H.B. Hopfenberg., Polymer, **19**, 489, 1978.
18. P. G. de Gennes, Scaling concept in polymer physics, Cornell University Press, Ithaca, New York ,1978.
19. J. Bastide and C. Picot., J. Polym. Sci., Polymer Phys. Ed., **17**, 1441, 1979.
20. H. Oikawa and K. Murakami, Macromolecules, **24**, 1117, 1991
21. K. K. Chee, Polymer gels and networks, **5**, 95, 1997
22. Encyclopedia of Polymer science and engineering, Second edition, Vol 5, Wiley Interscience publication, 1988
23. T. L. Varghese and V.N Krishnamurthy, J. Polym. Mater , **13**, 245, 1996
24. A. Takemura and H. Mizumachi, Adv. IPN, **3**, 25, 1991, Eds. D. Klempner and K.C. Frisch, Technomic, Lancaster, Pa.

25. Y. Suzuki, T. Fujimoto, S. Tsunoda and K. Shibayama, J. Macromol. Sci.-Physics, **B17(4)**, 787, 1980
26. M.C.O Chang, D.A. Thomas and L.H. Sperling, J. Polym. Mater., **6**, 61 1989
27. M.X. Xu, W.G. Liu and K.D. Yao, Polym. International, **38**, 205, 1995
28. D. J. Hourston and R. Satgurunathan, J. Appl. Polym. Sci., **29**, 2969, 1984
29. T. J. Hsu and L.J. Lee, J. Appl. Polym. Sci., **36**, 1157, 1988
30. Y.S. Yang and L.J. Lee, Macromolecules, **20**, 1490, 1987
31. C. Hepburn, Polyurethane elastomers, Applied science publishers, 1982
32. L. E. Nielsen, J. Compos. Mater., **1**, 100, 1967
33. L. E. Nielsen, Mechanical properties of polymers and composites, vol 2, Marcel Dekker, NY, 1974
34. M. Takayanagi, S. Vermura and S. Minami, J. Polym. Sci. **C 5**, 113, 1964
35. W.E.A. Davies, J. Phys. **D 4**, 1176, 1971
36. S. S. Lee and S.C. Kim, Polym. Eng. and Sci., **33(10)**, 598, 1993
37. K.J. Wang, T.J. Hsu and L.J. Lee, Polym. Eng. and Sci., **29(6)**, 397, 1989
38. S. C. Kim, D. Klempner, K.C. Frisch and S. K. Mukherjee, J. Appl. Polym. Sci., **21**, 1289, 1997
39. P. D. Nair, M. Jayabalan and V.N. Krishnamurthy, J. Polym. Sci., Part A, Polym. Chem., **28**, 3775,1990
40. G. M. Yenwo, J.A. Manson, J. Pulido and L.H. Sperling, J. Appl. Polym. Sci., **21**, 1531, 1977
41. A. A. Donatelli, L.H. Sperling and D.A. Thomas, Macromolecules, **9**, 671, 1976
42. Encyclopedia of polym. Sci and Eng., Second edition, Vol **12**, Wiley -Interscience publication, 1988, P-275
43. J. Selley, Encyclopedia of Polym. Sci. and Eng., Second edition, vol **12**,chapter II, Wiley - Interscience publication, 1988
44. L.J. Young, J. Polym. Sci., **54**, 411, 1961
45. J.R. Lawrence, Polyester resins, Reinhold plastics application series, Reinhold publishing corporation, New York,
46. I. Ludenwald, Developments in Polymer degradation -2, Chapter 3, Ed. N. Grassie, Applied science publishers,1979
47. H. H. G. Jellinek and S. R. Dankle, Degradation and stabilisation of polymers, vol **1**, chapter 2, Ed. H. H. G. Jellinek, Elsevier, 1983

48. D. J. David and H.B. Staley, Analytical chemistry of polyurethanes, vol XVI, Part III, High polymers, 1974

49. J.H. Saunders and K.C. Frisch, Polyurethane Chemistry and technology, Part I, Chemistry, High polymers, vol XVI, , Interscience publishers,1963

50. P. Patel and B. P. Suthar, Polymer, **31**, 339, 1990

51. A. Broido, J. Polym. Sci., **A 2(7)**, 1761, 1969

52. N. Nachimuthu, P. Rajalingam, G. Radhakrishnan and D. J. Francis, J. Appl. Polym. Sci.,**41**, 3059, 1990